Exploring multicomponent reactions

Kroon, Edwin

Exploring multicomponent reactions

From chemistry to drug design

Edwin Kroon

The research described in this thesis was carried out at the Department of Drug Design (Groningen Research Institute of Pharmacy, University of Groningen, The Netherlands) and was financially supported by the University of Groningen.

Printing of this thesis was financially supported by the University Library and the Graduate School of Science, Faculty of Mathematics and Natural Sciences, University of Groningen, The Netherlands.

ISBN: 978-90-367-9543-2 (printed version)

ISBN: 978-90-367-9542-5 (electronic version)

Printing: Ipskamp printing, Enschede

Cover design: Edwin Kroon. The tall ship on the cover was created by flordelys-stock (flordelys-stock.deviantart.com).

rijksuniversiteit
groningen

Exploring multicomponent reactions

From chemistry to drug design

Proefschrift

ter verkrijging van de graad van doctor aan de
Rijksuniversiteit Groningen
op gezag van de
rector magnificus prof. dr. E. Sterken
en volgens besluit van het College voor Promoties

De openbare verdediging zal plaatsvinden op

vrijdag 17 februari 2017 om 12.45 uur

door

Edwin Kroon

geboren op 14 oktober 1986
te Skarsterlân

Promotor
Prof. dr. A. S. S. Dömling

Beoordelingscommissie
Prof. dr. F. J. Dekker
Prof. dr. L. El Kaïm
Prof. dr. A. K. H. Hirsch

Sit and wait and all will be revealed
— Led Zeppelin, Kashmir

Table of Contents

Chapter 1

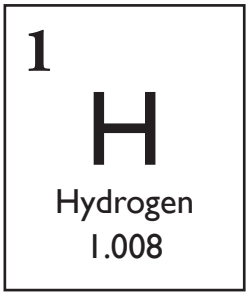

Introduction

In this chapter, the concept of multicomponent reactions is discussed and their application in drug design. Then, the biological target in this thesis, 3-phosphoinositide-dependent kinase-1 (PDK1), is introduced and the important allosteric PDK1-interacting-fragment pocket (PIF pocket) is presented. The structure and function of this pocket is discussed as well as an overview of molecules targeting this particular pocket is given.

1.1 Multicomponent reactions

In the early stages of multicomponent reaction (MCR), development revolved around the reactivity of carbonyl or imine groups. The first MCR, a chemical reaction with three or more starting materials that react together to form one product, was performed by Adolph Strecker in the 1850s; he reacted acetaldehyde with ammonia and hydrogen cyanide to form the amino acid alanine (Scheme 1a).[1,2] In the following decades several other MCR were developed including the Hantzsch pyrrole synthesis, Biginelli reaction, and Mannich reaction as well as the first application of MCR in the synthesis of the natural product tropinone. Around the same time a group of compounds was discovered that had a peculiar smell; these isocyanides, sometimes called isonitriles, have a special valence structure which allows them first to be nucleophiles and then behave as electrophiles (Scheme 1b). This reactivity was exploited by Passerini in the first isocyanide base multicomponent reaction (IMCR), the Passerini reaction.[3,4]

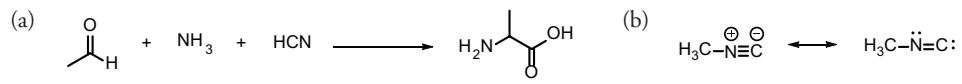

Scheme 1. (a) The Strecker reaction. (b) Resonance structure of methyl isocyanide.

In the years following the discovery of isocyanides the methods for isocyanide synthesis were improved and new IMCRs discovered. One of the most important discoveries after the Passerini reaction was made by Ivar Ugi; the Ugi reaction, a versatile reaction that, due to the nature of the starting materials, allows for the generation of diverse scaffolds.[5,6] In the years thereafter other isocyanide based multicomponent reactions were discovered (Scheme 2). After close to 100 years, multicomponent reactions are well-studied and addressing all novelties is beyond the scope of this introduction, however, several reviews cover the topic extensively.

The reason why multicomponent reactions have required so much attention is the fact that they have some advantages over classical chemical methods. First, the atom economy of MCRs is remarkable; the majority of the starting material atoms end up in the product and producing only water as the side product. Second, they are efficient in the sense that single reaction products can be obtained in one-step compared to sequential synthesis. Third, because the synthetic methodology of MCRs is general applicable to a wide range of starting materials it is well suited for parallel synthesis allowing for the generation of relatively large libraries. Finally, the number of compounds that can be formed is enormous with the chemical space largely not overlapping the chemical space that is accessible through classical synthesis.[8,12]

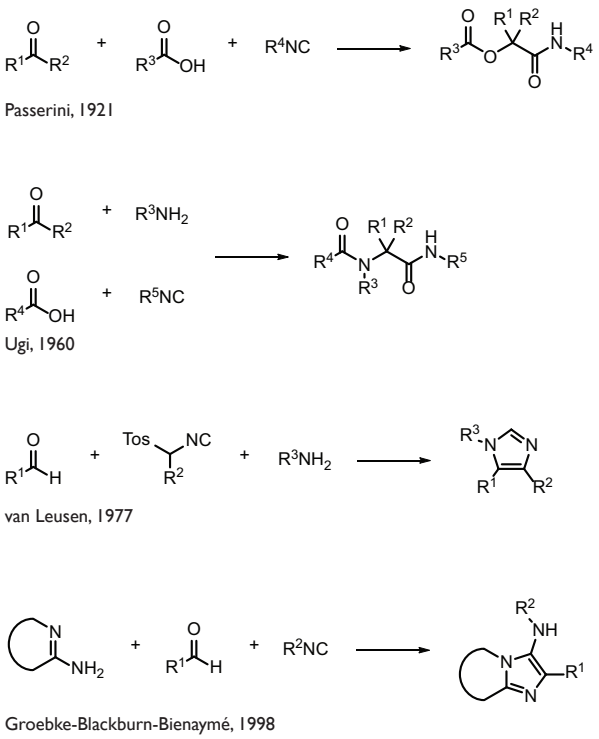

Scheme 2. Multicomponent reactions result in diverse scaffolds.

1.1.1 Multicomponent reactions in drug design

The nature of the starting materials allow MCRs to be versatile alternatives to classical chemical synthesis in the preparation of pharmaceutical products *e.g.*, the antihelmintic praziquantel.[13] Praziquantel is of particular interest because of its application in the treatment of schistosomiasis, a neglected tropical disease, caused by parasitic flatworms (schistosomes) which are largely prevalent in sub-Saharan Africa.[14,15] The reported syntheses are multistep (in general four or more) sequential procedures that yield racemic praziquantel, although, enantioselective procedures are known.[16] Recently, a MCR methodology was reported consisting of an Ugi reaction followed by a Pictet-Spengler cyclization that produced racemic praziquantel **1**. This two-step procedure started from cheap commercial starting materials **2–5**, through the intermediate Ugi product **6**, to form a number of novel praziquantel derivatives (Scheme 3).[17] This shows that MCRs are a useful tool in the chemist's toolbox for creating diversity and complexity in the synthesis of intricate molecules, pharmaceuticals and natural products.

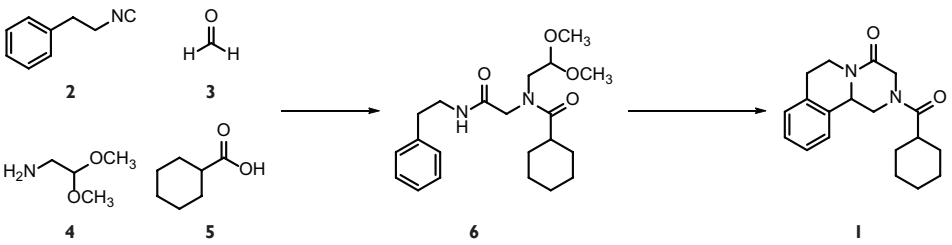

Scheme 3. Praziquantel synthesis *via* an Ugi/Pictet–Spengler strategy.

1.2 Drug discovery for protein kinases

Many aspects of cell life are regulated through protein phosphorylation, a process that is carried out by kinases; about two percent of all human genes make up for all 518 members of the human kinome.[18,19] Their main function is signal transduction within cells by alteration of substrate activity, protein kinases also govern many other cellular processes, including metabolism, cell cycle progression, and apoptosis. Protein kinases can be classified according to the amino acids they phosphorylate, the two major groups being serine/threonine kinases and tyrosine kinases. They exert their function by attaching a phosphate group to the hydroxyamino acid using adenosine triphosphate (ATP) as phosphate source (Figure 1).[20-22]

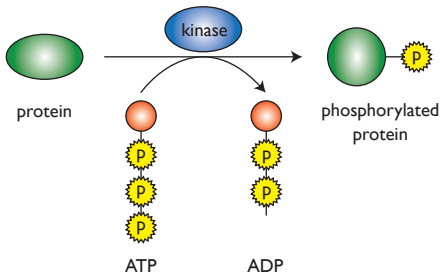

Figure 1. Phosphorylation by protein kinases.

Noticeably, because phosphorylation is such an important process in the cell it can be expected that dysregulation has major consequences for the human body, therefore, kinases are among the most important target for drug discovery.[23,24] The discovery of protein kinase inhibitors started in 1978 with the identification of the first oncogene; the transforming factor of the Rous sarcoma virus, a protein kinase called sarc (Src). Several years later the first inhibitors for protein kinases were synthesized based on a known sulfonamide targeting calmodulin; low micromolar compounds were obtained for protein kinase C (PKC), cyclic-AMP-dependent

protein kinase (PKA), and cyclic-GMP-dependent protein kinase (PKG, Figure 2). This compound was further developed into the drug fasudil, approved in Japan and China for the treatment of cerebral vasospasm.[24] Around the same time it was reported that staurosporine was a nanomolar inhibitor of PKC, this was the discovery that moved pharmaceutical companies into the field of protein tyrosine kinases developing bisindolyl maleimides derivatives like staurosporine (Figure 2).[23] In the following years a number of successes were achieved, but the hallmark in kinase inhibitor discovery was imatinib (Gleevec, Figure 2), developed by scientists from Ciba-Geigy (Novartis) and targeting Abelson tyrosine kinase (ABL).[25] Initially not given a high priority because chronic myeloid leukemia (CML) was not very prevalent, it later rapidly was approved due to a high efficacy and minimal side effects.[26,27]

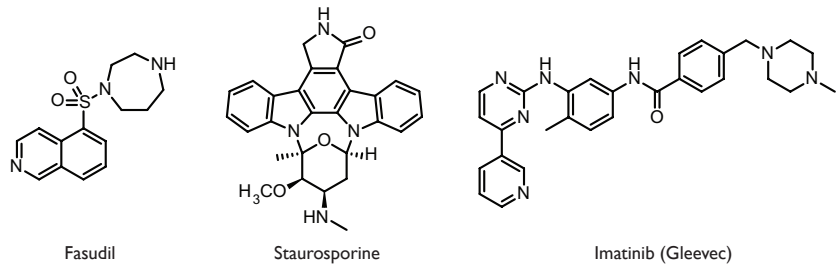

Figure 2. Selection of kinase inhibitors.

Since the United States Food and Drug Administration approved imatinib for the treatment of CML in 2001, twenty-seven other small molecule kinase inhibitors are approved, particularly, for oncology indications.[28,29] However, the exceptions not targeting cancer are tofacitinib (rheumatoid arthritis) and nintedanib (idiopathic pulmonary fibrosis), whereas, several other small molecules are currently in (pre)-clinical trials for anti-inflammatory treatment, central nervous system diseases, and cardiovascular disease.[24,29]

The focus by pharmaceutical companies on oncology also highlights a major challenge in the discovery of kinase inhibitors, namely selectivity.[30,31] Whereas in patients with a life-threatening disease severe side effects as a result of polypharmacology may be acceptable, in non-life-threatening diseases this is not desirable. The majority of kinase inhibitors, relatively flat and aromatic molecules, overlap to a certain extent with the ATP binding site; this site is highly conserved throughout the entire kinome, thus leading to selectivity problems.[32] Notwithstanding the fact that several selective ATP-competitive inhibitors are known.[24,28,33]

1.3 Phosphoinositide-dependent kinase-1 (PDK1)

The family of AGC kinases, after the representative members PKA, PKG, and PKC, consists of sixty-three serine/threonine protein kinases, twelve percent of the human kinome.[34] The family of AGC kinases plays a significant role in regulating physiological processes relevant to metabolism, growth, proliferation and survival, therefore dysregulation can have great consequences. Two main diseases associated with dysregulation in these physiological processes are cancer and diabetes mellitus type 2, on the other hand, mutations have been shown to cause various inherited syndromes.[35-37]

Within this family 3-phosphoinositide-dependent kinase-1 (PDK1) is an important member as it has a pivotal role as master kinase in the activation of at least twenty-three other AGC kinases. Upon interaction of insulin and growth factors with their respective receptors lead to activation of phosphatidylinositol 3-kinase (PI3K) which recruits PDK1 as major PI3K regulated AGC kinase (Figure 3).[38]

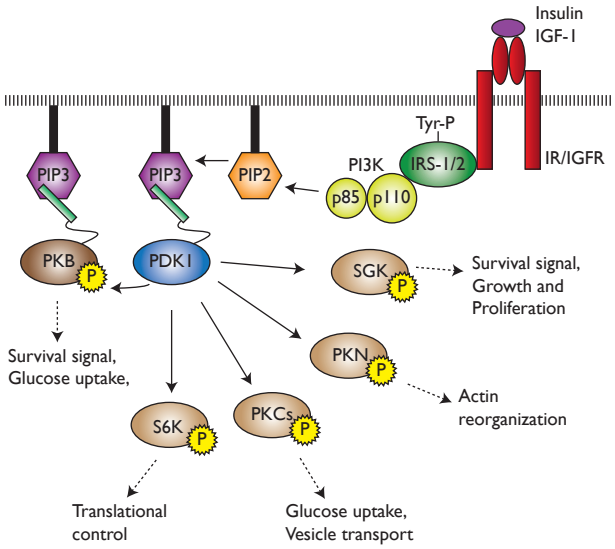

Figure 3. A selection of PDK1 substrates (adapted from reference 22).

This was supported with embryonic stem cells lacking PDK1; insulin-like growth factor-1 (IGF-1) failed to initiate activation of PKBα, p70 ribosomal S6 kinase-1 (S6K-1), and serum- and glucocorticoid-induced protein kinase-1 (SGK-1) under conditions where activation was achieved in wild-type cells, indicating that PDK1 is required for activation of these proteins.[39,40] Furthermore, PDK1 is responsible

for the T-loop activation of all PKC isoforms, and p90 ribosomal S6 kinase (RSK) where, consistent with previous observations, RSK cannot be activated and the majority of PKC isoforms are unstable, because T-loop phosphorylation stabilized the protein structure.[41] Finally, regulation of PDK1 activity is dictated by *trans*-autophosphorylation, thus PDK1 is constitutively active in mammalian cells. Evidence for *trans*-autophosphorylation was given by PDK1 obtained from unstimulated cells and growth factor or insulin-stimulated cells both showed a high catalytic activity.[36,41,42]

1.3.1 General structure of AGC kinases

The overall structure of an AGC kinase consists of an amino-terminal small lobe (N-lobe) and a large lobe on the carboxy terminal (C-lobe) that sandwich a molecule of ATP between them to form the typical bilobal kinase fold (Figure 4).[36]

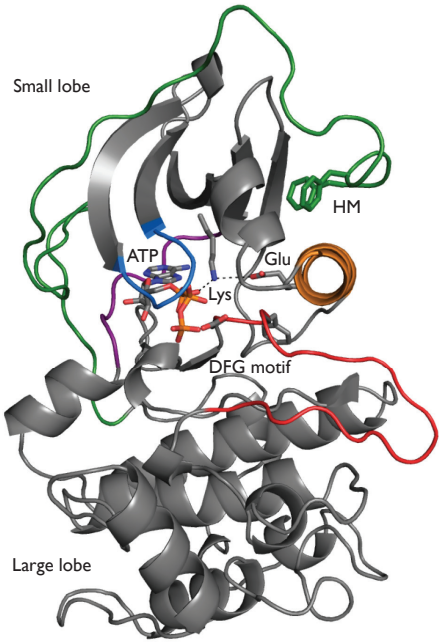

Figure 4. General structure of an AGC kinase, here represented by PKA (PDB ID: 1ATP). Color code: hinge region (purple), glycine-rich loop (blue), αC-helix (orange), T-loop (red), C-terminal tail (green) with the two phenylalanine residues (green sticks) of the hydrophobic motif (HM) binding to the HM pocket. Figures of this type were created with PyMol.[43]

In general, activation of AGC kinases involves two or three phosphorylations. First phosphorylation on the T-loop (activation loop) which is present on the C-lobe adjacent to the ATP binding pocket, and contains the important DFG motif necessary for phosphoryl transfer.[44] The αC-helix bridges the C-lobe and the N-lobe, phosphorylation of the activation loop causes a conformational change in the αC-helix and a hydrogen bond network is created between a glutamic acid residue on the αC-helix, a lysine on the N-lobe, and the γ-phosphate of ATP resulting in the catalytic activity of the enzyme.[45,46] Second, phosphorylation of the hydrophobic motif (HM), located on the C-terminal tail is required; after activation it wraps around the N-lobe and a regulatory interaction originates with the hydrophobic motif pocket stabilizing an active conformation of the αC-helix.[47,48] Finally, some AGC kinases need activation of the turn motif which is situated on the C-terminal tail, however, preceding the hydrophobic motif helping to position the HM for the HM pocket by interacting with a positively charged surface on the N-lobe; this interaction is required for full activity of these kinases.[49]

1.4 The PIF pocket of PDK1: structure and function

A strategy to overcome issues with selectivity is to find kinase inhibitors that bind to different sites than the ATP binding site of the protein kinase. A so-called allosteric site is remote from the ATP binding site, therefore ATP-noncompetitive, but through a structural conformational change has an influence on the ATP binding site.[50-52] The PIF pocket of PDK1 shows resemblance to the HM pocket of PKA in which intramolecularly the HM (FSEF-COOH) of PKA binds.[53] Key residues lining the PIF pocket of PDK1 and the HM pocket of PKA are conserved in all AGC group members, including PKB, PKC isoforms, SGK, S6K, PRK2, RSK, and ROCK.[47,54] Unlike all other AGC kinases PDK1 lacks the HM, therefore the PIF pocket is unoccupied and available for substrate recognition, thus PDK1 can exert its function as master kinase.[55] The PIF pocket is located remotely from the ATP binding site on the small lobe of PDK1 and is around 5 Å deep, the secondary structural features are two -helices (αB and αC) and two β-sheets (β4 and β5) being hydrophobic in the center and surrounded by polar residues (Figure 5).

The regulation of substrate AGC kinases by PDK1 can be divided into two different mechanisms. From all AGC kinases the three isoforms of protein kinase B (PKB) and PDK1 are the only ones to have a pleckstrin homology (PH) domain in their structure.[56] Upon extracellular stimulation by insulin or growth factors, PI3K phosphorylates phosphatidylinositol (4,5)-biphosphate (PIP_2) to phosphatidylinositol (3,4,5)-triphosphate (PIP_3), thereby allowing PKB and PDK1 to co-localize to the cell membrane and interact with their PH domain (Figure 6a;

also represented in Figure 3, Section 1.2).[57] Due to the close proximity PDK1 is able to phosphorylate PKB at the T-loop and the active PKB can phosphorylate its downstream substrates.

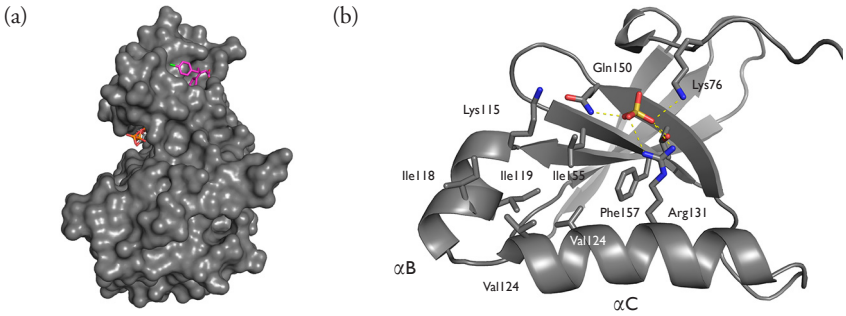

Figure 5. The PIF pocket of PDK1. (a) Location of the allosteric PIF pocket is remote from the ATP binding site (PDB ID: 3HRF). (b) close-up of the PIF pocket (PDB ID: 1H1W). Color code: (a) PDK1 (grey surface), ATP (orange sticks), small molecule in PIF pocket (magenta sticks). (b) PIF pocket (grey cartoon), residues lining the pocket (sticks), sulfate ion (yellow/red sticks).

All other PDK1 substrate kinases are devoid of the PH domain and have to be phosphorylated at the HM before they can interact with PDK1. Interaction of the phosphorylated HM of AGC substrates with the PIF pocket is required for

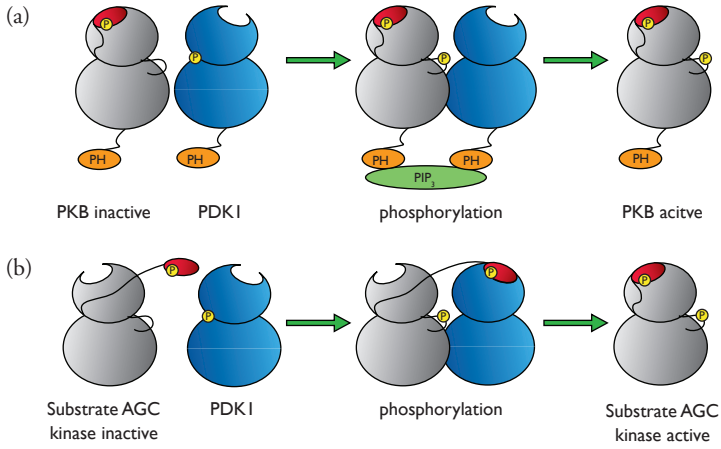

Figure 6. Regulation of AGC kinases by PDK1 follows two different pathways.(a) PDK1 regulation of PKB. After colocalization at the cell mebrane, through PIP_3 binding, PKB is phosphorylated at the T-loop and activated. No PIF pocket binding is required. (b) PDK1-dependent regulation of other AGC kinases. After phopshoryaltion of the hydrophobic motif (HM), the phosphoryalted HM binds to the PIF pocket of PDK1. Then, T-loop phosphoryaltion is initiated and the substrate AGC kinase activated (adapted from reference 15).

recognition and subsequent phosphorylation at the T-loop by PDK1.[54,59] After dissociation of the fully activated substrate from PDK1 the HM intramolecularly binds to its HM pocket and is fully active to exert its kinase function (Figure 6b).

1.5 Targeting the allosteric PIF pocket

That the PIF pocket is vital for PDK1 to interact and phosphorylate AGC kinases is investigated thoroughly, but to study if the interaction/phosphorylation remained, a mutation in the PIF pocket was introduced. Mutation of the PIF pocket's lysine to glutamic acid (L155E) significantly lowered the ability of PDK1 to activate S6K and SGK *in vitro*, but not the activation of PKB, in accordance with the mechanism of activation.[55] To confirm that the PIF pocket is necessary for PDK1 activity, the *in vivo* influence of the PIF pocket was examined in embryonic stem cells having the L155E knock-in mutation. Similar results were obtained as the in vitro experiments; SGK, S6K, and RSK were inactive while PKB was active.[40,60] These experiments provided the evidence that an intact PIF pocket is necessary for the activation of PH deficient AGC kinases, but not PKB. Moreover, applying HM peptides from different substrate AGC kinases revealed that the catalytic activity of PDK1 is enhanced, suggesting that complexation with the HM is necessary for full PDK1 activity as part of its regulatory mechanism.[45,47]

Importantly, this characterized the PIF pocket as an allosteric site on PDK1, transducing signals from interacting ligands to the active site.

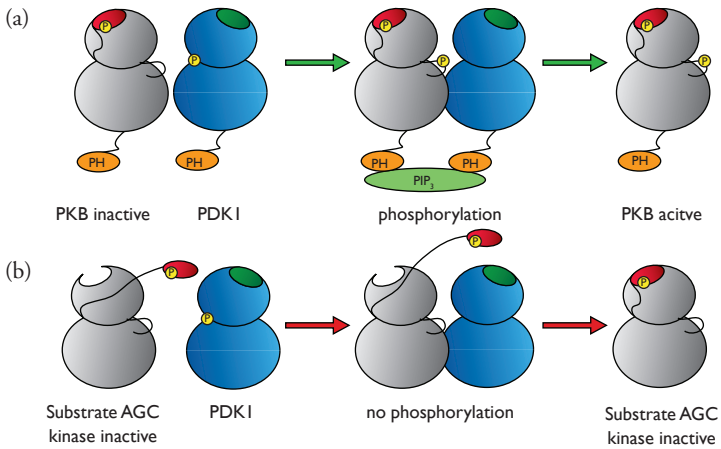

Figure 7. Effects of a small molecule binding to the PIF pocket of PDK1. (a) Although the PIF pocket is blocked by a small molecule, PKB is still phosphorylated at the T-loop, because PIF pocket binding is not required (b) AGC kinases requiring PIF pocket binding are not activated, the PIF pocket is blocked by a small molecule.

First, substrate AGC kinases that require PIF pocket binding can be prevented from doing so by occupying the PIF pocket with a small molecule, thus the AGC kinase cannot become activated while PKB can be activated (Figure 7). Second, because the PIF pocket is an allosteric site a small molecule modulator stabilizes a certain conformation, if one of these conformations induces reduced PDK1 activity it prevents not only the inhibition of substrate AGC kinases but PKB, also.

1.5.1 Small molecule modulators of the PIF pocket

Not surprisingly, since AGC kinases play such an important role in cellular processes they have been the subject of drug discovery research with a main focus on ATP-competitive inhibitors.[42] Nonetheless, in little over a decade several strategies were applied to find compounds that were active towards the PIF pocket in the search of selectivity. The first strategy was to mimic the HM with a small heptameric peptide (GFRDFDY), part of the high affinity PIFtide (part of the HM of PRK2), which proved to be unsuccessful in modulating PDK1 activity even at high concentration (500 μM). Then a pharmacophore based *in silico* screening was performed, starting with the HM of PKA, which identified close to 250 hits and screening them resulted in the first small molecule activator **7** (Figure 8).[61] Based on this initial hit a second series of PDK1 modulators was synthesized keeping the core structure the same; removing the chiral center and sulfur atom led to compound **8** (PS48, Figure 8). It exhibited similar activation potency (fourfold) as **7**, but with an AC_{50} that was more than four times lower (8 μM vs. 38 μM), moreover, the binding mode was confirmed with an X-ray cocrystal structure.[62,63] Recently, PS48 was further improved to obtain low micromolar PDK1 activators **9** and **10** (up to sevenfold activation with AC_{50}s of 2 μM).[64,65]

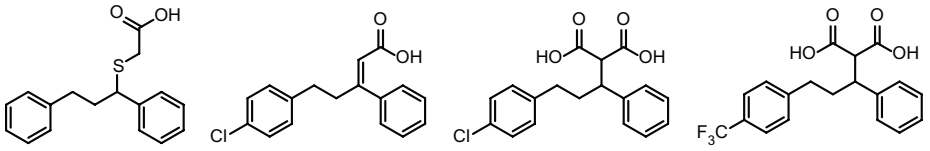

8 — 38 μM[a], 300%[b]

9 — 8 μM[a], 300%[b]

10 — 2 μM[a], 400%[b]

11 — 2 μM[a], 650%[b]

Figure 8. First small molecule activators of PDK1. [a] AC_{50}. [b] Maximum activation.

Another strategy used was saturation transfer difference nuclear magnetic resonance (STD-NMR)[66] to identify fragments targeting the PIF pocket. From

a library of 10,000 fragments more than 300 showed activity towards PDK1, unfortunately, the majority bound to the ATP binding site. Compounds **11** and **12** were found to target the PIF pocket, nonetheless, at high concentration (300 μM) **11** showed twofold activation, whereas **12** showed partial inhibition, but no comment was made on this discrepancy (Figure 9).[67] An alternative methodology is *de novo* design of compounds starting from known small molecules targeting the PIF pocket and this strategy was exploited for a series of benzoazepin-2-ones derived scaffolds. After *in silico* construction of the compounds they were virtually docked in the PIF pocket of PDK1. Not surprisingly, being closely related to the compounds in Figure 8, the more rigid scaffold **13** showed activity (EC_{50} = 23 μM) towards PDK1 (Figure 9).[68]

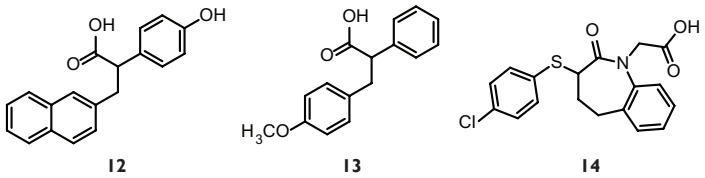

Figure 9. PDK1 modulators from STD-NMR (**12** and **13**) and *de novo* strategies (**14**).

Recently, structure based virtual screening was applied to a library of compounds using an ensemble of PDK1 structures. An initial hit was selected after performing a fluorescence polarization assay and a surface plasmon resonance assay, subsequent iterative synthesis of 300 compounds resulted in the weak activators **14** and **15** (Figure 10). Moreover, compound **14** blocked S6K1 activation *in vivo*, but not PKB activation where the PIF pocket is not necessary for activation (Section 1.3). Furthermore, blocking the activation of S6K1 and PKB by a known ATP-competitive inhibitor is more effective in the presence of **14**.[69]

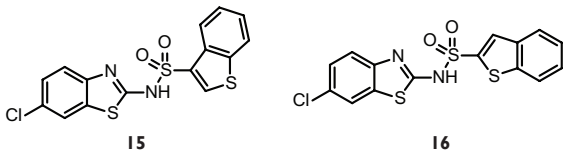

Figure 10. PDK1 modulators derived from high-throughput screening.

In the same report the cocrystal structure of PIFtide in the PIF pocket was presented, the small peptide extends into a shallow area adjacent to the PIF pocket (Figure 11). This could be useful for further discovery of PIF pocket modulators.

Altogether, some important observations can be made from these reported small molecule modulators of the PIF pocket: (1) a negatively charged carboxylate moiety is required for potent in vitro activation of PDK1, (2) two aromatic rings are required for proper interaction with the PIF pocket; they mimic the two phenylalanine residues present in the HM of substrate AGC kinases, and (3) no potent reversible small molecule inhibitor of the PIF pocket is known to date. Moreover, the presence of a negatively charged carboxylate, poses a challenge for the compounds to display proper pharmacological properties e.g., crossing membranes and protein binding. However, these challenges could be overcome by several strategies like prodrug formation or bioisosteres.[70,71]

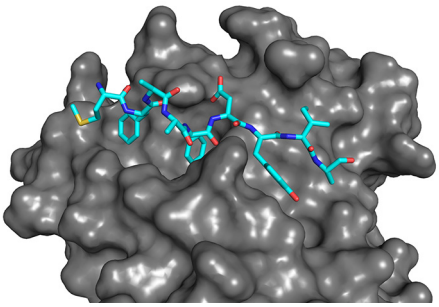

Figure 11. Cocrystal structure of PIFtide in the PIF pocket. Color code: PDK1 (grey surface), PIFtide (cyan sticks).

1.6 Project goals and outline of the thesis

Since dysregulation of protein kinases has major implications in the development of severe diseases such as cancer, design and validation of new compounds that target kinases is important. With respect to selectivity, allosteric modulators could play a significant role and in this thesis, we describe the use of multicomponent reaction chemistry for the synthesis of compounds targeting the allosteric PIF pocket of PDK1. Furthermore, we describe the use of new starting materials in multicomponent reactions to expand the applicability of these useful reactions.

In Chapter 2, we describe the application of the recently reported AnchorQuery for the design and synthesis of small molecule modulators of the PIF pocket. First we describe the pharmacophore based design followed by the synthesis of the compounds and their ability to modulate PDK1 activity is tested. Furthermore, we describe the binding mode and an in-depth SAR with in vitro testing for PDK1 activity.

In Chapter 3, a new cleavable isocyanide is presented for the Ugi tetrazole

reaction. The scope for the reaction is investigated and our cleavable isocyanide is compared with other cleavable isocyanides. Finally, the potential application in other multicomponent reactions is briefly discussed.

In Chapter 4, we describe our efforts using mixed cyclic anhydrides in the Castagnoli reaction. A detailed discussion is presented for the viability of using cyclic mixed anhydrides in this reaction.

In Chapter 5, we will discuss the latest applications of domino transformations in organic synthesis with a special focus on additions to carbon–nitrogen double bonds and nitriles. After a short introduction, different strategies for postcondensation of Ugi reaction products are discussed followed by the final part that has an emphasis on the addition to nitriles.

1.7 References

1 Strecker, A. Ueber die künstliche bildung der milchsäure und einen neuen, dem glycocoll homologen körper. *Justus Liebigs Ann. Chem.* **75,** 27–45 (1850).

2 Strecker, A. Ueber einen neuen aus aldehyd - ammoniak und blausäure entstehenden Körper. *Justus Liebigs Ann. Chem.* **91,** 349–351 (1854).

3 Passerini, M. Isonitriles. I. Compound of *p*-isonitrileazobenzene with acetone and acetic acid. *Gazz. Chim. Ital.* **51,** 126–129 (1921).

4 Passerini, M. Isonitrile. II. Compounds with aldehydes or with ketones and monobasic organic acids. *Gazz. Chim. Ital.* **51,** 181–189 (1921).

5 Ugi, I. & Steinbrückner, C. Über ein neues kondensations-prinzip. *Angew. Chem.* **72,** 267–268 (1960).

6 Ugi, I. Neuere methoden der präparativen organischen chemie IV mit sekundär-reaktionen gekoppelte α-additionen von immonium-ionen und anionen an isonitrile. *Angew. Chem.* **74,** 9–22; *Angew. Chem., Int. Ed. Engl.* **1,** 8–21 (1962).

7 Dömling, A. & Ugi, I. Multicomponent reactions with isocyanides. *Angew. Chem., Int. Ed.* **39,** 3168–3210; *Angew. Chem.* **112,** 3300–3344 (2000).

8 Dömling, A. Recent developments in isocyanide based multicomponent reactions in applied chemistry. *Chem. Rev.* **106,** 17–89 (2006).

9 Dömling, A., Wang, W. & Wang, K. Chemistry and biology of multicomponent reactions. *Chem. Rev.* **112,** 3083–3135 (2012).

10 de Graaff, C., Ruijter, E. & Orru, R. V. A. Recent developments in asymmetric multicomponent reactions. *Chem. Soc. Rev.* **41,** 3969–4009 (2012).

11 Wessjohann, L. A. *et al.* in *Multicomponent Reactions 1* (ed Müller, T. J. J.) 415–502 (Georg Thieme Verlag KG, 2014).

12 Dömling, A. Recent advances in isocyanide-based multicomponent chemistry. *Curr. Opin. Chem. Biol.* **6,** 306–313 (2002).

13 Ruijter, E. & Orru, R. V. A. Multicomponent reactions – opportunities for the pharmaceutical industry. *Drug Discovery Today: Technol.* 10, e15–e20 (2013).

14 Colley, D. G., Bustinduy, A. L., Secor, W. E. & King, C. H. Human schistosomiasis. *Lancet* **383,** 2253–2264 (2014).

15 Njoroge, M. *et al.* Recent approaches to chemical discovery and development against malaria and the neglected tropical diseases human african trypanosomiasis and schistosomiasis. *Chem. Rev.* **114,** 11138–11163 (2014).

16 Dömling, A. & Khoury, K. Praziquantel and schistosomiasis. *ChemMedChem* **5,** 1420–1434 (2010).

17 Liu, H., William, S., Herdtweck, E., Botros, S. & Dömling, A. MCR synthesis of praziquantel derivatives. *Chem. Biol. Drug Des.* **79,** 470–477 (2012).

18 Manning, G., Whyte, D. B., Martinez, R., Hunter, T. & Sudarsanam, S. The protein kinase complement of the human genome. *Science* **298,** 1912–1934 (2002).

19 Cohen, P. The origins of protein phosphorylation. *Nat. Cell Biol.* **4,** E127–E130 (2002).

20 Hanks, S. K. Eukaryotic protein kinases. *Curr. Opin. Struct. Biol.* **1,** 369–383 (1991).

21 Johnson, L. N. & Lewis, R. J. Structural basis for control by phosphorylation. *Chem. Rev.* **101,** 2209–2242 (2001).

22 Adams, J. A. Kinetic and catalytic mechanisms of protein kinases. *Chem. Rev.* **101,** 2271–2290 (2001).

23 Cohen, P. Protein kinases — the major drug targets of the twenty-first century? *Nat. Rev. Drug Discov.* **1,** 309–315 (2002).

24 Cohen, P. & Alessi, D. R. Kinase drug discovery – what's next in the field? *ACS Chem. Biol.* **8,** 96–104 (2013).

25 Buchdunger, E. *et al.* Inhibition of the Abl protein-tyrosine kinase *in vitro* and *in vivo* by a 2-phenylaminopyrimidine derivative. *Cancer Res.* **56,** 100–104 (1996).

26 Druker, B. J. *et al.* Effects of a selective inhibitor of the Abl tyrosine kinase on the growth of Bcr-Abl positive cells. *Nat. Med.* **2,** 561–566 (1996).

27 Druker, B. J. *et al.* Efficacy and safety of a specific inhibitor of the BCR-ABL tyrosine kinase in chronic myeloid leukemia. *N. Engl. J. Med.* **344,** 1031–1037 (2001).

28 Zhang, J., Yang, P. L. & Gray, N. S. Targeting cancer with small molecule kinase inhibitors. *Nat. Rev. Cancer* **9,** 28–39 (2009).

29 Wu, P., Nielsen, T. E. & Clausen, M. H. Small-molecule kinase inhibitors: an analysis of FDA-approved drugs. *Drug Discovery Today* **21,** 5–10 (2016).

30 Anastassiadis, T., Deacon, S. W., Devarajan, K., Ma, H. & Peterson, J. R. Comprehensive assay of kinase catalytic activity reveals features of kinase inhibitor selectivity. *Nat. Biotechnol.* **29,** 1039–1045 (2011).

31 Davis, M. I. *et al.* Comprehensive analysis of kinase inhibitor selectivity. *Nat. Biotechnol.* **29,** 1046–1051 (2011).

32 Engel, M. in *Protein-Protein Interactions in Drug Discovery* (ed. Dömling, A.) 187-223 (Wiley-VCH Verlag GmbH & Co. KGaA, 2013).

33 Knight, Z. A. & Shokat, K. M. Features of selective kinase inhibitors. *Chem. Biol.* **12,** 621–637 (2005).

34 Hanks, S. K. & Hunter, T. Protein kinases 6. The eukaryotic protein kinase superfamily: kinase (catalytic) domain structure and classification. *FASEB J.* **9,** 576–596 (1995).

35 Hennessy, B. T., Smith, D. L., Ram, P. T., Yiling, L. & Mills, G. B. Exploiting the PI3K/Akt pathway for cancer drug discovery. *Nat. Rev. Drug Discov.* **4,** 988–1004 (2005).

36 Pearce, L. R., Komander, D. & Alessi, D. R. The nuts and bolts of AGC protein kinases. *Nat. Rev. Mol. Cell Biol.* **11,** 9–22 (2010).

37 Mochly-Rosen, D., Das, K. & Grimes, K. V. Protein kinase C, an elusive therapeutic target? *Nat. Rev. Drug Discov.* **11,** 937–957 (2012).

38 Kikani, C. K., Dong, L. Q. & Liu, F. "New"-clear functions of PDK1: beyond a master kinase? *J. Cell. Biochem.* **96,** 1157–1162 (2005).

39 Williams, M. R. *et al.* The role of 3-phosphoinositide-dependent protein kinase 1 in activating AGC kinases defined in embryonic stem cells. *Curr. Biol.* **10,** 439–448 (2000).

40 Collins, B. J., Deak, M., Murray-Tait, V., Storey, K. G. & Alessi, D. R. *In vivo* role of the phosphate groove of PDK1 defined by knockin mutation. *J. Cell Sci.* **118,** 5023–5034 (2005).

41 Mora, A., Komander, D., van Aalten, D. M. F. & Alessi, D. R. PDK1, the master regulator of AGC kinase signal transduction. *Semin. Cell Dev. Biol.* **15,** 161–170 (2004).

42 Arencibia, J. M., Pastor-Flores, D., Bauer, A. F., Schulze, J. O. & Biondi, R. M. AGC protein kinases: from structural mechanism of regulation to allosteric drug development for the treatment of human diseases. *Biochim. Biophys. Acta, Proteins and Proteomics* **1834,** 1302–1321 (2013).

43 The Pymol Molecular Graphics System, Version 1.3, Schrödinger, LLC

44 Johnson, L. N., Noble, M. E. M. & Owen, D. J. Active and inactive protein kinases: structural basis for regulation. *Cell* **85,** 149–158 (1996).

45 Yang, J. *et al.* Molecular mechanism for the regulation of protein kinase B/Akt by hydrophobic motif phosphorylation. *Mol. Cell* **9,** 1227–1240 (2002).

46 Komander, D., Kular, G., Deak, M., Alessi, D. R. & van Aalten, D. M. F. Role of T-loop phosphorylation in PDK1 activation, stability, and substrate binding. *J. Biol. Chem.* **280,** 18797–18802 (2005).

47 Biondi, R. M. *et al.* Identification of a pocket in the PDK1 kinase domain that interacts with PIF and the C–terminal residues of PKA. *EMBO J.* **19,** 979–988 (2000).

48 Biondi, R. M. *et al.* High resolution crystal structure of the human PDK1 catalytic domain defines the regulatory phosphopeptide docking site. *EMBO J.* **21,** 4219–4228 (2002).

49 Hauge, C. *et al.* Mechanism for activation of the growth factor–activated AGC kinases by turn motif phosphorylation. *EMBO J.* **26,** 2251–2261 (2007).

50 Goodey, N. M. & Benkovic, S. J. Allosteric regulation and catalysis emerge via a common route. *Nat. Chem. Biol.* **4,** 474–482 (2008).

51 Fang, Z., Grütter, C. & Rauh, D. Strategies for the selective regulation of kinases with allosteric modulators: exploiting exclusive structural features. *ACS Chem. Biol.* **8,** 58–70 (2013).

52 Wu, P., Clausen, M. H. & Nielsen, T. E. Allosteric small-molecule kinase inhibitors. *Pharmacol. Ther.* **156,** 59–68 (2015).

53 Zheng, J. *et al.* 2.2 Å refined crystal structure of the catalytic subunit of cAMP-dependent protein kinase complexed with MnATP and a peptide inhibitor. *Acta Crystallogr., Sect. D: Struct. Biol.* **49,** 362–365 (1993).

54 Frödin, M. *et al.* A phosphoserine/threonine–binding pocket in AGC kinases and PDK1 mediates activation by hydrophobic motif phosphorylation. *EMBO J.* **21,** 5396–5407 (2002).

55 Biondi, R. M., Kieloch, A., Currie, R. A., Deak, M. & Alessi, D. R. The PIF-binding pocket in PDK1 is essential for activation of S6K and SGK, but not PKB. *EMBO J.* **20,** 4380-4390 (2001).

56 Thomas, C. C., Deak, M., Alessi, D. R. & van Aalten, D. M. F. High-resolution structure of the pleckstrin homology domain of protein kinase B/Akt bound to phosphatidylinositol (3,4,5)-trisphosphate. *Curr. Biol.* **12,** 1256–1262 (2002).

57 Currie, R. A. *et al.* Role of phosphatidylinositol 3,4,5-trisphosphate in regulating the activity and localization of 3-phosphoinositide-dependent protein kinase-1. *Biochem. J.* **337,** 575–583 (1999).

58 Manning, B. D. & Cantley, L. C. AKT/PKB signaling: navigating downstream. *Cell* **129,** 1261–1274 (2007).

59 Balendran, A. *et al.* A 3-phosphoinositide-dependent protein kinase-1 (PDK1) docking site is required for the phosphorylation of protein kinase Cζ (PKCζ) and PKC-related kinase 2 by PDK1. *J. Biol. Chem.* **275,** 20806–20813 (2000).

60 Collins, B. J., Deak, M., Arthur, J. S. C., Armit, L. J. & Alessi, D. R. *In vivo* role of the PIF-binding docking site of PDK1 defined by knock-in mutation. *EMBO J.* **22,** 4202–4211 (2003).

61 Engel, M. *et al.* Allosteric activation of the protein kinase PDK1 with low molecular weight compounds. *EMBO J.* **25,** 5469–5480 (2006).

62 Hindie, V. *et al.* Structure and allosteric effects of low-molecular-weight activators on the protein kinase PDK1. *Nat. Chem. Biol.* **5,** 758–764 (2009).

63 Stroba, A. *et al.* 3,5-Diphenylpent-2-enoic acids as allosteric activators of the protein kinase PDK1: structure–activity relationships and thermodynamic characterization of binding as paradigms for PIF-binding pocket-targeting compounds. *J. Med. Chem.* **52,** 4683–4693 (2009).

64 Busschots, K. *et al.* Substrate-selective inhibition of protein kinase PDK1 by small compounds that bind to the PIF-pocket allosteric docking site. *Chem. Biol.* **19,** 1152–1163 (2012).

65 Wilhelm, A. *et al.* 2-(3-Oxo-1,3-diphenylpropyl)malonic acids as potent allosteric ligands of the PIF pocket of phosphoinositide-dependent kinase-1: development and prodrug concept. *J. Med. Chem.* **55,** 9817–9830 (2012).

66 Lepre, C. A., Moore, J. M. & Peng, J. W. Theory and applications of NMR-based screening in pharmaceutical research. *Chem. Rev.* **104,** 3641–3676 (2004).

67 Stockman, B. J. *et al.* Identification of allosteric PIF-pocket ligands for PDK1 using NMR-based fragment screening and ^{1}H-^{15}N TROSY experiments. *Chem. Biol. Drug Des.* **73,** 179–188 (2009).

68 Wei, L. *et al.* Design and synthesis of benzoazepin-2-one analogs as allosteric binders targeting the PIF pocket of PDK1. *Bioorg. Med. Chem. Lett.* **20,** 3897–3902 (2010).

69 Rettenmaier, T. J. *et al.* A small-molecule mimic of a peptide docking motif inhibits the protein kinase PDK1. *Proc. Natl. Acad. Sci. U. S. A.* **111,** 18590–18595 (2014).

70 Rautio, J. *et al.* Prodrugs: design and clinical applications. *Nat. Rev. Drug Discov.* **7,** 255–270 (2008).

71 Meanwell, N. A. Synopsis of some recent tactical application of bioisosteres in drug design. *J. Med. Chem.* **54,** 2529–2591 (2011).

Chapter 2

He
Helium
4.003

A potent allosteric kinase inhibitor: beyond traditional drug design

Rational design of allosteric kinase modulators is challenging but rewarding. In this chapter, we describe how we use the ANCHOR.QUERY software to discover a potent allosteric PDK1 kinase modulator. We are able to generate several new scaffolds binding to the allosteric target site and validate one example for which the binding mode is discussed with an X-ray cocrystal structure.

Part of this chapter has been published:

Kroon, E., Schulze, J. O., Süß, E., Camacho, C. J., Biondi, R. M. & Dömling, A. Discovery of a Potent Allosteric Kinase Modulator by Combining Computational and Synthetic Methods. *Angew. Chem., Int. Ed.* **54,** 13933–13936; *Angew. Chem.* **127,** 14139–14142 (2015).

The work described in this chapter resulted from collaboration with the Biondi research group (University Hospital Frankfurt, Germany). The in vitro experiments were performed by E. Süß, the in vivo experiments by Dr. A. E. Leroux and the cocrystal structure determination was performed by Dr. J. O. Schulze, all members from the group of Dr. R. M. Biondi. The X-ray strucutres are determined by Dr. K. Kurpiewska and Dr. J. Kalinowska-Tłuścik (Jagiellonian University, Poland). AnchorQuery is co-developed by Prof. Dr. J. J. Camacho (University of Pittsburgh, USA).

2.1 AnchorQuery design of new kinase modulators

It is a misconception that the term pharmacophore was first introduced by Paul Ehrlich in the early 1900s, in his paper he never mentioned the term pharmacophore. However, he did use the terms haptophore and toxophore, which indicated the stable non–toxic and toxic part of a molecule, respectively.[1] Actually, the concept of a pharmacophore was first described by the American chemist Lemont Kier whom initially called it receptor pattern, but later coined the term pharmacophore (Figure 1).[2–4]

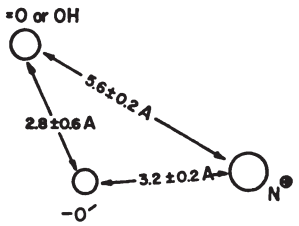

Figure 1. The first published receptor pattern (i.e. pharmacophore) for muscarinic agonists. Reprinted with permission: from Lemont B. Kier, Molecular Orbital Calculation of Preferred Conformations of Acetylcholine, Muscarine, and Muscarone, *Mol. Pharmacol.* **1967,** 3, 487–494.

A pharmacophore is an ensemble of steric and electronic features that is necessary to ensure the optimal supramolecular interactions with a specific biological target structure and to trigger (or block) its biological response. However, it should not be regarded as a molecule or set of functional groups, but a more abstract concept that is a common denominator shared by a group of active molecules.[5]

The pharmacophore concept grew over the decades following Kier's pioneering work and it was adapted for virtual screening applications (*e.g.*, Catalyst, Phase) which use a pharmacophore query to search a three-dimensional compound library.[6] Pharmacophores are now widely used by scientists who study structure-activity relationships to give them insight in how a molecule's three-dimensional properties give rise to that SAR.

2.1.1 AnchorQuery

Recently, AnchorQuery was introduced as specialized pharmacophore search technology to facilitate the rational design of small molecules targeting protein-protein interactions (PPIs).[7] The challenge with PPIs is, however, that they exhibit large, flat contact surfaces that lack the grooves and pockets present at the surfaces of proteins that bind small molecules. Therefore, the design of de novo molecules or the

use of high–throughput screening is rather limited. On the other hand PPIs tend to have hotspot residues; those residues are important for a particular PPI, make up less than half of the contact surface, and are generally found near the center of the PPI.[8]

AnchorQuery, an inexpensive and user-friendly software, utilizes those deeply buried hotspot residues, required for molecular recognition, as anchor and the technology is able to combine the advantages of ligand-based virtual screening, docking, and pharmacophore-based searches.[7,9] Unlike other software, AnchorQuery is leveraging more than thirty-one million compounds with a preformed two billion conformer space of low molecular weight compounds easily accessible by multicomponent reaction (MCR) chemistry.[10] Although, the anchor is the same in all the results, the scaffold of which it is part of is different and allows for easy scaffold hopping when a particular scaffold is not active towards the PPI. Until now the AnchorQuery software was mainly applied to design antagonists of the protein-protein interaction between p53 and MDM2 using a deeply buried tryptophan as anchor and template.[11] Multiple active scaffolds containing an indole moiety mimicking the trypthophan, one of four hotspot residues, were discovered and validated by cocrystal structures.[12–17] In this research it was the first time that AnchorQuery was applied to a small-molecule-protein interaction.

2.1.2 AnchorQuery design of novel PIF pocket modulators

The starting points for the discovery were the cocrystal structures of the known small molecule PS48 and PS114 in the PIF pocket of PDK1.[18,19] The ligand was loaded in AnchorQuery which, in both cases, automatically proposed the deeply buried phenyl group as the highest energy contributing fragment of the molecule, and as anchor for drug design (Figure 2).

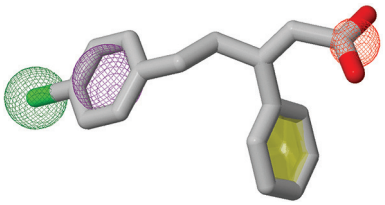

Figure 2. The phamacophore from AnchorQuery. Color code: Phenyl anchor (yellow), Second aromatic phenyl ring (purple), Negative ion (red), Hyrophobic region (green).

Further analysis of the crystal structure revealed that the carboxylic acid of PS48 and PS114 formed multiple hydrogen bonds and charge-charge interactions to

Lys76 and Arg131 of the receptor. Finally, the second aromatic group resided on a hydrophobic, but solvent exposed patch of amino acids forming a rather flat pocket. Next, the receptor was loaded and the pharmacophore queried against the virtual library. The results were ranked according to pharmacophore match (*i.e.*, number of pharmacophore points identical to the pharmacophore), but could be ranked according to molecular weight, root-mean-square deviation (RMSD), or rotatable bonds as well. The results were downloaded and an energy minimization was performed using Moloc.[20,21]

Amongst the top results from the pharmacophore search on PS48 were several different MCR scaffolds including Ugi, van Leusen, and Castagnoli. The Castagnoli

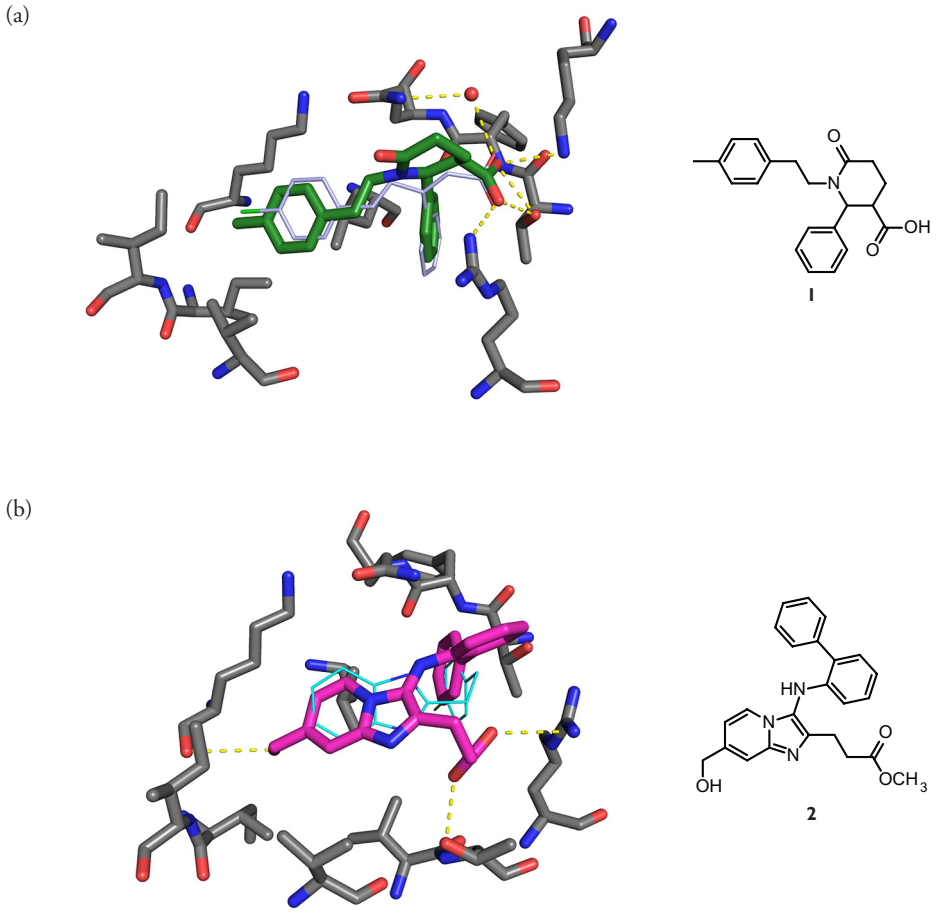

Figure 3. Superimposition of the proposed energy-minimized AnchorQuery result of (a) the template PS48 (PDB ID: 3HRF) with the Castagnoli scaffold and (b) the template PS114 (PDB ID: 4A06) with the GBB scaffold. Color code: Residues lining the PIF pocket (grey sticks), Castagnoli scaffold (green sticks), PS48 (teal lines), GBB scaffold (green sticks, PS114 (cyan lines).

scaffold **1** (Figure 3a) was chosen because it had several advantages over the other scaffolds: first, there was no need for starting material synthesis (*i.e.*, isocyanide), second, has a non-flat 3D-structure and therefore would be less likely to bind in the adenosine triphosphate binding site, and third exhibits a certain structural rigidity due to the δ-lactam core. From the pharmacophore search on PS114 the Groebke-Blackburn-Bienaymé (GBB) scaffold **2** (Figure 3b) was selected, because of similar reasons; a non-flat, rigid molecule and only the aldehyde and isocyanide have to be prepared according to known procedures.

2.2 Scaffold 1: Castagnoli

The Castagnoli (or Castagnoli-Cushman) reaction is the addition of imines to cyclic anhydrides described for the first time by Neal Castagnoli Jr. (Scheme 1).[22] These chemical structures are prevalent motifs present in natural products and synthetic pharmaceuticals and the reaction is in general carried out in non-polar solvents like toluene or xylene. Mechanistically it starts with condensation of the aldehyde and amine to form the imine, which then condenses with the cyclic anhydride.[23,24]

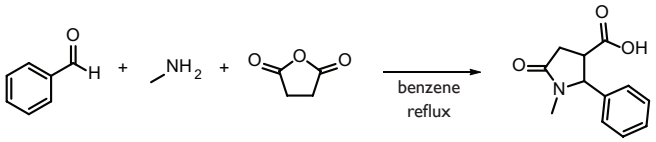

Scheme 1. The first Castagnoli reaction.

2.2.1 Synthesis of the Castagnoli scaffold

Scaffold **1** was proposed amongst the top results of the AnchorQuery search and can be synthesized from benzaldehyde (**3**), 2-(*p*-tolyl)ethylamine (**4**), and glutaric anhydride (**5**) (Scheme 2). Although the reaction can be performed in one step, pre-formation of the imine is desired to obtain satisfactory yields. One of the side reactions that could occur is acylation of the amine with the cyclic anhydride, thus reducing the conversion towards the product. Moreover, the side product is a carboxylic acid too, hence, difficult to separate from the Castagnoli product.

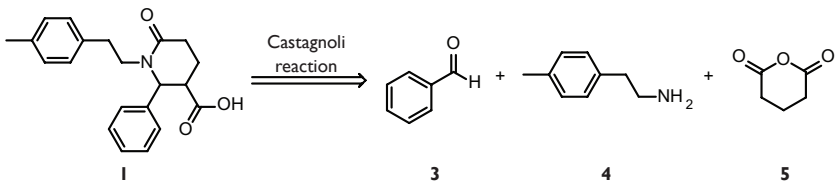

Scheme 2. Retrosynthetic pathway for the Castagnoli compound **1**.

Synthesis of compound **1** was achieved by stirring benzaldehyde (**3**) and 2-(*p*-tolyl)ethylamine (**4**) in CH_2Cl_2 with $MgSO_4$ as water scavenger overnight followed by a solvent switch to *p*-xylene. Glutaric anhydride (**5**) was added and the reaction was stirred at reflux for six hours (Scheme 3).

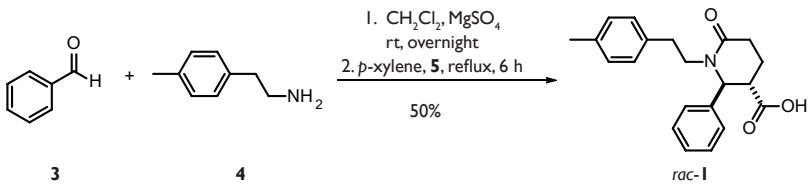

Scheme 3. Synthesis of the AnchorQuery proposed Castagnoli compound **1**.

Upon cooling, the product precipitated, which was conveniently collected by filtration from the reaction mixture. The thermodynamically favored *trans*-isomer was obtained in accordance with previously observed results, however, as a racemate.[25] A number of other Castagnoli compounds were synthesized under the same reaction conditions with satisfactory yields (Table 1) and with these few compounds the kinase activity was tested.

Table 1. Synthesis of a number of Castagnoli compounds.

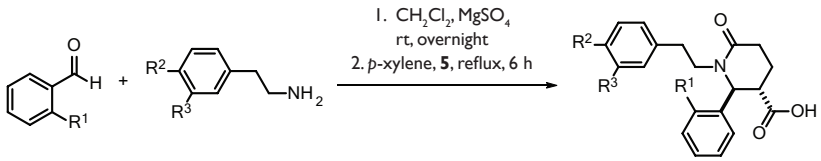

Compound	R^1	R^2	R^3	Yield (%)[a]
rac-**6**	H	H	Cl	42
rac-**7**	H	Cl	H	47
rac-**8**	Cl	Cl	H	58

[a] Isolated yield.

2.2.2 Biochemical activity

To gain insight in the ability of the Castagnoli scaffold to modulate the activity of PDK1, a kinase activity assay was performed. Different concentrations of the compounds were incubated with PDK1, the substrate T308tide, and [γ-^{32}P]ATP after which the activity was determined with a phosphorimager.[26,27] The Castagnoli scaffold indeed was able to activate PDK1 with the original proposed AnchorQuery compound *rac*-**1** activating up to fourfold (Table 2). The 2-(4-chlorophenyl)ethyl side chain in *rac*-**7** appeared slightly more active than the 2-(3-chlorophenyl)ethyl side chain in *rac*-**6**, moreover, substitution in the 2-position of the aldehyde component to chloro, *rac*-**8**, further improved the ability to activate PDK1.

Table 2. *In vitro* influence of Castagnoli compounds on PDK1 activity.

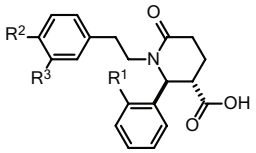

Compound	R^1	R^2	R^3	2 μM^a (%)^b	50 μM^a (%)^b	200 μM^a (%)^b
rac-**1**	H	CH_3	H	189	418	442
rac-**6**	H	H	Cl	88	162	218
rac-**7**	H	Cl	H	116	291	301
rac-**8**	Cl	Cl	H	186	430	545

^{a} Concentration small molecule. ^{b} Average activity of experiments performed in duplicate.

2.2.3 Evaluation of the structure-activity-relationship (SAR)

After identification of the Castagnoli scaffold as a PDK1 modulator the structure-activity relationship was evaluated by preparing a library of compounds ,by changing the amine or aldehyde component, to further improve this scaffold. The synthesis was accomplished by preforming the imine in the microwave followed by the addition of the cyclic anhydride and refluxing in *p*-xylene for six hours. In general, moderate to good yields were obtained and all products were obtained as solids (Table 3). In several cases lower yields were obtained, in these cases imine formation could be incomplete or the imine reversed back to the starting materials. Then the amine could be acetylated with the cyclic anhydride, therefore, reducing the yield.

Table 3. Castagnoli library synthesis for the SAR.

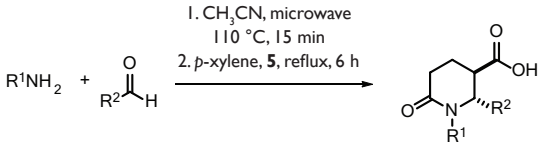

Compound	R^1	R^2	Yield[a]
rac-**9**	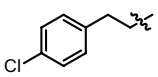		43
rac-**10**	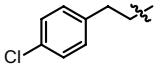		24
rac-**11**	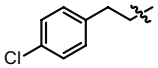		40
rac-**12**	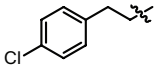		45
rac-**13**	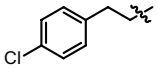	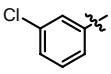	31
rac-**14**	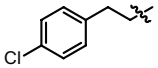	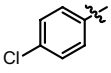	38
rac-**15**	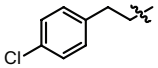	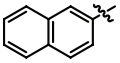	67
rac-**16**	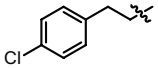		31
rac-**17**	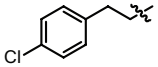		22
rac-**18**	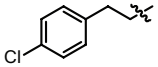		46
rac-**19**	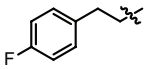		31

[a] Isolated yield.

Compound	R^1	R^2	Yield[a]
rac-**20**	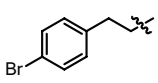		65
rac-**21**	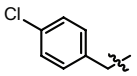		20
rac-**22**	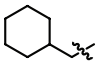		14
rac-**23**			31
rac-**24**	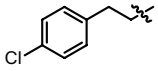	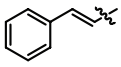	33

[a] Isolated yield.

Synthesis of Castagnoli derivatives

In the introduction it was already mentioned that a carboxylic acid functionality was necessary for good PDK1 modulation, nevertheless, other Castagnoli derivatives lacking the carboxylic acid were synthesized to gain an insight in the influence of the functional group for this particular scaffold. Initially, to obtain the ester of *rac*-**8** a Fischer esterification was performed, however, this resulted in opening of the lactam ring. Fortunately, activation of *rac*-**8** to the acyl chloride was achieved with thionyl chloride and subsequent esterification with methanol resulted in the formation of ester *rac*-**25** in 74% yield (Scheme 4).

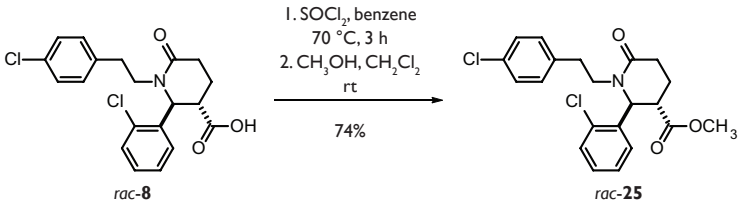

Scheme 4. Synthesis of the ester derivative *rac*-**25**.

To investigate the effect of the separate enantiomers of *rac*-**8** the ester *rac*-**25** was subjected to preparative chiral SFC, which failed on compound *rac*-**8**, to separate the two enantiomers. The separate enantiomers of *rac*-**25** were hydrolyzed

to the corresponding carboxylic acids and obtained in moderate yield to excellent yield with excellent enantiomeric excesses (Scheme 5). The absolute configuration was assigned after the single crystal X-ray structure of (*S*,*S*)-**8** was obtained (Figure 4).

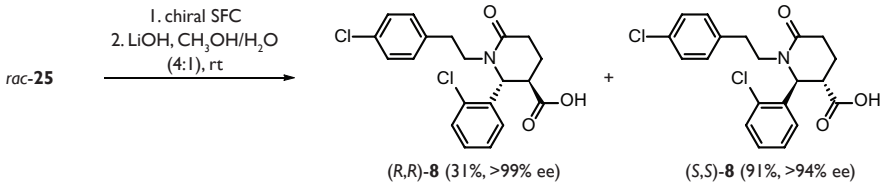

Scheme 5. Chiral separation and hydrolysis of *rac*-**25**.

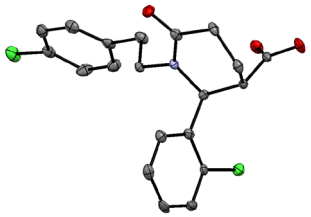

Figure 4. Single crystal X-ray structure of (*S*,*S*)-**8**. Hydrogen atoms are omitted for clarity.

The other carboxylic acid derivative we wanted to synthesize was the primary amide *rac*-**26**, which was prepared by activating the acid *rac*-**8** with 1,1'-carbonyldiimidazole (CDI) in DMF. Subsequent addition of ammonium carbonate and heating at 70 °C for two days gave the amide in 82% yield (Scheme 6).

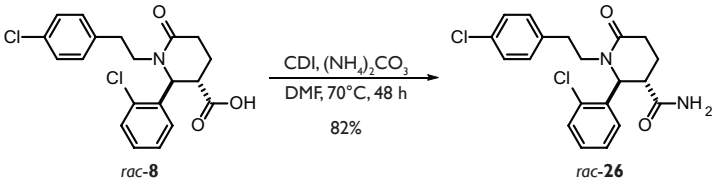

Scheme 6. Synthesis of *rac*-**26**.

Recently, the cocrystal structure of PIFtide in the PIF pocket was reported which showed that part of PIFtide bound to a shallow area adjacent to the PIF pocket.[28] Therefore, we wanted to extend the Castagnoli scaffold towards this area

by making the 2-phentylethyl amide derivative of *rac*-**8** (Scheme 7). The amide *rac*-**27** was prepared in moderate yield (62%) according to the protocol used for *rac*-**25**, however, using 2-phenethylamine as the nucleophile. To examine if a bioisostere of the carboxylic acid was active towards PDK1 we decided to synthesize the tetrazole derivative, which is conveniently obtained from the primary amide *rac*-**26**. Dehydration of the amide to the nitrile *rac*-**28** was achieved with phosphorous oxychloride in good yield (80%); subsequent cycloaddition with sodium azide resulted in the formation of the tetrazole derivative *rac*-**29**, unfortunately, in 25% yield (Scheme 8). Finally, the lactam ring size was reduced from six to five by performing the Castagnoli reaction with succinic anhydride. Reaction of 2-(4-chlorphenyl) ethylamine (**30**) with 2-chlorobenzaldehyde (**31**) and succinic anhydride resulted in the formation of *rac*-**32** in moderate yield (43%, Scheme 9).

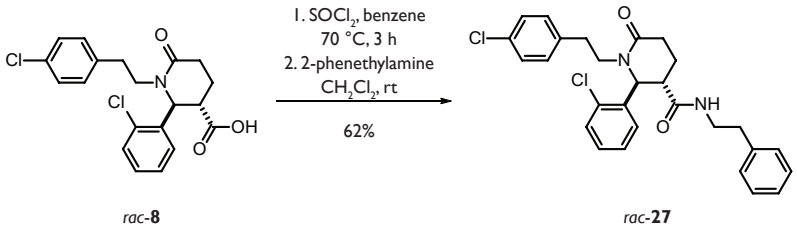

rac-**8** *rac*-**27**

Scheme 7. Synthesis of *rac*-**27**.

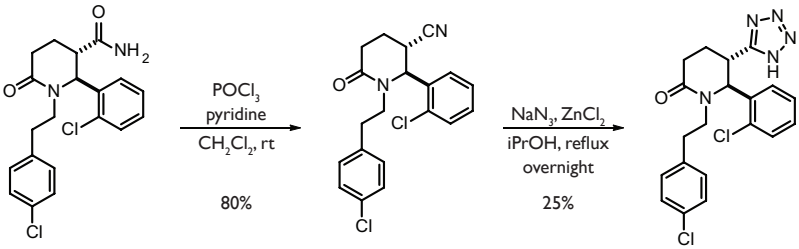

rac-**26** *rac*-**28** *rac*-**29**

Scheme 8. Synthesis of *rac*-**29**.

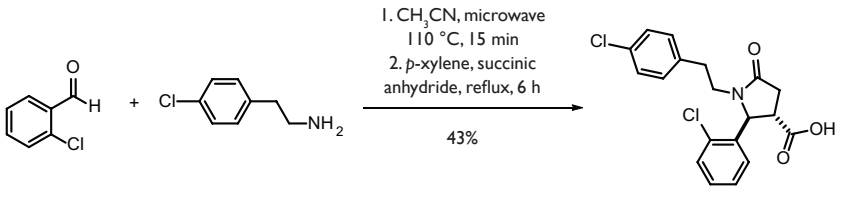

30 **31** *rac*-**32**

Scheme 9. Synthesis of *rac*-**32**.

2.2.4 Alphascreen

To assess the SAR, the compounds were tested in an Alphascreen interaction-displacement assay. PIFtide, the C-terminal sequence of PRK2, has vastly higher affinity than the hydrophobic motif sequences derived from other substrates,[29] however, the majority of the Castagnoli compounds were able to fully disrupt its high–affinity interaction with PDK1 (Table 4).

Table 4. Displacement of the PIFtide-PDK1 interaction.

Compound	IC_{50} (μM)	95% CI (μM)[a]	Compound	IC_{50} (μM)	95% CI (μM)[a]
rac-**6**	41	33–51	*rac*-**17**	nd	
rac-**27**	43	36–52	*rac*-**18**	26	15–46
rac-8	11	9.9–12	*rac*-**19**	26	22–31
(*R*,*R*)-**8**	7.0	6.1–8.0	*rac*-**20**	8.1	7.0–9.3
(*S*,*S*)-**8**	15	13–17	*rac*-**21**	nd[b]	
rac-**9**	28	22–36	*rac*-**22**	nd[b]	
rac-**10**	8.5	7.9–9.2	*rac*-**23**	nd[b]	
rac-**11**	9.4	7.9–11	*rac*-**24**	32	28–37
rac-**12**	42	38–47	*rac*-**25**	40	31–52
rac-**13**	21	17–26	*rac*-**26**	nd[b]	
rac-**14**	29	23–37	*rac*-**27**	nd[b]	
rac-**15**	5.6	5.1–6.3	*rac*-**29**	22	16–30
rac-**16**	7.8	5.5–11	*rac*-**32**	17	14–20

[a] 95% CI = 95% confidence interval. [b] nd = no displacement.

There is an indication of halogen bonding in the phenylethyl side chain, with chloro (*rac*-**8**, 11 μM) and bromo (*rac*-**20**, 8.1 μM) being more potent than the fluoro counterpart (*rac*-**19**, 26 μM) that is not capable of halogen bonding.[30] Shortening of the linker at the δ-lactam nitrogen from phenethyl to benzyl, or replacing it with an aliphatic *tert*-butyl group eliminated the ability to replace PIFtide. The aldehyde component favored a phenyl ring with substitution in the 2-position, the most potent substituents were chloro (*rac*-**8**, 11 μM) and bromo (*rac*-**10**, 8.5 μM), both displaying around threefold better potency than fluoro (*rac*-**9**, 28 μM). Also methyl (*rac*-**11**, 9.4 μM) was favored, whereas, heteroaromatic replacements displayed no or less potency (*rac*-**17** and *rac*-**18**, respectively). Additionally, employing 2-naphthaldehyde or 1-naphthaldehyde resulted in the most potent compounds *rac*-**15** (5.6 μM) and *rac*-**16** (7.8 μM, Figure 5). Moreover, an aliphatic group reduced the ability to displace PIFtide entirely. The carboxylic acid moiety was favored, whereas, the analogous ester

derivative and tetrazole bioisostere were less potent (*rac*-**25**, 40 μM; *rac*-**29**, 22 μM) and the primary amide (*rac*-**26**) was not able to displace PIFtide at all. Extending the scaffold towards the shallow area adjacent the PIF pocket did not show any displacement (*rac*-**27**). Finally, *rac*-**8** showed good potency, separation of the two enantiomers by chiral SFC illustrated a difference between the two enantiomers; (*R*,*R*)-**8** (7.0 μM) was twofold more potent than (*S*,*S*)-**8** (15 μM) for displacing the PDK1-PIFtide interaction. Such difference may be due to the off–rate by (*R*,*R*)-**8**, a feature that is more relevant for the displacement of PIFtide from PDK1. These results showed that the Castagnoli scaffold displaces PIFtide with higher potency than, for example, the currently best compound PS210 (20 μM)[31] and is amongst the most potent compounds described.

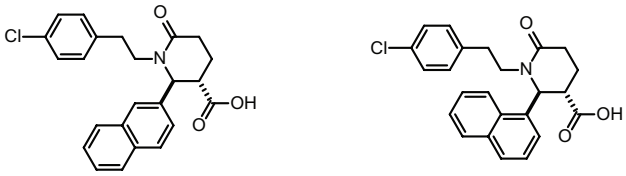

rac-**15** *rac*-**16**

Figure 5. The most potent Castagnoli compounds, *in vitro*.

2.2.5 *In vivo* inhibition of S6K

A small selection of Castagnoli compounds were tested *in vivo* by overnight serum starvation of HEK293 cells followed by incubation (4 hours) with the compounds (10 μM). Then the cells were stimulated with IGF-1, lysed after 30 min, and a western blot analysis was performed (Figure 6). Although, the Alphascreen showed that the majority of the Castagnoli compounds were potent modulators, the *in vivo* test showed that the large part of the compounds were not able to appreciatively inhibit the phosphorylation of S6K compared to RS1 or GSK (a). Perhaps the carboxylic acid moiety prevents the compounds from entering the cells and, therefore, no inhibition is observed. In the phosphorylation of PKB no effect was observed (Figure 6b), which is due to the mechanism of phosphorylation; no PIF pocket binding is required (Section 1.4). Finally, the amide compound *rac*-**27** was tested at different concentrations compared to RS1, while there is a concentration dependent inhibition of S6K, it is not as potent as RS1. That *rac*-**27** is active most likely arises from intracellular amide cleavage by a protease, resulting in the active compound *rac*-**8** (Figure 6c).

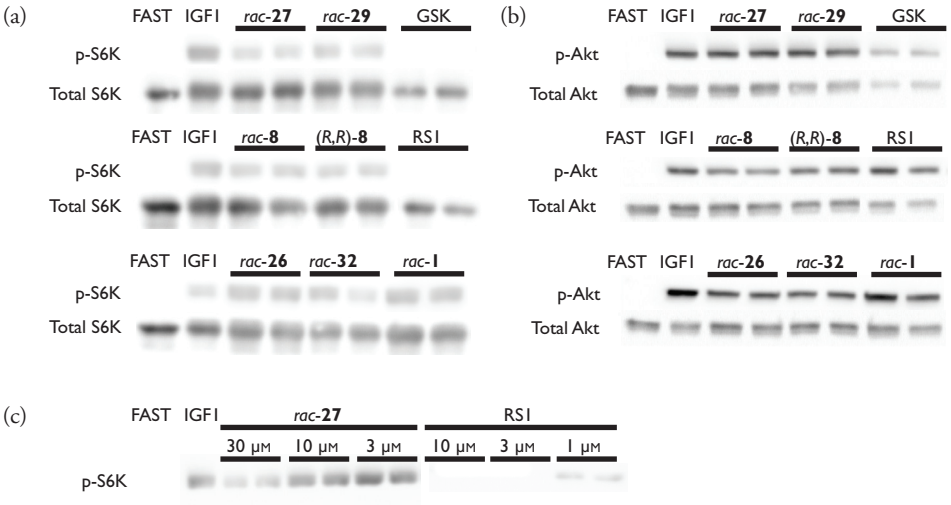

Figure 6. The immunoblots show the effects of the Castagnoli compounds on the PDK1 signaling pathway compared to RS1[28] and GSK2334470[32] (GSK). HEK293 cells were treated with 10 µM of the different compounds and stimulated with IGF-1 30 min prior to lysis. Western blots were probed with antibodies against (a) phosphor-S6K and (b) phosphor-PKB/Akt. The blots were reprobed with antibodies against the total amount of the S6K and PKB/Akt as loading control. (c) HEK293 cells were treated with different concentrations of *rac*-**27** and RS1 and stimulated with IGF-1 30 min prior to lysis, and western blotting using antibodies against phospho-S6K.

2.2.6 Binding mode of the Castagnoli scaffold

In order to elucidate the structural mode-of-action of this scaffold, a cocrystal structure of *rac*-**8** with PDK1 was obtained, solved to 1.24 Å resolution. Different to previous crystal structures in complex with small molecules, Lys76 is invisible due to side-chain movement. Interestingly, both enantiomers of *rac*-**8** cocrystallized in the structure with a ratio of approximately 1:1. The receptor-ligand interactions are dominated by hydrophobic contacts, electrostatic, and halogen bonding (Figure 7).[30,33]

In both molecules the 2-chloro phenyl represents the anchor deeply buried in the pocket equally to PS48.[18] The orientation, however, of the 2-chloro phenyl substituent is different in the two enantiomers. Whereas in the structure of the (*S*,*S*)-**8** isomer the 2-chloro substituent is forming a short contact (3.2 Å) to the backbone carbonyl oxygen of Phe149, it is turned by ≈180° in the other enantiomer. The carboxyl moiety of the (*R*,*R*)-**8** isomer appears to displace the usual conformation of the Arg131 head group in the crystal structure, nonetheless, a charge-charge interaction would be feasible with different conformations of Arg131. The different orientation of the other enantiomer precludes this interaction. Instead the (*S*,*S*)-**8**

isomer carboxyl forms hydrogen bonds with the Gln150 side chain amide, and the Thr148 hydroxyl, and a water–mediated hydrogen bond to Phe149. The δ-lactam carbonyl oxygen from (*R,R*)-**8** forms an additional hydrogen bond with Gln150. In both enantiomers the 4-chlorophenylethyl side chain displays hydrophobic interactions with Leu155, Ile118, Ile119 Lys115, Val127, and, additionally, a halogen bond to the backbone carbonyl oxygen of Lys115.

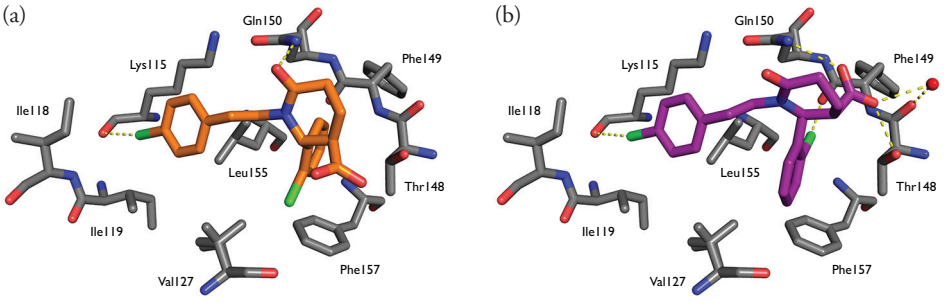

Figure 7. Crystal structure of *rac*-**8** in the PIF pocket of PDK1 with (left) (*R,R*)-**8** and (right) (*S,S*)-**8**. Color code: residues within 4 Å (grey sticks), (*R,R*)-**8** (orange sticks), (*S,S*)-**8** (purple sticks).

2.2.7 Selectivity

All AGC kinases have a pocket similar to the PIF pocket and therefore selectivity can be challenging. To investigate the selectivity, a kinase profiling was performed, which showed no significant activity (activity ~100%) for any of the fifty tested kinases that provide a representative sample of the human kinome (Table 5). However, this particular kinase profiling is performed with PDKtide, a construct of PIFtide and T308tide.[34] Although the compound tested showed low micromolar affinity for the PIF pocket it was probably not sufficient to displace PDKtide from the kinase and hence did not show appreciative selectivity.

Table 5. Kinase profiling study of compound *rac*-**8**.

Kinase[a]	Activity (%)[b]	SD[c]	Kinase[a]	Activity (%)[b]	SD[c]
MKK1	94	13	CK2	110	4
JNK1	102	7	DYRK1A	97	0
p38a MAPK	96	7	NEK6	103	1

[a] Most kinases were assayed at a concentration of ATP at or below the calculated K_m for that kinase.
[b] Kinase activity tested with *rac*-**8** (10 μM). c Standard deviation.

Kinase[a]	Activity (%)[b]	SD[c]	Kinase[a]	Activity (%)[b]	SD[c]
RSK1	122	8	TBK1	106	5
PDK1	100	5	PIM1	102	0
PKBα	110	5	SRPK1	112	3
SGK1	101	5	EF2K	85	5
S6K1	93	11	HIPK2	96	7
PKA	110	3	PAK4	111	0
ROCK 2	111	3	MST2	119	12
PRK2	110	4	MLK3	100	1
PKCα	105	8	TAK1	103	8
PKD1	107	7	IRAK4	103	6
MSK1	98	2	RIPK2	115	2
CAMKKβ	106	6	TTK	106	9
CAMK1	102	2	Src	108	6
SmMLCK	101	1	Lck	103	12
CHK2	95	20	BTK	104	3
GSK3β	99	2	JAK2	102	5
PLK1	99	2	SYK	86	17
Aurora B	97	0	EPH-A2	118	13
LKB1	104	0	HER4	102	16
AMPK (hum)	100	4	IGF-1R	80	2
MARK3	107	13	TrkA	76	0
CK1δ	94	3	VEG-FR	99	7

[a] Most kinases were assayed at a concentration of ATP at or below the calculated K_m for that kinase.
[b] Kinase activity tested with *rac*-**8** (10 μM). c Standard deviation.

2.3 Scaffold 2: Groebke-Blackburn-Bienaymé

In 1998, three groups led by Katrin Groebke, Cristopher Blackburn, and Hugues Bienaymé independently discovered that aldehydes, 2-aminoazines and isocyanides reacted together to form fused 3-aminoimidazole derivatives (Scheme 10).[35–37] The reaction is generally performed in methanol and catalyzed by both Brønsted and Lewis acids. Mechanistically the reaction is initiated by the condensation of the aldehyde with the amine and the resulting imine is involved in a nonconcerted [4+1] cycloaddition. Finally, a 1,3-protonshift leads to the formation of the Groebke-Blackburn-Bienaymé scaffold.[38]

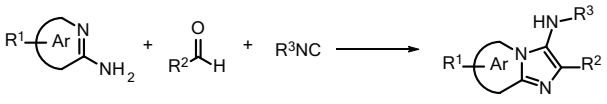

Scheme 10. The Groebke-Blackburn-Bienaymé reaction.

2.3.1 Synthesis of starting materials

Formylation of commercial available 2-aminobiphenyl (**33**) was achieved with zinc oxide in formic acid and the *N*-formylated product **34** was obtained in 83% yield.[39] Subsequent formation of isocyanide **35** was performed under standard dehydrating conditions in 68% yield (Scheme 11a).[40] The required aldehyde **37** was obtained by catalytic hydrogenation of the corresponding commercially available acyl chloride **36** in 86% yield (Scheme 11b).[41]

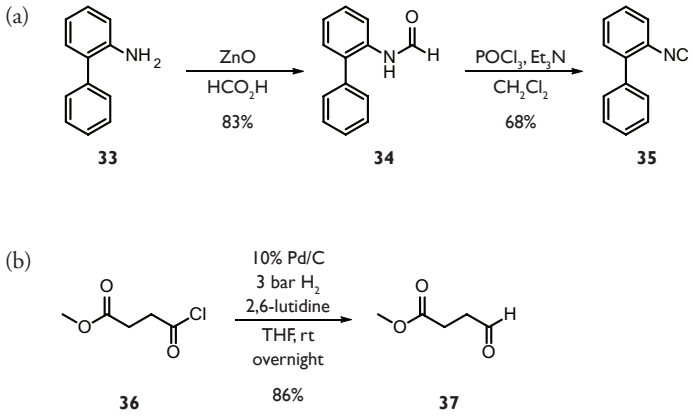

Scheme 11. Starting material synthesis of (a) 2-isocyanobiphenyl (**35**) and (b) methyl 4-oxobutanoate (**37**).

2.3.2 Synthesis of the Groebke–Blackburn–Bienaymé scaffold

First a screening for the optimal reaction conditions to perform the GBB reaction was carried out (Table 6). Initial results showed that scandium(III) triflate (63% yield) outperformed zirconium chloride (52% yield) and perchloric acid (48% yield) in the reaction of aldehyde **37** with 2-aminopyridine (**38**) and 2-isocyanobiphenyl (**35**) to form imidazo[1,2-*a*]pyridine **39**. Although scandium(III) triflate is more expensive than the other two, it was chosen as catalyst for further GBB reactions.

Afterwards, a small set of compounds were synthesized according to the protocol obtained with the test reaction (Table 7). The yields of compounds **40** and **41** were comparable with the test reaction, however, the reactions with acetaldehyde gave the GBB products **42** and **43** in significant lower yields which was probably the consequence of the high volatility of acetaldehyde. Perhaps, to limit evaporation of acetaldehyde, the reaction should be performed at lower temperature or a small

excess of acetaldehyde could be used to obtain satisfactory yields.

Table 6. Catalyst screening for the GBB reaction.

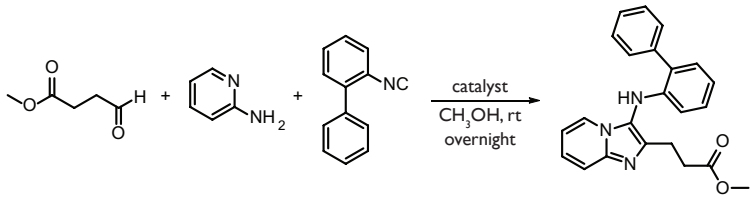

37 **38** **35** **39**

Catalyst	Loading (mol%)	Yield[a]
$ScOTf_3$	5	63
$ZrCl_4$	5	52
$HClO_4$	10	48

[a] Isolated yield.

Table 7. Synthesis of a small set of GBB compounds.

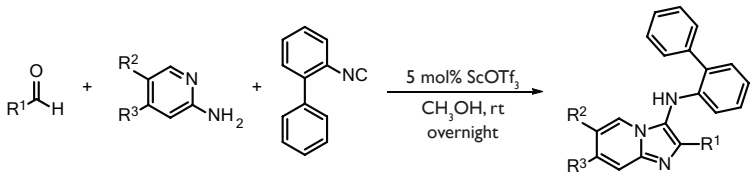

Compound	R^1	R^2	R^3	Yield[a]
40	$(CH_2)_2CO_2CH_3$	H	Cl	57
41	$(CH_2)_2CO_2CH_3$	Cl	H	61
42	CH_3	H	Cl	37
43	CH_3	Cl	H	33

[a] Isolated yield.

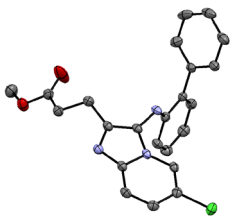

Figure 8. Single crystal X-ray structure of **41**. Hydrogens atoms omitted for clarity.

An X-ray crystal structure of compound **41** clearly showed a perpendicular orientation of the biphenyl side chain with the imidazo[1,2-*a*]pyridine core as well as a perpendicular rotation between the two phenyl groups (Figure 8).

The ester compounds **40** and **41** were hydrolyzed with lithium hydroxide to the corresponding carboxylic acids **44** and **45** in moderate yield (Scheme 12); the carboxylic acids tend to be more active towards the PIF pocket.

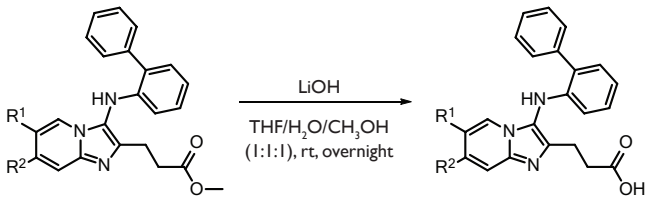

Scheme 12. Synthesis of the carboxylic acid derivatives **44** and **45**.

2.3.3 Biochemical activity

For the GBB scaffold the same kinase activity assay was performed as described for the Castagnoli scaffold (see Section 2.2.2). Surprisingly, these compounds appear to inhibit PDK1 activity, however, there are two reasons why this inhibition could be observed (Table 8).

Table 8. *In vitro* influence of GBB compounds on PDK1 activity.

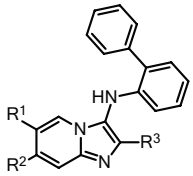

Compound	R^1	R^2	R^3	2 μM (%)[ab]	50 μM (%) [ab]	200 μM (%)[ab]
40	H	Cl	$(CH_2)_2CO_2CH_3$	80	71%	37
41	Cl	H	$(CH_2)_2CO_2CH_3$	56	47	41
42	H	Cl	CH_3	91	106	104
43	Cl	H	CH_3	81	100	95
44	H	Cl	$(CH_2)_2CO_2H$	81	89	35
45	Cl	H	$(CH_2)_2CO_2H$	100	102	52

[a] Concentration small molecule. [b] Average activity of two experiments.

First, although the three–dimensional structure showed a non-flat relationship between the biphenyl side-chain and the imidazopyridine core in the X-ray structure, there could be the possibility that the compounds bound in the ATP binding site and prevent ATP from binding, therefore, inhibiting the phosphorylation of T308tide. Second, there is not a clear linear correlation between the concentration and the activity, therefore, most likely an artifact was observed. To investigate this, kinetic studies that monitor ATP consumption have to be performed to ratify binding to the ATP binding site.

2.4 Conclusions and outlook

AnchorQuery is a powerful tool for the design of novel scaffolds that target protein-protein interactions, moreover, here the first application for a protein-small molecule interaction is described resulting in two scaffolds, the Castagnoli and the Groebke-Blackburn-Bienaymé.

The Castagnoli scaffold was selected for further research, while the GBB scaffold showed inhibition in the performed kinase activity assay, it was concluded that more detailed investigation is needed to confirm these results. The initial Castagnoli compounds showed up to fivefold activation (at 200 μM) and the structure-activity-relationship was evaluated by synthesizing a library of Castagnoli compounds. The ability of the compounds to displace the high-affinity interaction between PDK1 and PIFtide was tested with an Alphascreen and the majority of the compounds were able to fully disrupt this interaction. The most potent compound rac-**15** (IC_{50} = 5.6 μM) is amongst the most potent described so far.

Unfortunately, the Castagnoli scaffold was not able to in vivo inhibit the phosphorylation of S6K, most likely the carboxylic acid moiety prevents the compounds from entering the cell. Although, *rac*-**27** showed a concentration dependent inhibition of S6K, full inhibition was not achieved.

A cocrystal structure was obtained for PDK1 and one of the more potent Castagnoli compounds, surprisingly, both enantiomers were present in the PIF pocket. Moreover, the overall binding mode showed a good resemblance with the original, energy minimized, AnchorQuery result.

Although, these compounds showed good modulating activities towards PDK1, several hurdles remain. First, a carboxylic acid moiety is still present in these compounds, therefore, most likely exhibiting poor pharmacokinetic properties and strategies to improve this (e.g., bioisostere) were not as potent as the carboxylic acid counterpart. Second, to obtain more potent compounds and perhaps some selectivity the scaffolds should be extended towards the shallow area that was present in the cocrystal structure between PDK1 and PIFtide. Two strategies can be applied to

achieve this; extend the current Castagnoli scaffold towards this area by synthesizing more derivatives or use this crystal structure in AnchorQuery and design new scaffolds (Figure 9).

When more potent compounds (nM) can be designed for the PIF pocket it remains an interesting target as PDK1 plays such an pivotal part in the activation of other AGC kinases, moreover, these kinases play crucial roles in cellular processes and dysregulation has major consequences.

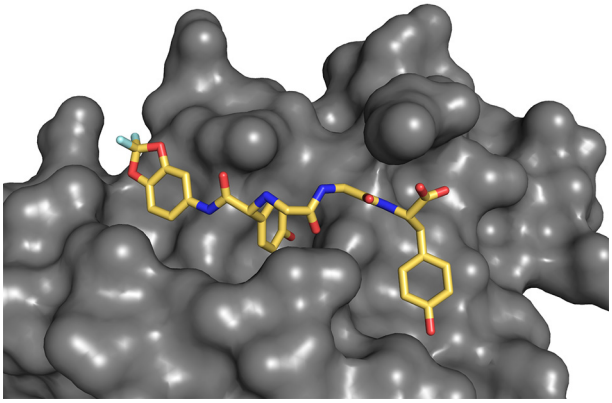

Figure 9. Potential new scaffold designed with AnchorQuery interacting with the shallow area next to the PIF pocket. Color code: PDK1 (grey surface), AnchorQuery result (gold sticks).

2.5 Experimental section

General remarks

Reagents were available from commercial suppliers and used without any purification unless otherwise noted. Solvents were dried according to standard procedures and moisture sensitive reactions were performed under nitrogen. Thin layer chromatography was performed on Merck TLC silica gel 60 F_{254}. Column chromatography was performed on a Grace Reveleris X2 or Teledyne Isco Combiflash R_F using silica gel columns with petroleum ether/ethyl acetate or dichloromethane/methanol as eluent. Melting points were measured on an Electrothermal IA8103 melting point apparatus. IR was recorded on a Thermo Scientific Nicolet 380 FT-IR. Nuclear magnetic resonance spectra were recorded on a Bruker Avance 500 spectrometer. Chemical shifts for ^{1}H NMR were reported relative to TMS (for $CDCl_3$, δ 0 ppm) or internal solvent (DMSO-d_6 δ 2.50 ppm, CD_3OD δ 3.31 ppm or D_2O δ 4.79 ppm) and coupling constants (*J*) were in hertz (Hz). The following abbreviations were used for spin multiplicity: s = singlet, d = doublet, t = triplet, q = quartet, m = multiplet, br. = broad, or combinations thereof (*e.g.*, dd = doublet of doublets). Chemical shifts for ^{13}C NMR were reported in ppm relative to the solvent peak ($CDCl_3$ δ 77.23 ppm, DMSO-d_6 δ 39.52 ppm, CD_3OD δ 49.00 ppm). Mass spectra were measured on a Waters Investigator Supercritical Fluid Chromatograph with a 3100 MS Detector (ESI) using a solvent system of methanol and CO_2 on either a Viridis 2-ethyl pyridine column (4.6 × 250 mm, 5 μm particle size) or a Viridis silica gel column (4.6 × 250 mm, 5 μm particle size) and reported as (*m*/*z*). Analytical chiral SFC was performed on a Reprosil Chiral-AM column (4.6 × 250 mm, 5 μm) and semi-preparative SFC was performed with a stacked injector (25 μL injections) on a Reprosil Chiral-AM column (10 × 250 mm, 5μm) with 30% MeOH/CO_2 as mobile phase.

Molecular biology techniques were performed using standard protocols The polypeptides used were synthesized by JPT Peptide Technologies GmbH. PIFtide (Biotin-REPRILSEEEQEMFRDFDYIADWC) is derived from the C-terminal 24 amino acids of the PDK1 substrate PRK2. The antibodies for the cell experiments were purchased from Cell Signaling. The outsourced kinase profiling was performed by the International Centre for Kinase Profiling (MRC Protein Phosphorylation unit, University of Dundee, Scotland).

Compounds **34**,[39] **35**,[40] and **37**[41] were synthesized according to literature procedures and the spectral data were consistent with those reported in literature.

General procedure for the Castagnoli reaction:

A solution of aldehyde (1.0 mmol) and amine (1.0 mmol) in acetonitrile (1 mL, 1.0 M) was heated in the microwave at 110 °C for 15 min. The reaction was concentrated *in vacuo* and to the residue was added *p*-xylene (2 mL, 0.5 M) and glutaric anhydride (114 mg, 1.0 mmol). The resulting reaction mixture was heated at reflux for 6 h. Upon cooling, to room temperature, the product precipitated from solution. The solid was collected by filtration, washed with ice-cold ether (3 × 5 mL) and dried. Products were recrystallized from acetonitrile or an alcoholic solvent (methanol, ethanol, or isoporpanol). The reaction diastereoselectively gives the *trans*-product, however, as a racemate.

***rac*-1-(4-Methylphenethyl)-6-oxo-2-phenylpiperidine-3-carboxylic acid (*rac*-1)**

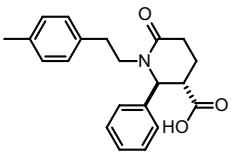

Obtained from benzaldehyde (102 μL) and 2-(*p*-tolyl) ethylamine (145 μL) as a white solid (170 mg, 0.50 mmol, 50%). Melting point: 194 °C; ^{1}H NMR (500 MHz, $CDCl_3$) δ 7.37 (t, *J* = 7.5, 2H), 7.30 (t, *J* = 7.3, 1H), 7.20 (d, *J* = 7.4, 2H), 7.02 (apparent s, 4H), 5.08 (d, *J* = 3.3, 1H), 4.17 – 4.10 (m, 1H), 2.90 (dd, *J* = 8.8, *J* = 4.2, 1H), 2.86 – 2.81 (m, 2H), 2.75 – 2.63 (m, 2H), 2.58 (dt, *J* = 18.3, *J* = 5.3, 1H), 2.27 (s, 3H), 2.12 – 2.02 (dt, *J* = 16.9, *J* = 5.5, 1H), 2.02 – 1.88 (m, 1H); ^{13}C NMR (126 MHz, $CDCl_3$) δ = 175.40, 170.65, 140.10, 135.99, 135.92, 129.26, 129.19, 128.86, 128.30, 126.87, 62.25, 48.60, 46.53, 32.80, 29.58, 21.20, 19.45; MS (ESI): *m/z* (%): 360.2 (100) [M^++Na], 338.2 (55) [M^++H].

***rac*-1-(3-Chlorophenethyl)-6-oxo-2-phenylpiperidine-3-carboxylic acid (*rac*-6)**

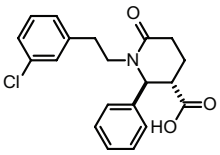

Obtained from benzaldehyde (102 μL) and 2-(3-chlorophenyl) ethylamine (139 μL) as a white solid (150 mg, 0.42 mmol, 42%). Melting point: 182 °C; ^{1}H NMR (500 MHz, $CDCl_3$) δ 7.38 (t, *J* = 7.5, 2H), 7.32 (t, *J* = 7.3, 1H), 7.20 (d, *J* = 7.3, 2H), 7.17 – 7.07 (m, 3H), 7.02 (dd, *J* = 6.2, *J* = 2.0, 1H), 5.08 (d, *J* = 3.3, 1H), 4.12 (ddd, *J* = 13.3, *J* = 9.7, *J* = 6.3, 1H), 2.99 – 2.79 (m, 3H), 2.78 – 2.63 (m, 2H), 2.59 (ddd, *J* = 18.4, *J* = 6.3, *J* = 4.3, 1H), 2.20 – 2.03 (m, 1H), 2.03 – 1.86 (m, 1H); ^{13}C NMR (126 MHz, $CDCl_3$) δ = 175.50, 170.85, 141.14, 139.89, 134.33, 129.89, 129.30, 129.10, 128.46, 127.20, 126.84, 126.70, 62.39, 48.30, 46.44, 32.99, 29.51, 19.28; MS (ESI): *m/z* (%): 358.2 (100) [M^++H], 380.2 (60) [M^++Na].

rac-1-(4-Chlorophenethyl)-6-oxo-2-phenylpiperidine-3-carboxylic acid (_rac_-7)

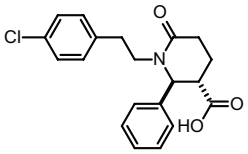

Obtained from benzaldehyde (102 µL) and 2-(4-chlorophenyl)ethylamine (140 µL) as a white solid (168 mg, 0.47 mmol, 47%). Melting point: 229 °C; ^{1}H NMR (500 MHz, $CDCl_3$) δ 7.36 (t, *J* = 7.4, 2H), 7.30 (t, *J* = 7.5, 1H), 7.22 – 7.17 (m, 4H), 7.08 (d, *J* = 8.4, 2H), 5.10 (d, *J* = 3.6, 1H), 4.10 (ddd, *J* = 13.3, *J* = 10.3, *J* = 6.1, 1H), 2.90 – 2.77 (m, 3H), 2.70 – 2.58 (m, 2H), 2.51 (ddd, *J* = 18.1, *J* = 6.1, *J* = 4.7, 1H), δ 2.14 –1.99 (m, 1H), 1.98 – 1.79 (m, 1H); ^{13}C NMR (126 MHz, $CDCl_3$) δ 173.96, 170.01, 140.51, 137.71, 131.91, 130.21, 128.96, 128.47, 127.98, 126.72, 62.24, 47.86, 46.58, 32.58, 29.71, 19.48; MS (ESI): *m/z* (%): 358.2 (100) [M^++H], 380.2 (60) [M^++Na].

rac-1-(4-Chlorophenethyl)-2-(2-chlorophenyl)-6-oxopiperidine-3-carboxylic acid (_rac_-8)

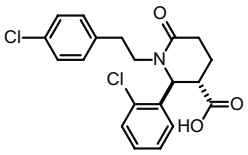

Obtained from 2-chlorobenzaldehyde (113 µL) and 2-(4-chlorophenyl)ethylamine (140 µL) as a white solid (227 mg, 0.58 mmol, 58 %). Melting point: 258 °C; ^{1}H NMR (500 MHz, $CDCl_3$) δ 7.44 – 7.39 (m, 1H), 7.33 – 7.24 (m, 2H), 7.19 (d, *J* = 7.7, 2H), 7.16 – 7.07 (m, 3H), 5.55 (br. s, 1H), 4.15 (dt, *J* = 13.4, *J* = 8.0, 1H), 2.97 (br. s, 1H), 2.88 (t, *J* = 8.1, 2H), 2.65 – 2.55 (m, 2H), 2.55 – 2.43 (m, 2H), 2.20 – 2.01 (m, 1H), 1.93 – 1.70 (m, 1H); ^{13}C NMR (126 MHz, $CDCl_3$) δ 173.54, 169.94, 137.59, 137.34, 132.71, 131.79, 130.35, 130.14, 129.24, 128.38, 128.01, 127.14, 59.15, 48.03, 42.63, 32.33, 29.07, 18.60; MS (ESI): *m/z* (%): 390.1 (100) [M^--H].

rac-1-(4-Chlorophenethyl)-2-(2-fluorophenyl)-6-oxopiperidine-3-carboxylic acid (_rac_-9)

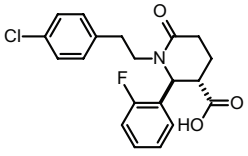

Obtained from 2-fluorobenzaldehyde (105 µL) and 2-(4-chlorophenyl)ethylamine (140 µL) as a white solid (161 mg, 0.43 mmol, 43%). Melting point: 237 °C; ^{1}H NMR (500 MHz, $CDCl_3$) δ 7.38 – 7.21 (m, 1H), 7.16 (d, *J* = 7.9, 2H), 7.13 – 6.98 (m, 5H), 5.40 (br. s, 1H), 4.20 – 3.98 (m, 1H), 2.90 (br. s, 1H), 2.86 – 2.72 (m, 2H), 2.65 – 2.52 (m, 2H), 2.51 – 2.40 (m, 1H), 2.17 – 1.95 (m, 1H), 1.94 – 1.71 (m, 1H); ^{13}C NMR (126 MHz, $CDCl_3$) δ = 173.64, 170.14, 161.18, 159.21, 137.60, 131.93, 130.22, 129.83, 129.76, 128.49, 128.23, 128.21, 127.46, 127.36, 124.52, 124.49, 116.16, 115.99, 56.58, 48.06, 44.10, 32.45, 29.43, 19.47 (^{13}C–^{19}F coupling observed); MS (ESI): *m/z* (%): 398.1 (100) [M^++Na], 376.2 (60) [M^++H].

rac-2-(2-Bromophenyl)-1-(4-chlorophenethyl)-6-oxopiperidine-3-carboxylic acid (_rac_-10)

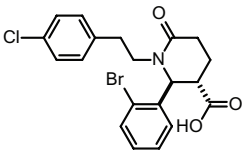

Obtained from 2-bromobenzaldehyde (117 µL) and 2-(4-chlorophenyl)ethylamine (140 µL) as a white solid (106 mg, 0.24 mmol, 24%). Melting point: 261 °C; ^{1}H NMR (500 MHz, $CDCl_3$) δ 7.60 (d, *J* = 7.9, 1H), 7.33 (t, *J* = 7.5, 1H), 7.22 – 7.18 (m, 3H), 7.12 (apparent d, *J* = 8.0, 3H), 5.52 (br. s, 1H), 4.15 (dt, *J* = 13.3, *J* = 8.2, 1H), 2.97 (br. s, 1H), 2.89 (t, *J* = 8.1, 2H), 2.67 – 2.37 (m, 3H), 2.24 – 2.04 (m, 1H), 1.95 – 1.67 (m, 1H); ^{13}C NMR (126 MHz, $CDCl_3$) δ 173.49, 169.89, 138.73, 137.56, 133.65, 131.74, 130.13, 129.52, 128.36, 128.15, 127.71, 122.83, 61.21, 48.00, 42.60, 32.28, 28.99, 18.34; MS (ESI): *m/z* (%): 460.1 (100) [M^++Na], 438.1 (60) [M^++H].

rac-1-(4-Chlorophenethyl)-6-oxo-2-(_o_-tolyl)piperidine-3-carboxylic acid (_rac_-11)

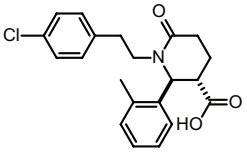

Obtained from *o*-tolualdehyde (116 µL) and 2-(4-chlorophenyl)ethylamine (140 µL) as a white solid (148 mg, 0.40 mmol, 40%). Melting point: 274 °C; ^{1}H NMR (500 MHz, $CDCl_3$) δ 7.36 (br. s, 1H), 7.27 – 7.14 (m, 4H), 7.09 (d, *J* = 8.0, 2H), 7.07 – 6.97 (m, 1H), 5.33 (br. s, 1H), 4.10 (dt, *J* = 13.6, *J* = 8.0, 1H), 2.85 (t, *J* = 7.9, 2H), 2.73 (br. s, 1H), 2.69 – 2.58 (m, 1H), 2.57 – 2.47 (m, 2H), 2.14 – 2.00 (m, 1H), 1.98 – 1.83 (m, 1H); ^{13}C NMR (126 MHz, $CDCl_3$) δ 173.83, 169.88, 137.94, 137.69, 135.04, 131.68, 131.14, 130.05, 128.31, 127.67, 126.19, 126.07, 58.81, 47.80, 43.39, 32.48, 29.12, 18.79, 18.50; MS (ESI): *m/z* (%): 394.2 (100) [M^++Na], 372.2 (50) [M^++H].

rac-1-(4-Chlorophenethyl)-2-(2-methoxyphenyl)-6-oxopiperidine-3-carboxylic acid (_rac_-12)

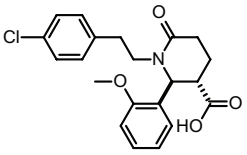

Obtained from 2-methoxybenzaldehyde (121 µL) and 2-(4-chlorophenyl)ethylamine (140 µL) as a white solid (174 mg, 0.45 mmol, 45%). Melting point: 278 °C; ^{1}H NMR (500 MHz, $CDCl_3$) δ 7.29 (t, *J* = 7.6, 1H), 7.18 (d, *J* = 8.0, 2H), 7.11 (d, *J* = 8.1, 2H), 7.01 (d, *J* = 7.3, 1H), 6.93 (dd, *J* = 14.4, *J* = 7.7, 2H), 5.44 (br. s, 1H), 4.12 (dt, *J* = 13.2, *J* = 8.2, 1H), 3.87 (s, 3H), 2.98 (s, 1H), 2.87 (t, *J* = 8.1, 2H), 2.64 – 2.52 (m, 3H), 2.47 (dd, *J* = 18.1, *J* = 3.8, 1H), 2.15 – 1.97 (m, 1H), 1.91 – 1.72 (m, 1H); ^{13}C NMR (126 MHz, $CDCl_3$) δ 174.32, 170.17, 156.35, 137.83, 131.58, 130.11, 128.91, 128.24, 127.77, 127.23, 120.39, 110.56, 57.05, 55.27, 47.93, 42.59, 32.33, 29.21, 19.16;

MS (ESI): *m/z* (%): 410.1 (100) [M^++Na], 388.1 (50) [M^++H].

rac-1-(4-Chlorophenethyl)-2-(3-chlorophenyl)-6-oxopiperidine-3-carboxylic acid (_rac_-13)

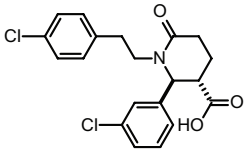

Obtained from 3-chlorobenzaldehyde (113 µL) and 2-(4-chlorophenyl)ethylamine (140 µL) as a white solid (121 mg, 0.31 mmol, 31%). Melting point: 234 °C; ^{1}H NMR (500 MHz, $CDCl_3$) δ 7.38 – 7.25 (m, 2H), 7.20 (apparent d, *J* = 8.3, 3H), 7.09 (apparent d, *J* = 7.6, 3H), 5.07 (br. s, 1H), 4.20 – 4.03 (m, 1H), 2.96 – 2.70 (m, 3H), 2.69 – 2.55 (m, 2H), 2.54 – 2.41 (m, 1H), 2.11 – 1.99 (m, 1H), 1.97 – 1.83 (m, 1H); ^{13}C NMR (126 MHz, $CDCl_3$) δ 173.67, 169.87, 142.87, 137.53, 135.00, 132.03, 130.33, 130.23, 128.55, 128.25, 126.89, 124.90, 61.80, 47.86, 46.51, 32.52, 29.72, 19.56; MS (ESI): *m/z* (%): 414.1 (100) [M^++Na], 392.1 (60) [M^++H].

rac-1-(4-Chlorophenethyl)-2-(4-chlorophenyl)-6-oxopiperidine-3-carboxylic acid (_rac_-14)

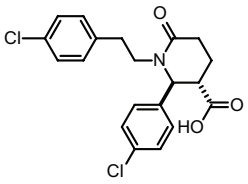

Obtained from 4-chlorobenzaldehyde (141 mg) and 2-(4-chlorophenyl)ethylamine (140 µL) as an off-white solid (151 mg, 0.38 mmol, 38%). Melting point: 227 °C; ^{1}H NMR (500 MHz, $CDCl_3$) δ 7.34 (d, *J* = 8.0, 2H), 7.20 (d, *J* = 8.1, 2H), 7.15 (d, *J* = 8.2, 2H), 7.08 (d, *J* = 8.1, 2H), 5.06 (d, *J* = 3.6, 1H), 4.11 (ddd, *J* = 13.5, *J* = 9.9, *J* = 6.5, 1H), 2.95 – 2.70 (m, 3H), 2.70 – 2.55 (m, 2H), 2.50 (dt, *J* = 18.1, *J* = 5.3, 1H), 2.13 – 1.97 (m, 1H), 1.96 – 1.82 (m, 1H); ^{13}C NMR (126 MHz, $CDCl_3$) δ 173.69, 169.83, 139.14, 137.52, 133.77, 131.97, 130.17, 129.13, 128.50, 128.12, 61.68, 47.70, 46.60, 32.50, 29.75, 19.59; MS (ESI): *m/z* (%): 414.1 (100) [M^++Na], 392.1 (60) [M^++H].

rac-1-(4-Chlorophenethyl)-2-(naphthalen-2-yl)-6-oxopiperidine-3-carboxylic acid (_rac_-15)

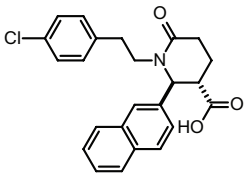

Obtained from 2-naphthaldehyde (156 mg) and 2-(4-chlorophenyl)ethylamine (140 µL) as an off-white solid (273 mg, 0.67 mmol, 67%). Melting point: 224 °C; ^{1}H NMR (500 MHz, $CDCl_3$) δ 7.98 – 7.74 (m, 3H), 7.61 (s, 1H), 7.55 – 7.42 (m, 2H), 7.33 (d, *J* = 8.4, 1H), 7.17 (d, *J* = 7.9, 2H), 7.07 (d, *J* = 7.9, 2H), 5.26 (d, *J* = 2.7, 1H), 4.29 – 4.09 (m, 1H), 2.93 (br. s, 1H), 2.90 – 2.81 (m, 2H), 2.75 – 2.61 (m, 2H), 2.61 – 2.49 (m, 1H), 2.14 – 2.01 (m, 1H), 2.00 – 1.82 (m, 1H); ^{13}C NMR (126 MHz, $CDCl_3$) δ 173.99,

170.08, 137.84, 137.65, 133.23, 132.95, 131.90, 130.20, 129.04, 128.46, 127.91, 127.74, 126.70, 126.40, 125.67, 124.41, 62.38, 47.82, 46.43, 32.61, 29.83, 19.63; MS (ESI): *m/z* (%): 430.1 (100) [M^++Na], 408.1 (70)[M^++H].

rac-1-(4-Chlorophenethyl)-2-(naphthalen-1-yl)-6-oxopiperidine-3-carboxylic acid (_rac_-16)

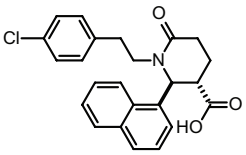

Obtained from 1-naphthaldehyde (136 μL) and 2-(4-chlorophenyl)ethylamine (140 μL) as an off-white solid (126 mg, 0.31 mmol, 31%). ^{1}H NMR (500 MHz, DMSO) δ 8.03 (dd, *J* = 16.1, *J* = 8.3, 2H), 7.92 (d, *J* = 8.1, 1H), 7.66 (t, *J* = 7.0, 1H), 7.59 (t, *J* = 7.2, 1H), 7.54 (t, *J* = 7.7, 1H), 7.25 (d, *J* = 8.3, 3H), 7.13 (d, *J* = 8.4, 2H), 5.87 (br. s, 1H), 4.13 – 3.89 (m, 1H), 3.00 (br. s, 1H), 2.90 – 2.77 (m, 1H), 2.77 – 2.61 (m, 1H), 2.49 – 2.41 (m, 2H), 2.01 – 1.83 (m, 1H), 1.76 – 1.59 (m, 1H); ^{13}C NMR (126 MHz, DMSO) δ 173.85, 170.12, 135.89, 134.04, 132.96, 132.57, 131.75, 130.46, 129.30, 128.75, 128.70, 128.58, 126.68, 126.65, 126.43, 125.17 62.16, 47.56, 45.96, 32.84, 29.79, 19.23; MS (ESI): *m/z* (%): 430.1 (100) [M^++Na], 408.0 (90) [M^++H].

rac-1-(4-Chlorophenethyl)-6-oxo-2-(pyridin-3-yl)piperidine-3-carboxylic acid (_rac_-17)

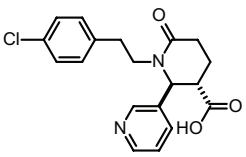

Obtained from 3-pyridinecarboxaldehyde (94 μL) and 2-(4-chlorophenyl)ethylamine (140 μL) as an off-white solid (79 mg, 0.22 mmol, 22%). ^{1}H NMR (500 MHz, $CDCl_3$) δ 8.63 – 8.51 (m, 2H), 7.64 (d, *J* = 7.9, 1H), 7.42 (dd, *J* = 7.8, *J* = 5.0, 1H), 7.20 (d, *J* = 8.3, 2H), 7.07 (d, *J* = 8.3, 2H), 5.10 (d, *J* = 5.1, 1H), 4.20 – 4.06 (m, 1H), 2.96 – 2.76 (m, 3H), 2.75 – 2.52 (m, 3H), 2.19 – 2.05 (m, 1H), 2.04 – 1.92 (m, 1H); ^{13}C NMR (126 MHz, $CDCl_3$) δ 173.88, 170.68, 148.41, 147.67, 137.22, 137.08, 135.49, 132.48, 130.35, 128.85, 124.73, 76.98, 60.71, 47.78, 47.76, 32.62, 30.41, 20.75; MS (ESI): *m/z* (%): 459.2 (100) [M^++H].

rac-1-(4-Chlorophenethyl)-6-oxo-2-(thiophen-2-yl)piperidine-3-carboxylic acid (_rac_-18)

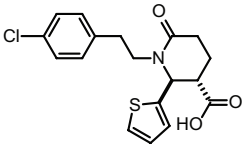

Obtained from 2-thiophenecarboxaldehyde (93 μL) and 2-(4-chlorophenyl)ethylamine (140 μL) as a white solid (167 mg, 0.46 mmol, 46%). ^{1}H NMR (500 MHz, DMSO) δ 7.50 (d, *J* = 4.8, 1H), 7.30 (d, *J* = 8.1, 2H), 7.16 (d,*J* = 8.1, 2H), 7.07 (br. s, 1H), 7.02 (t, *J* = 4.3, 1H), 5.26 (d,

J = 4.5, 1H), 3.93 – 3.79 (m, 1H), 3.01 – 2.89 (m, 1H), 2.88 – 2.71 (m, 2H), 2.68 – 2.53 (m, 1H), 2.47 – 2.20 (m, 2H), 2.04 – 1.83 (m, 2H); ^{13}C NMR (126 MHz, DMSO) δ 173.03, 167.97, 144.77, 138.06, 130.76, 130.42, 128.29, 127.15, 126.11, 125.78, 125.59, 57.70, 46.79, 46.61, 32.09, 29.44, 20.32; MS (ESI): *m/z* (%): 486.1 (100) [M^++Na], 464.1 (55) [M^++H].

rac-2-(2-Chlorophenyl)-1-(4-fluorophenethyl)-6-oxopiperidine-3-carboxylic acid (_rac_-19)

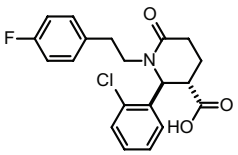

Obtained from 2-chlorobenzaldehyde (113 μL) and 4-fluorophenethylamine (131 μL) as an off-white solid (118 mg, 0.31 mmol, 31%). Melting point: 237 °C; ^{1}H NMR (500 MHz, $CDCl_3$) δ 7.48 – 7.38 (m, 1H), 7.35 – 7.23 (m, 2H), 7.14 (apparent t, *J* = 6.7, 3H), 6.92 (t, *J* = 8.6, 2H), 5.55 (br. s, 1H), 4.15 (dt, *J* = 13.5, *J* = 8.3, 1H), 2.97 (s, 1H), 2.88 (t, *J* = 8.1, 2H), 2.68 – 2.56 (m, 1H), 2.55 – 2.42 (m, 2H), 2.17 – 2.02 (m, 1H), 1.90 – 1.70 (m, 1H); ^{13}C NMR (126 MHz, $CDCl_3$) δ 173.57, 169.96, 162.30, 160.36, 137.35, 134.74, 134.71, 132.69, 130.33, 130.19, 130.13, 129.21, 128.01, 127.12, 115.11, 114.94, 59.16, 48.29, 42.61, 32.14, 29.06, 18.58. (^{13}C–^{19}F coupling observed); MS (ESI): *m/z* (%): 398.2 (100) [M^++Na], 376.2 (50) [M^++H].

rac-1-(4-Bromophenethyl)-2-(2-chlorophenyl)-6-oxopiperidine-3-carboxylic acid (_rac_-20)

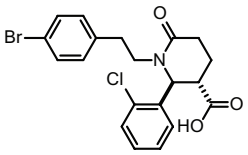

Obtained from 2-chlorobenzaldehyde (113 μL) and 4-bromophenethylamine (155 μL) as a white solid (283 mg, 0.65 mmol, 65 %). Melting point: 272 °C; ^{1}H NMR (500 MHz, $CDCl_3$) δ 7.44 – 7.37 (m, 1H), 7.35 (d, *J* = 8.3, 2H), 7.31 – 7.21 (m, 2H), 7.18 – 7.09 (m, 1H), 7.07 (d, *J* = 8.3, 2H), 5.53 (br. s, 1H), 4.13 (dt, *J* = 13.4, *J* = 8.2, 1H), 2.96 (br. s, 1H), 2.86 (t, *J* = 8.1, 2H), 2.64 – 2.55 (m, 1H), 2.55 – 2.42 (m, 2H), 2.18 – 2.04 (m, 1H), 1.93 – 1.91 (m, 1H); ^{13}C NMR (126 MHz, $CDCl_3$) δ 173.20, 169.53, 137.81, 136.94, 132.33, 131.01, 130.25, 130.04, 128.98, 127.68, 126.87, 119.51, 47.56, 42.30, 32.06, 28.76, 18.29; MS (ESI): *m/z* (%): 460.0 (100) [M^++Na], 438.0 (50) [M^++H].

rac-1-(4-Chlorobenzyl)-2-(2-chlorophenyl)-6-oxopiperidine-3-carboxylic acid (_rac_-21)

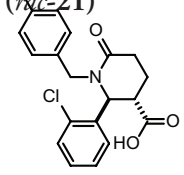

Obtained from 2-chlorobenzaldehyde (113 μL) and 4-chlorobenzylamine (122 μL) as a white solid (75 mg, 0.20 mmol, 20%). Melting point: 241 °C; ^{1}H NMR (500 MHz, $CDCl_3$) δ 7.53 – 7.36 (m, 1H), 7.35 – 7.26 (m, 2H), 7.22 (d, *J*

= 8.1, 2H), 7.20 – 7.08 (m, 3H), 5.40 (br. s, 1H), 5.30 (d, *J* = 14.8, 1H), 3.46 (d, *J* = 14.8, 1H), 2.88 (br. s, 1H), 2.70 (ddd, *J* = 18.4, *J* = 11.5, *J* = 6.9, 1H), 2.65 – 2.48 (m, 1H), 2.18– 2.01 (d, *J* = 13.5, 1H), 1.93 – 1.74 (s, 1H); ^{13}C NMR (126 MHz, $CDCl_3$) δ 173.29, 170.23, 136.81, 135.06, 132.80, 132.68, 130.33, 130.00, 129.19, 128.23, 127.99, 127.05, 58.73, 48.32, 42.52, 40.14, 39.97, 39.80, 39.63, 29.03, 18.40; MS (ESI): *m/z* (%): 400.1 (100) [M^++Na], 378.2 (30) [M^++H].

***rac*-1-(*tert*-Butyl)-2-cyclohexyl-6-oxopiperidine-3-carboxylic acid (*rac*-22)**

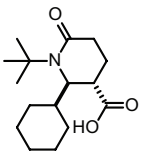

Obtained from cyclohexanecarboxaldehyde (121 μL) and *t*-butylamine (105 μL) as a white solid (39 mg, 0.14 mmol, 14%). Melting point: 251 °C; ^{1}H NMR (500 MHz, $CDCl_3$) δ = 4.04 (dd, *J* = 7.9, *J* = 3.0, 1H), 2.90 – 2.73 (m, 1H), 2.53 – 2.39 (m, 1H), 2.35 – 2.22 (m, 1H), 2.12 – 1.89 (m, 2H), 1.80 (d, *J* = 12.2, 2H), 1.72 (d, *J* = 13.7, 3H), 1.60 – 1.48 (m, 1H), 1.43 (s, 9H), 1.26 – 1.08 (m, 3H), 1.08 – 0.88 (m, 2H); ^{13}C NMR (126 MHz, $CDCl_3$) δ = 176.58, 172.68, 59.68, 57.63, 42.80, 41.37, 32.27, 30.34, 29.49, 28.66, 26.71, 26.47, 26.34, 19.81; MS (ESI): *m/z* (%): 304.3 (100) [M^++Na].

***rac*-2-(2-Chlorophenyl)-1-(cyclohexylmethyl)-6-oxopiperidine-3-carboxylic acid (*rac*-23)**

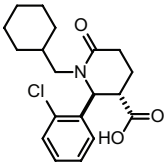

Obtained from 2-chlorobenzaldehyde (113 μL) and cyclohexanemethylamine (130 μL) as a white solid (110 mg, 0.31 mmol, 31%). Melting point: 220 °C; ^{1}H NMR (500 MHz, $CDCl_3$) δ 7.41 (d, *J* = 7.4, 1H), 7.28 (apparent p, *J* = 7.2, 2H), 7.09 (d, *J* = 7.3, 1H), 5.54 (br. s, 1H), 3.98 (dd, *J* = 13.4, 8.9, 1H), 2.96 (br. s, 1H), 2.77 – 2.62 (m, 1H), 2.48 (dd, *J* = 18.2, *J* = 5.9, 1H), 2.14 – 2.02 (m, 2H), 1.86 – 1.71 (m, 2H), 1.71 – 1.55 (m, 5H), 1.34 – 1.02 (m, 3H), 1.02 – 0.79 (m, 2H); ^{13}C NMR (126 MHz, $CDCl_3$) δ 173.79, 170.64, 137.68, 132.81, 130.38, 129.11, 127.92, 127.13, 59.31, 51.78, 42.43, 35.91, 30.98, 30.93, 30.80, 29.03, 26.48, 25.96, 25.90; MS (ESI): *m/z* (%): 372.2 (100) [M^++Na], 350.2 (30) [M^++H].

***rac*-(*E*)-1-(4-Chlorophenethyl)-6-oxo-2-styrylpiperidine-3-carboxylic acid (*rac*-24)**

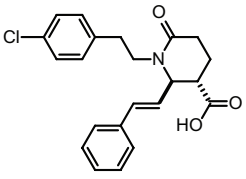

Obtained from cinnamaldehyde (126 μL) and 2-(4-chlorophenyl)ethylamine (140 μL) as an off-white solid (127 mg, 0.33 mmol, 33%). Melting point: 175 °C; ^{1}H NMR (500 MHz, $CDCl_3$) δ 7.46 – 7.31 (m, 5H), 7.27 (t, *J* = 6.9, 1H), 7.21 (d, *J* = 8.3, 2H), 7.14 (d, *J* = 8.4,

2H), 6.48 (d, *J* = 15.8, 1H), 6.08 (dd, *J* = 15.8, *J* = 7.0, 1H), 4.59 (dd, *J* = 6.6, *J* = 3.9, 1H), 4.06 (dt, *J* = 13.3, *J* = 7.8, 1H), 3.02 (dt, *J* = 9.2, *J* = 7.3, 1H), 2.87 (t, *J* = 8.0, 2H), 2.77 (dd, *J* = 9.2, *J* = 4.3, 1H), 2.62 – 2.57 (m, 1H), 2.54 (dd, *J* = 9.4, *J* = 7.0, 1H), 2.43 (dt, *J* = 18.1, *J* = 5.6, 1H), 2.16 – 2.02 (m, 2H); ^{13}C NMR (126 MHz, $CDCl_3$) δ 173.78, 169.38, 137.70, 135.68, 132.52, 131.77, 130.16, 128.64, 128.39, 128.11, 128.04, 126.47, 60.51, 47.37, 43.97, 32.72, 29.65, 20.09; MS (ESI): *m/z* (%): 406.2 (90) [M^++Na], 384.2 (100) [M^++ H].

rac-1-(4-Chlorophenethyl)-2-(2-chlorophenyl)-5-oxopyrrolidine-3-carboxylic acid (_rac_-32)

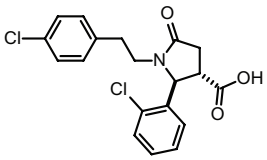

Obtained from 2-chlorbenzaldehyde (126 µL), 2-(4-chlorophenyl)ethylamine (140 µL) and succinic anhydride as an off-white solid (162 mg, 0.43 mmol, 43%). ^{1}H NMR (500 MHz, $CDCl_3$) δ 7.33 (d, *J* = 4.5, 1H), 7.24 – 7.16 (m, 2H), 7.12 (d, *J* = 7.9, 2H), 7.03 – 6.92 (3H), 5.36 (s, 1H), 3.85 (s, 1H), 3.06 – 2.83 (m, 1H), 2.79 – 2.56 (m, 5H). ^{13}C NMR (126 MHz, $CDCl_3$) δ 174.03, 173.15, 137.59. 136.89, 133.22, 131.99, 130.03, 129.50, 128.47, 127.67, 127.43, 60.20, 44.61, 42.19, 33.48, 32.58; MS (ESI): *m/z* (%): 400.1 (100) [M^++Na], 378.1 (60) [M^++H].

***rac*-Methyl-1-(4-chlorophenethyl)-2-(2-chlorophenyl)-6-oxopiperidine-3-carboxylate (*rac*-25)**

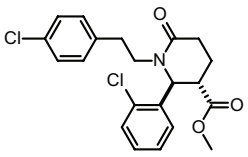

To a 0 °C suspension of *rac*-**8** (250 mg, 0.64 mmol, 1.0 equiv) in benzene (5 mL) was added dropwise thionyl chloride (251 µL, 3.2 mmol, 5.0 equiv.). The resulting mixture was heated at 70 °C until a clear solution was obtained (~3 h). The reaction was concentrated *in vacuo* and CH_2Cl_2 (5 mL) was added to the residue under a nitrogen atmosphere. The reaction was cooled to 0 °C and methanol (1 mL, 25 mmol, 39 equiv.) was added. The reaction was stirred until TLC showed full conversion of the starting material. The reaction was concentrated *in vacuo* and purified by column chromatography (SiO_2, ethyl acetate/petroleum ether). The product was obtained as a white solid (193 mg, 74%). Melting point: 120°C; ^{1}H NMR (500 MHz, $CDCl_3$) δ 7.46 – 7.37 (m, 1H), 7.30 – 7.27 (m, 2H), 7.21 (d, *J* = 8.4, 1H), 7.16 – 7.07 (m, 3H), 5.49 (br. s, 1H), 4.17 (ddd, *J* = 13.4, *J* = 10.1, *J* = 6.4, 1H), 3.78 (s, 3H), 3.02 (dd, *J* = 6.9, *J* = 4.1, 1H), 2.95 – 2.79 (m, 2H), 2.58 – 2.44 (m, 3H), 2.16 – 2.06 (dq, *J* = 13.5, *J* = 4.4, 1H), 1.94 – 1.76 (m, 1H); ^{13}C NMR (126 MHz, $CDCl_3$) δ 172.30, 169.88, 137.54, 137.15, 132.96, 132.24, 130.67, 130.34, 129.66, 128.71, 128.30, 127.49, 59.37, 52.71, 48.17, 43.12, 32.59, 29.34, 19.08; MS (ESI): *m/z* (%): 428.1

(100) [M^++Na], 406.2 (30) [M^++H]. Preparative chiral separation (Reprosil chiral-AM) was performed on racemic 25 (MeOH, 50 mg/mL) as described in the general remarks to obtain the two *trans*-enantiomers **25A** (t_R = 4.0 min) and **25B** (t_R = 4.9 min).

(2*R*,3*R*)-1-(4-Chlorophenethyl)-2-(2-chlorophenyl)-6-oxopiperidine-3-carboxylic acid [(*R*,*R*)-8]

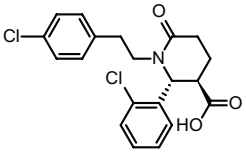

To a suspension of **25A** (40 mg, 98 µmol, 1.0 equiv.) and LiOH (7.1 mg, 296 µmol, 3.0 equiv.) in methanol (800 µL) was added dropwise water (200 µL) to prevent precipitation of the ester. The reaction was stirred at room temperature overnight. The reaction mixture was concentrated *in vacuo*. To the residue was added water (1 mL), the pH adjusted to 4, and the solid was collected by filtration, washed with cold ether (2 × 1 mL) and dried. The product was obtained as a white solid (12 mg, 31 µmol, 31%). Melting point: 259 °C; ^{1}H and ^{13}C NMR were identical to *rac*-**8**. Enantiomeric excess: >99% which was determined by esterification (TMS-diazomethane in benzene/methanol 4:1) of a small amount (3 mg) and performing analytical chiral SFC as described in the general remarks. The absolute configuration was assigned based on the crystal structure obtained for the *S*,*S*-enantiomer.

(2*S*,3*S*)-1-(4-Chlorophenethyl)-2-(2-chlorophenyl)-6-oxopiperidine-3-carboxylic acid [(*S*,*S*)-8]

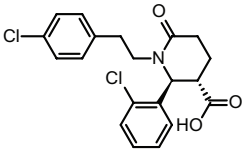

To a suspension of **25B** (40 mg, 98 µmol, 1.0 equiv.) and LiOH (7.1 mg, 296 µmol, 3.0 equiv.) in methanol (800 µL) was added dropwise water (200 µL) to prevent precipitation of the ester. The reaction was stirred at room temperature overnight. The reaction mixture was concentrated *in vacuo*. To the residue was added water (1 mL), the pH adjusted to 4, and the solid was collected by filtration, washed with cold ether (2 × 1 mL) and dried. The product was obtained as a white solid (35 mg, 89 µmol, 91%). Melting point: 258 °C; ^{1}H and ^{13}C NMR were identical to *rac*-**8**. Enantiomeric excess: 94% which was determined by esterification (TMS-diazomethane in benzene/methanol 4:1) of a small amount (3 mg) and performing analytical chiral SFC as described in the general remarks. The absolute configuration was determined by single crystal X-ray crystallography. The supplementary crystallographic data can be obtained, free of charge, from the Cambridge Crystallographic Data Centre (CCDC 1506780).

rac-1-(4-Chlorophenethyl)-2-(2-chlorophenyl)-6-oxopiperidine-3-carboxamide (*rac*-26)

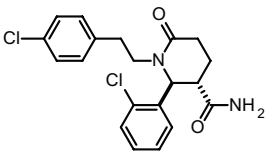

A solution of *rac*-**8** (109 mg, 0.28 mmol, 1.0 equiv.) and 1,1'-carbonyldiimidazole (CDI, 48 mg, 0.29 mmol, 1.05 equiv.) in DMF (500 µL) under nitrogen was heated at 50 °C for 1 h. Then ammonium carbonate (81 mg, 0.84 mmol, 3.0 equiv.) was added and the reaction heated at 70 °C for 2 days. The reaction was cooled and water (5 mL) was added which precipitated the product that was collected by filtration, washed with water, and dried. The product was obtained as a white solid (91 mg, 0.23 mmol, 82%). Melting point: 222 °C; ^{1}H NMR (500 MHz, $CDCl_3$) δ 7.48 – 7.36 (m, 1H), 7.35 – 7.23 (m, 2H), 7.23 – 7.14 (m, 3H), 7.09 (d, *J* = 8.3, 2H), 6.04 (br. s, 1H), 5.77 (br. s, 1H), 5.32 (d, *J* = 2.9, 1H), 4.09 (ddd, *J* = 13.6, *J* = 10.2, *J* = 5.8, 1H), 3.02 – 2.74 (m, 3H), 2.70 – 2.62 (m, 1H), 2.59 – 2.43 (m, 2H), 2.03 – 1.84 (m, 2H); ^{13}C NMR (126 MHz, $CDCl_3$) δ 173.60, 169.88, 137.69, 137.42, 132.75, 131.80, 130.42, 130.17, 129.33, 128.68, 128.41, 127.29, 59.84, 47.63, 44.07, 32.30, 29.65, 20.99; MS (ESI): *m/z* (%): 413.1 (100) [M^++Na], 391.1 (20) [M^++H].

rac-1-(4-Chlorophenethyl)-2-(2-chlorophenyl)-6-oxo-*N*-phenethylpiperidine-3-carboxamide (*rac*-27)

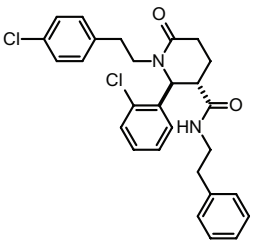

To a 0 °C suspension of *rac*-**8** (392 mg, 1.0 mmol, 1.0 equiv) in benzene (5 mL) was added dropwise thionyl chloride (235 µL, 3.0 mmol, 3.0 equiv.). The resulting mixture was heated at 70 °C until a clear solution was obtained (~3 h). The reaction was concentrated *in vacuo* and CH_2Cl_2 (5 mL) was added to the residue under a nitrogen atmosphere. The reaction was cooled to 0 °C and 2-phenethylamine (378 µL, 3.0 mmol, 3.0 equiv.) was added. The reaction was stirred until TLC showed full conversion of the starting material. The reaction was concentrated *in vacuo* and purified by column chromatography (SiO_2, ethyl acetate/petroleum ether). The product was obtained as an off-white solid (307 mg, 62%). ^{1}H NMR (500 MHz, $CDCl_3$) δ 7.46 – 7.35 (m, 1H), 7.34 – 7.25 (m, 4H), 7.25 – 7.17 (m, 3H), 7.18 – 7.12 (m, 1H), 7.07 (d, *J* = 8.1, 4H), 5.48 (br. s, 1H), 5.25 (br, 1H), 4.22 – 3.92 (m, 1H), 3.69 – 3.30 (m, 2H), 3.00 – 2.64 (m, 5H), 2.63 – 2.36 (m, 3H), 1.86 (dd, *J* = 12.2, *J* = 6.1, 2H); ^{13}C NMR (126 MHz, $CDCl_3$) δ 176.12, 170.36, 139.08, 138.31, 135.91, 135.43, 132.99, 131.79, 130.43, 129.99, 129.30, 129.19, 128.83, 128.23, 126.81, 126.13, 61.75, 47.94, 45.38, 42.54, 35.92, 35.06, 31.88, 24.98; MS (ESI): *m/z* (%): 517.1 (100) [M^++Na], 495.3 (50) [M^++H].

***rac*-1-(4-Chlorophenethyl)-2-(2-chlorophenyl)-6-oxopiperidine-3-carbonitrile (*rac*-28)**

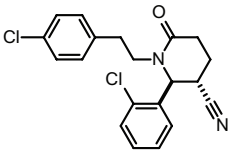

To a 0 °C solution *rac*-**26** (196 mg, 0.5 mmol, 1.0 equiv.) and pyridine (131 µL, 1.6 mmol, 3.0 equiv.) in CH_2Cl_2 (5 mL) was added dropwise $POCl_3$ (93 µL, 1.0 mmol, 1.0 equiv.). After 15 min. at the same temperature the reaction was allowed to warm to room temperature and stirred until TLC showed full conversion. The reaction was poured in 1 M HCl (10 mL), extracted with CH_2Cl_2 (3 × 5 mL). The organic layer was washed with brine (10 mL), dried over $MgSO_4$, concentrated *in vacuo*, and purified by column chromatography (SiO_2, EtOAc/petroleum ether). The product was obtained as a yellow oil (150 mg, 0.40 mmol, 80%). ^{1}H NMR (500 MHz, $CDCl_3$) δ 7.43 (d, *J* = 8.6, 1H), 7.41 – 7.29 (m, 2H), 7.25 (d, *J* = 8.3, 2H), 7.14 (d, *J* = 8.3, 2H), 7.11 – 6.99 (m, 1H), 5.04 (br. s, 1H), 4.42 – 4.13 (m, 1H), 3.22 (br. s, 1H), 2.99 – 2.75 (m, 3H), 2.65 (apparent d, *J* = 17.1, 1H), 2.56 – 2.38 (m, 1H), 2.01 – 1.74 (m, 2H); ^{13}C NMR (126 MHz, $CDCl_3$) δ 168.85, 137.02, 134.66, 132.89, 132.53, 130.95, 130.53, 130.37, 128.96, 128.27, 127.71, 119.05, 60.38, 48.22, 33.13, 30.22, 28.85, 19.47.

***rac*-1-(4-Chlorophenethyl)-6-(2-chlorophenyl)-5-(1*H*-tetrazol-5-yl)piperidin-2-one (*rac*-29)**

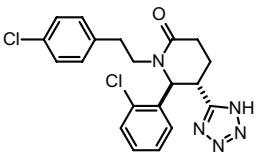

To a solution *rac*-**28** (100 mg, 270 µmol) in isopropanol (1.5 mL) was added $ZnCl_2$ (8 mg, 0.054 mmol) and NaN_3 (52 mg, 0.81 mmol). The resulting mixture was heated at reflux overnight. The solvent was evaporated under reduced pressure, to the residue was added H_2O (10 mL), and extracted with EtOAc (3 × 10 mL). The organic layer was washed with H_2O (5 mL), dried over $MgSO_4$, and concentrated *in vacuo*. The residue was triturated with ether, the solid collected by filtration and washed with little Et_2O. The product was obtained as an off-white solid (28 mg, 67 µmol, 25%). ^{1}H NMR (500 MHz, $CDCl_3$) δ = 7.48 – 7.36 (m, 1H), 7.32 – 7.24 (m, 2H), 7.16 (d, *J* = 7.7, 2H), 7.13 – 7.07 (m, 3H), 5.51 (br. s, 1H), 3.87 (dt, *J* = 13.4, *J* = 8.0, 1H), 2.97 (br. s, 1H), 2.86 (t, *J* = 8.1, 2H), 2.67 – 2.59 (m, 1H), 2.56 – 2.39 (m, 2H), 2.13 – 2.07 (m, 1H), 1.93 – 1.70 (m, 1H) ^{13}C NMR (126 MHz, $CDCl_3$) δ = 169.94, 154.61, 137.59, 137.34, 132.71, 131.79, 130.35, 130.14, 129.24, 128.38, 128.01, 127.14, 59.15, 48.03, 42.63, 32.33, 29.07, 18.60; MS (ESI): *m/z* (%): 414.0 (100) [*M*$^-$-H].

General procedure for the Groebke–Blackburn–Bienaymé reaction:

To a solution of aldehyde (1.0 mmol) and amine (1.0 mmol) in methanol (4 mL, 0.5 M) was added 2-isocyanobiphenyl (1.0 mmol, 179 mg) followed by $ScOTf_3$ (5 mol%, 20 mg). The resulting mixture was stirred at room temperature overnight. A precipitate formed during the course of the reaction which was collected by filtration, washed with cold Et_2O (3 × 5 mL), and dried *in vacuo*.

Methyl 3-(3-([1,1'-biphenyl]-2-ylamino)imidazo[1,2-*a*]pyridin-2-yl) propanoate (39)

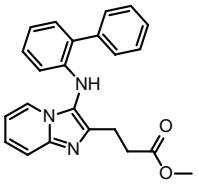

Obtained from methyl 4-oxobutanoate (105 μL) and 2-aminopyridine (94 mg) and catalyst as an off white solid. Yields: 5 mol% $ScOTf_3$ (63%), 5 mol% $ZrCl_4$ (52%), 10 mol% $HClO_4$ (48%). ^{1}H NMR (500 MHz, $CDCl_3$) δ 7.75 (d, *J* = 6.8, 1H), 7.61 (d, *J* = 7.3, 2H), 7.58 – 7.48 (m, 3H), 7.41 (t, *J* = 7.4, 1H), 7.23 (dd, *J* = 7.5, 1.2, 1H), 7.15 (dd, *J* = 11.7, 4.0, 1H), 7.14 – 7.03 (m, 1H), 6.90 (t, *J* = 7.3, 1H), 6.73 (t, *J* = 6.7, 1H), 6.13 (d, *J* = 8.1, 1H), 5.88 (s, 1H), 3.54 (s, 3H), 2.99 (t, *J* = 7.3, 2H), 2.78 (t, *J* = 7.3, 2H); ^{13}C NMR (126 MHz, $CDCl_3$) δ 173.74, 142.81, 142.28, 140.61, 138.99, 130.90, 129.57, 129.36, 129.07, 128.26, 127.84, 124.37, 122.86, 119.62, 119.19, 117.53, 112.21, 111.93, 51.70, 33.20, 22.57; MS (ESI): *m/z* (%): 372.25 (100) [M^++H].

Methyl 3-(3-([1,1'-biphenyl]-2-ylamino)-7-chloroimidazo[1,2-*a*]pyridin-2-yl) propanoate (40)

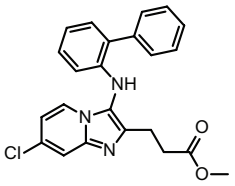

Obtained from methyl 4-oxobutanoate (105 μL) and 2-amino-4-chloropyridine (129 mg) as an off-white solid (231 mg, 0.58 mmol, 58%). R_f = 0.55 (55% EtOAc/ petroleum ether). ^{1}H NMR (500 MHz, $CDCl_3$) δ 7.66 (d, *J* = 7.2, 1H), 7.59 (d, *J* = 7.4, 2H), 7.56 – 7.48 (m, 3H), 7.41 (t, *J* = 7.4, 1H), 7.31 – 7.21 (m, 1H), 7.17 – 7.05 (m, 1H), 6.91 (t, *J* = 7.4, 1H), 6.72 (dd, *J* = 7.2, 1.9, 1H), 6.11 (d, *J* = 8.1, 1H), 5.93 (s, 1H), 3.53 (s, 3H), 2.96 (t, *J* = 7.2, 2H), 2.76 (t, *J* = 7.1, 2H); ^{13}C NMR (126 MHz, $CDCl_3$) δ 173.66, 142.41, 141.97, 141.34, 138.84, 131.01, 129.54, 129.39, 129.11, 128.40, 127.91, 123.23, 119.90, 119.73, 116.46, 113.56, 112.17, 100.18, 51.76, 33.02, 22.52; MS (ESI): *m/z* (%): 406.16 (100) [M^++H], 374.09 (80) [M^+-OCH_3].

Methyl 3-(3-([1,1'-biphenyl]-2-ylamino)-6-chloroimidazo[1,2-*a*]pyridin-2-yl) propanoate (41)

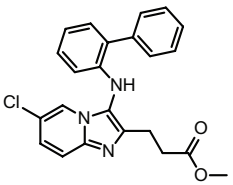

Obtained from 4-oxobutanoate (105 μL) and 2-amino-5-chloropyridine (129 mg) as an off-white solid (248 mg, 0.61 mmol, 61%). R_f = 0.43 (55% EtOAc/petroleum ether). ^{1}H NMR (500 MHz, $CDCl_3$) δ 7.79 (d, *J* = 1.9, 1H), 7.61 (d, *J* = 7.4, 2H), 7.52 (t, *J* = 7.7, 2H), 7.49 – 7.38 (m, 2H), 7.25 (dd, *J* = 7.8, 1.7, 1H), 7.17 – 7.05 (m, 2H), 6.93 (t, *J* = 7.4, 1H), 6.12 (d, *J* = 8.1, 1H), 5.91 (s, 1H), 3.53 (s, 3H), 2.96 (t, *J* = 7.2, 2H), 2.76 (t, *J* = 7.2, 2H); ^{13}C NMR (126 MHz, $CDCl_3$) δ 173.61, 141.94, 141.68, 141.06, 138.81, 131.01, 129.55, 129.37, 129.14, 128.43, 127.89, 125.70, 120.69, 120.48, 120.01, 119.96, 117.91, 112.12, 51.74, 32.98, 22.50; MS (ESI): *m/z* (%): 406.16 (100) [M^++H], 374.10 (90) [M^+-OCH_3].

***N*-([1,1'-Biphenyl]-2-yl)-7-chloro-2-methylimidazo[1,2-*a*]pyridin-3-amine (42)**

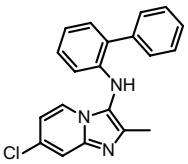

Obtained from freshly distilled acetaldehyde (56 μL) and 2-amino-4-chloropyridine (129 mg) as an off-white solid (124 mg, 0.37 mmol, 37%). ^{1}H NMR (500 MHz, $CDCl_3$) δ 7.69 (d, *J* = 7.2, 1H), 7.54 (ddd, *J* = 12.4, 6.3, 1.3, 5H), 7.42 (dd, *J* = 10.4, 4.1, 1H), 7.22 (dd, *J* = 7.5, 1.3, 1H), 7.17 – 7.03 (m, 1H), 6.91 (t, *J* = 7.4, 1H), 6.72 (dd, *J* = 7.2, 1.9, 1H), 6.15 (d, *J* = 8.1, 1H), 5.51 (s, 1H), 2.33 (s, 3H); ^{13}C NMR (126 MHz, $CDCl_3$) δ 142.33, 142.05, 140.00, 138.88, 130.93, 129.50, 129.48, 129.18, 128.17, 128.02, 122.88, 119.89, 119.27, 116.23, 113.50, 112.12, 13.15; MS (ESI): *m/z* (%): 334.12 (100) [M^++H].

***N*-([1,1'-Biphenyl]-2-yl)-6-chloro-2-methylimidazo[1,2-*a*]pyridin-3-amine (43)**

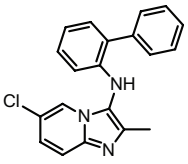

Obtained from freshly distilled acetaldehyde (56 μL) and 2-amino-5-chloropyridine (129 mg) as an off-white solid (103 mg, 0.31 mmol, 31%). ^{1}H NMR (500 MHz, $CDCl_3$) δ 7.82 (s, 1H), 7.56 (dd, *J* = 20.0, 7.3, 4H), 7.43 (dd, *J* = 13.4, *J* = 8.1, 2H), 7.23 (d, *J* = 7.5, 1H), 7.17 – 7.04 (m, 2H), 6.92 (t, *J* = 7.4, 1H), 6.17 (d, *J* = 8.1, 1H), 5.50 (s, 1H), 2.32 (s, 3H); ^{13}C NMR (126 MHz, $CDCl_3$) δ 142.01, 140.96, 140.29, 138.86, 130.94, 129.49, 129.19, 128.21, 128.01, 125.65, 120.41, 119.96, 119.57, 117.70, 112.11, 13.19; MS (ESI): *m/z* (%): 334.11 (100) [M^++H].

3-(3-([1,1'-Biphenyl]-2-ylamino)-7-chloroimidazo[1,2-*a*]pyridin-2-yl) propanoic acid (44)

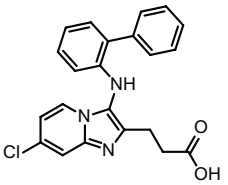

To a suspension of **40** (0.25 mmol, 101 mg) in H_2O/CH_3OH/THF (1:1:1, 1.5 mL) was added LiOH (0.5 mmol, 12 mg, 2.0 equiv.). The resulting mixture was stirred until TLC showed full conversion. The solvent was evaporated till dryness and the residue was dissolved in H_2O (10 mL). The solution was acidified to pH 4 and the formed precipitate was collected by filtration, washed with little cold water, and dried *in vacuo*. The product was obtained as an off-white solid (62 mg, 0.16 mmol, 63%). ^{1}H NMR (500 MHz, $CDCl_3$) δ 7.70 (d, *J* = 7.1, 1H), 7.62 (s, 1H), 7.59 – 7.45 (m, 4H), 7.39 (t, *J* = 7.3, 1H), 7.33 – 7.16 (m, 2H), 7.09 (t, *J* = 7.6, 1H), 6.92 (t, *J* = 7.4, 1H), 6.78 (d, *J* = 6.7, 1H), 6.13 (d, *J* = 8.1, 1H), 5.72 (s, 1H), 2.97 (t, *J* = 6.2, 2H), 2.76 (s, 2H); ^{13}C NMR (126 MHz, $CDCl_3$) δ 175.02, 142.09, 141.55, 140.62, 138.70, 131.17, 129.48, 129.49, 129.22, 128.51, 128.06, 124.58, 120.64, 119.95, 116.81, 113.38, 111.71, 100.16, 33.90, 21.96; MS (ESI): *m/z* (%): 390.12 (100) [*M*-H].

3-(3-([1,1'-Biphenyl]-2-ylamino)-6-chloroimidazo[1,2-*a*]pyridin-2-yl) propanoic acid (45)

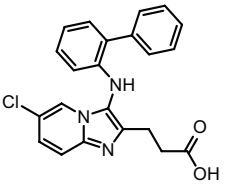

This compound was prepared from **41** according to the procedure of **44**. The product was obtained as an off-white solid (72mg, 0.18 mmol, 73%). ^{1}H NMR (500 MHz, $CDCl_3$) δ 7.70 (d, *J* = 7.1, 1H), 7.62 (s, 1H), 7.59 – 7.45 (m, 4H), 7.39 (t, *J* = 7.3, 1H), 7.33 – 7.16 (m, 2H), 7.09 (t, *J* = 7.6, 1H), 6.92 (t, *J* = 7.4, 1H), 6.78 (d, *J* = 6.7, 1H), 6.13 (d, *J* = 8.1, 1H), 5.72 (s, 1H), 2.97 (t, *J* = 6.2, 2H), 2.76 (s, 2H); ^{13}C NMR (126 MHz, $CDCl_3$) δ 174.94, 141.61, 141.27, 140.36, 138.65, 131.15, 129.50, 129.47, 129.24, 128.52, 128.06, 127.07, 121.47, 120.72, 120.37, 119.79, 117.44, 112.11, 33.87, 21.84; MS (ESI): *m/z* (%): 390.10 (100) [*M*-H].

Biochemistry

Expression, purification, and crystallization of PDK

PDK1 50-359 [Y288G,Q292A] was expressed, purified, concentrated, crystallized, and soaked with compounds as previously described.[18,26] In brief, PDK1 was expressed in Sf9 insect cells as His6-tagged PDK1 50-359 [Y288G,Q292A] using a baculovirus expression system (Invitrogen) and purified through Ni-NTA affinity chromatography, cleavage of the His-tag with TEV protease, followed by clean up

through another Ni-NTA resin. As a final purification step, the protein was isolated essentially pure using gel filtration chromatography. Using this double mutant protein construct, PDK1 crystallized in crystal packing II and diffracted to high resolution. His6-tagged PDK1 that was used for biochemical assays was expressed and purified essentially as described above but without TEV protease cleavage and without re-chromatography through the Ni-NTA column.

Data collection and structure determination

Diffraction data were collected on BL14.1 operated by the Helmholtz-Zentrum Berlin (HZB) at the BESSY II electron storage ring.[42] Data were processed and scaled using the XDS program package.[43] Human PDK1 (PDB ID: 3HRC) was used as a model for molecular replacement in Phaser.[44] The Phenix software suite was used for refinement.[45] Coot was used for manual model building and structural analysis and PyMol (Schrödinger) for molecular depictions.[46,47] The coordinates have been deposited in the Protein Data Bank under accession code 5ACK

PDK1 activity assay

Protein kinase activity tests were performed essentially as previously described.[29,34] Alternatively, assays were performed in a 96-well format, aliquots spotted on p81 phosphocellulose papers (Whatmann), washed in 0.01% phosphoric acid, dried and then exposed and analyzed using PhosphoImager technology (Storm, Molecular Dynamics). Activity measurements were performed in duplicates with less than 10% difference between duplicate pairs. Experiments were repeated at least twice, although most of the experiments were repeated multiple times, with similar results. PDK1 activity assay was performed in a 20 μL mix containing 50 mM Tris–HCl (pH 7.5), 0.05 mg/mL BSA, 0.1% beta-mercaptoethanol, 10 mM $MgCl_2$, 100 μM [γ-^{32}P]ATP (5–50 c.p.m./pmol), 300 ng PDK1 and T308tide (from 0.05 to 1 mM). We should note that the specific activity of PDK1 towards T308tide greatly depends on the peptide concentration as the K_m toward T308tide is >10 mM.[34] For screening purposes, the concentration of T308tide in the assay and the specific activity of the ATP used was in the lower range, with the sole purpose of saving material. Linearity was ensured by performing the assays under conditions in which the product was less than 2% of the least concentrated substrate.

Displacement of the interaction between His-PK1 and biotin-PIFtide using AlphaScreen technology

The AlphaScreen assay was performed according to the manufacturer's protocol (Perkin Elmer). Reactions were performed in a 25 μL final volume in white 384-well microtiter plates (Greiner). The reaction buffer contained 50 mM Tris-HCl (pH 7.4), 100 mM NaCl, 2 mM dithiotreitol, 0.01% (v/v) Tween-20 and 0.1% (w/v) BSA. 25 nM His6-tagged PDK150–359 and 25 nM Biotin-PIFtide (REPRILSEEEQEMFRDFDYIADWS) were mixed with varying concentrations of unlabeled compounds. Subsequently, 5 μL of beads solution containing nickel chelate-coated acceptor beads and streptavidin-coated donor beads (20 μg/mL final concentrations) was added to the reaction mix. Proteins and beads were incubated in the dark for 90 min at room temperature and the emission of light from the acceptor beads was measured in the EnVision reader (Perkin Elmer) and analyzed using the GraphPad Prism software.

Cell-Based Experiments

HEK293 cells were grown in 6-well culture dishes, serum starved overnight and incubated for 1 h and 4 h with the positive control and test compounds, respectively. All compound dilutions were added as duplicates. Cells treated with 0.2% DMSO served as controls. The cells were stimulated 30 min, prior to lysis, with 50 ng/mL IGF1. The lysis was performed on ice in a buffer containing 50 mM Tris-HCl (pH 7.4), 1.0 mM EGTA, 1.0 mM EDTA, 1% (w/v) Triton X-100, 1.0 mM sodium orthovanadate, 50 mM sodium fluoride, 5.0 mM sodium pyrophosphate, 0.27 M sucrose, 0.1% beta-mercaptoethanol, and one tablet of protease inhibitor cocktail (Roche) per 50 mL of buffer. For the western blot analysis, we used antibodies against phospho-S6K [Ser235/236], phospho-Akt [S473], Akt total, and S6K total. The IgG horseradish peroxidase coupled secondary antibodies (anti-mouse and anti-rabbit) were obtained from Biorad. The chemiluminescence image was obtained using the West Dura ECL (Thermo Fisher Scientific) and detected on a G:Box (Syngene). Acid stripping was performed incubating the blots with 50 mM glycine pH 2.2 as previously described.[48]

Crystallographic data

Data collection and refinement statistics (Table ES1). The values in parentheses refer to the shell of highest resolution.

Table ES1. Data collection and refinement statistics for the cocrystal strucutre of PDK1 and *rac*-**8**.

Data collection	
Unit cell dimensions *a*, *b*, *c* (Å)	148.0, 44.5, 47.8
Unit cell dimensions α, β, γ (°)	90, 101.3, 90
Space group	C2
Wavelength	0.91853
Number of unique reflections	83263
Resolution range (Å)	73-1.24 (1.34-1.24)
Completeness of data (%)	96.1 (94.7)
Redundancy	2.6 (2.6)
R_{sym} (%)	2.8 (55.7)
$<I/\sigma(I)>$	17.0 (2.0)
Refinement	
Maximal resolution (Å)	1.24 (1.254–1.24)
No. of atoms: protein, water	2391, 335
Monomers per asymmetric unit	1
R-factor (%)	13.9 (26.9)
R_{free} (%)	16.6 (30.7)
Wilson *B*-factor (Å^2)	21.3
R.m.s.d. bond length (Å)	0.015
R.m.s.d. bond angles (°)	1.7
Ramachandran plot[a]	96.5/3.5/0

[a] Coot: preferred regions/allowed regions/outliers.

2.6 References

1 Ehrlich, P. Über den jetzigen Stand der Chemotherapie. *Ber. Dtsch. Chem. Ges.* **42,** 17–47 (1909).

2 Kier, L. B. Molecular orbital calculation of preferred conformations of acetylcholine, muscarine, and muscarone. *Mol. Pharmacol.* **3,** 487–494 (1967).

3 Kier, L. B. *Molecular Orbital Theory in Drug Research.* pp. 164–169 (Academic Press, 1971).

4 Van Drie, J. H. Monty Kier and the origin of the pharmacophore concept. *Internet Electron. J. Mol. Des.* **6,** 271–279 (2007).

5 Wermuth, C. G., Ganellin, C. R., Lindberg, P. & Mitscher, L. A. Glossary of terms used in medicinal chemistry (IUPAC recommendations 1998). *Pure Appl. Chem.* **70,** 1129–1143 (1998).

6 Leach, A. R., Gillet, V. J., Lewis, R. A. & Taylor, R. Three-dimensional pharmacophore methods in drug discovery. *J. Med. Chem.* **53,** 539–558 (2010).

7 Koes, D. *et al.* Enabling large-scale design, synthesis and validation of small molecule protein-protein antagonists. *PLoS One* **7,** e32839 (2012).

8 Wells, J. A. & McClendon, C. L. Reaching for high-hanging fruit in drug discovery at protein-protein interfaces. *Nature* **450,** 1001–1009 (2007).

9 Rajamani, D., Thiel, S., Vajda, S. & Camacho, C. J. Anchor residues in protein–protein interactions. *Proc. Natl. Acad. Sci. U. S. A.* **101,** 11287–11292 (2004).

10 *AnchorQuery™*, http://anchorquery.csb.pitt.edu (2010).

11 Czarna, A. *et al.* Robust generation of lead compounds for protein–protein interactions by computational and MCR chemistry: p53/Hdm2 antagonists. *Angew. Chem., Int. Ed.* **49,** 5352–5356; *Angew. Chem.* **122,** 5480–5484 (2010).

12 Popowicz, G. M. *et al.* Structures of low molecular weight inhibitors bound to MDMX and MDM2 reveal new approaches for p53-MDMX/MDM2 antagonist drug discovery. *Cell Cycle* **9,** 1104–1111 (2010).

13 Huang, Y. J. *et al.* 1,4-Thienodiazepine-2,5-diones via MCR (I): synthesis, virtual space and p53-Mdm2 activity. *Chem. Biol. Drug Des.* **76,** 116–129 (2010).

14 Huang, Y. *et al.* Exhaustive fluorine scanning toward potent p53–Mdm2 antagonists. *ChemMedChem* **7,** 49–52 (2012).

15 Wang, W. *et al.* Benzimidazole-2-one: a novel anchoring principle for antagonizing p53-Mdm2. *Bioorg. Med. Chem.* **21,** 3982–3995 (2013).

16 Bista, M. *et al.* Transient protein states in designing inhibitors of the MDM2-p53 interaction. *Structure* **21,** 2143–2151 (2013).

17 Huang, Y. *et al.* Discovery of highly potent p53-MDM2 antagonists and structural basis for anti-acute myeloid leukemia activities. *ACS Chem. Biol.* **9,** 802–811 (2014).

18 Hindie, V. *et al.* Structure and allosteric effects of low-molecular-weight activators on the protein kinase PDK1. *Nat. Chem. Biol.* **5,** 758–764 (2009).

19 Lopez-Garcia, Laura A. *et al.* Allosteric regulation of protein kinase PKCζ by the N-terminal C1 domain and small compounds to the PIF-pocket. *Chem. Biol.* **18,** 14631473 (2011).

20 Gerber, P. R. & Müller, K. MAB, a generally applicable molecular force field for structure modelling in medicinal chemistry. *J. Comput.–Aided Mol. Des.* **9,** 251–268 (1995).

21 Gerber, P. R. Charge distribution from a simple molecular orbital type calculation and non-bonding interaction terms in the force field MAB. *J. Comput.–Aided Mol. Des.* **12,** 37–51 (1998).

22 Castagnoli, N. J. Condensation of succinic anhydride with *N*-benzylidene-*N*-methylamine. Stereoselective synthesis of *trans*- and *cis*-1-methyl-4-carboxy-5-phenyl-2-pyrrolidinone. *J. Org. Chem.* **34,** 3187–3189 (1969).

23 O'Hagan, D. Pyrrole, pyrrolidine, pyridine, piperidine and tropane alkaloids. *Nat. Prod. Rep.* **17,** 435–446 (2000).

24 Krasavin, M. & Dar'in, D. Current diversity of cyclic anhydrides for the Castagnoli–Cushman-type formal cycloaddition reactions: prospects and challenges. *Tetrahedron Lett.* **57,** 1635–1640 (2016).

25 Burdzhiev, N. T. & Stanoeva, E. R. Reaction between glutaric anhydride and *N*-benzylidenebenzylamine, and further transformations to new substituted piperidin-2-ones. *Tetrahedron* **62,** 8318–8326 (2006).

26 Biondi, R. M. *et al.* High resolution crystal structure of the human PDK1 catalytic domain defines the regulatory phosphopeptide docking site. *EMBO J.* **21,** 4219–4228 (2002).

27 Engel, M. *et al.* Allosteric activation of the protein kinase PDK1 with low molecular weight compounds. *EMBO J.* **25,** 5469–5480 (2006).

28 Rettenmaier, T. J. *et al.* A small-molecule mimic of a peptide docking motif inhibits the protein kinase PDK1. *Proc. Natl. Acad. Sci. U. S. A.* **111,** 18590–18595 (2014).

29 Biondi, R. M., Kieloch, A., Currie, R. A., Deak, M. & Alessi, D. R. The PIF-binding pocket in PDK1 is essential for activation of S6K and SGK, but not PKB. *EMBO J.* **20,** 4380-4390 (2001).

30 Wilcken, R., Zimmermann, M. O., Lange, A., Joerger, A. C. & Boeckler, F. M. Principles and applications of halogen bonding in medicinal chemistry and chemical biology. *J. Med. Chem.* **56,** 1363–1388 (2012).

31 Busschots, K. *et al.* Substrate-selective inhibition of protein kinase PDK1 by small compounds that bind to the PIF-pocket allosteric docking site. *Chem. Biol.* **19,** 1152–1163 (2012).

32 Najafov, A., Sommer, Eeva M., Axten, Jeffrey M., Deyoung, M. P. & Alessi, Dario R. Characterization of GSK2334470, a novel and highly specific inhibitor of PDK1. *Biochem. J.* **433,** 357–369 (2010).

33 Bissantz, C., Kuhn, B. & Stahl, M. A medicinal chemist's guide to molecular interactions. *J. Med. Chem.* **53,** 5061–5084 (2010).

34 Biondi, R. M. *et al.* Identification of a pocket in the PDK1 kinase domain that interacts with PIF and the C–terminal residues of PKA. *EMBO J.* **19,** 979–988 (2000).

35 Groebke, K., Weber, L. & Mehlin, F. Synthesis of imidazo[1,2-*a*] annulated pyridines, pyrazines and pyrimidines by a novel three-component condensation. *Synlett* **1998,** 661–663 (1998).

36 Bienaymé, H. & Bouzid, K. A new heterocyclic multicomponent reaction for the combinatorial synthesis of fused 3-aminoimidazoles. *Angew. Chem., Int. Ed.* **37,** 2234–2237; *Angew. Chem.* **110,** 2349–2352 (1998).

37 Blackburn, C., Guan, B., Fleming, P., Shiosaki, K. & Tsai, S. Parallel synthesis of 3-aminoimidazo[1,2-*a*]pyridines and pyrazines by a new three-component condensation. *Tetrahedron Lett.* **39,** 3635–3638 (1998).

38 Devi, N., Rawal, R. K. & Singh, V. Diversity-oriented synthesis of fused-imidazole derivatives via Groebke–Blackburn–Bienayme reaction: a review. *Tetrahedron* **71,** 183–232 (2015).

39 Hosseini-Sarvari, M. & Sharghi, H. ZnO as a new catalyst for *N*-formylation of amines under solvent-free conditions. *J. Org. Chem.* **71,** 6652–6654 (2006).

40 Kobiki, Y., Kawaguchi, S.-i. & Ogawa, A. Palladium-catalyzed synthesis of α-diimines from triarylbismuthines and isocyanides. *Org. Lett.* **17,** 3490–3493 (2015).

41 Corey, E. J. & Mehrotra, M. M. Total synthesis of (±)-clavulones. *J. Am. Chem. Soc.* **106,** 3384–3384 (1984).
42 Mueller, U. *et al.* Facilities for macromolecular crystallography at the Helmholtz-Zentrum Berlin. *J. Synchrotron Radiat.* **19,** 442–449 (2012).
43 Kabsch, W. XDS. *Acta Crystallogr., Sect. D: Biol. Crystallogr.* **66,** 125–132 (2010).
44 McCoy, A. J. *et al.* Phaser crystallographic software. *J. Appl. Crystallogr.* **40,** 658–674 (2007).
45 Adams, P. D. *et al.* PHENIX: a comprehensive Python-based system for macromolecular structure solution. *Acta Crystallogr., Sect. D: Biol. Crystallogr.* **66,** 213-221 (2010).
46 The Pymol Molecular Graphics System, Version 1.3, Schrödinger, LLC
47 Emsley, P., Lohkamp, B., Scott, W. G. & Cowtan, K. Features and development of Coot. *Acta Crystallogr., Sect. D: Biol. Crystallogr.* **66,** 486–501 (2010).
48 Legocki, R. P. & Verma, D. P. S. Multiple immunoreplica technique: screening for specific proteins with a series of different antibodies using one polyacrylamide gel. *Anal. Biochem.* **111,** 385–392 (1981).

Chapter 3

Li
Lithium
6.941

A new cleavable isocyanide in the Ugi tetrazole reaction

In this chapter, we introduce a new cleavable isocyanide for the Ugi tetrazole reaction. Our findings show a broad scope for the reaction, moreover, the β-cyanoethyl isocyanide is cleaved with short reaction times providing a valuable alternative to known procedures. Due to these features it could be applied in medicinal chemistry for the synthesis of biologically active 1H-tetrazoles.

Part of this chapter has been published:

Kroon, E., Kurpiewska, K., Kalinowska-Tłuścik, J. & Dömling, A. Cleavable β-Cyanoethyl Isocyanide in the Ugi Tetrazole Reaction. *Org. Lett.* **18,** 4762–4765 (2016).

The X-ray structures in this chapter are determined by Dr. K. Kurpiewska and Dr. J. Kalinowska-Tłuścik (Jagiellonian University, Poland).

3.1 Introduction

The Ugi reaction is a well-known multicomponent reaction that has a comprehensive range of starting materials.[1] Numerous reported examples revealed that aldehydes, ketones, primary or secondary amines, and isocyanides react with suitable acid components to yield a variety of scaffolds.[2–9] Moreover it is well established that multicomponent reaction chemistry has several advantages over sequential step chemistry. They show a high degree of diversity due to the nature of the starting materials, and are efficient, mild, one-pot procedures; their atom economy is remarkable since almost all atoms from the starting materials are retained in the final product (Scheme 1).[5,6]

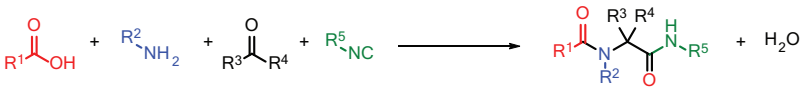

Scheme 1. The classical Ugi reaction.

The 1*H*-tetrazole moiety has attracted much attention in the field of medicinal chemistry as bioisostere of the carboxylic acid functional group. This is mainly due to a combination of a similar pK_a (4–5) and, more importantly, a tenfold higher lipophilicty, which is potentially more beneficial when cell membrane permeability is desired.[10,11]

Traditionally, there are two methods to introduce the tetrazole moiety, addition of an azide source to a nitrile or the addition of an azide source to an amide reacting through its imidoyl derivative (Scheme 2a and b).[12,13] However, both methods have limitations that include multistep synthesis of starting materials, expensive reagents, or a great amount of chemical waste. In this respect the Ugi multicomponent reaction, with trimethylsilyl azide (TMS-N_3) as acid component, is a valuable alternative, provided that an efficient method for deprotection of *N*-1 is available (Scheme 2c).[3] A large set of compounds can potentially be synthesized because most of the two retained starting materials, carbonyl and amine compounds, are commercially available, eliminating the need for starting-material synthesis.

3.2 Cleavable isocyanides

The concept of cleavable (or convertible) isocyanides was introduced as early as 1963 by Ugi with cyclohexenyl isocyanide, which can be cleaved in the Ugi reaction product using acidic conditions.[14] The concept was later extended by many

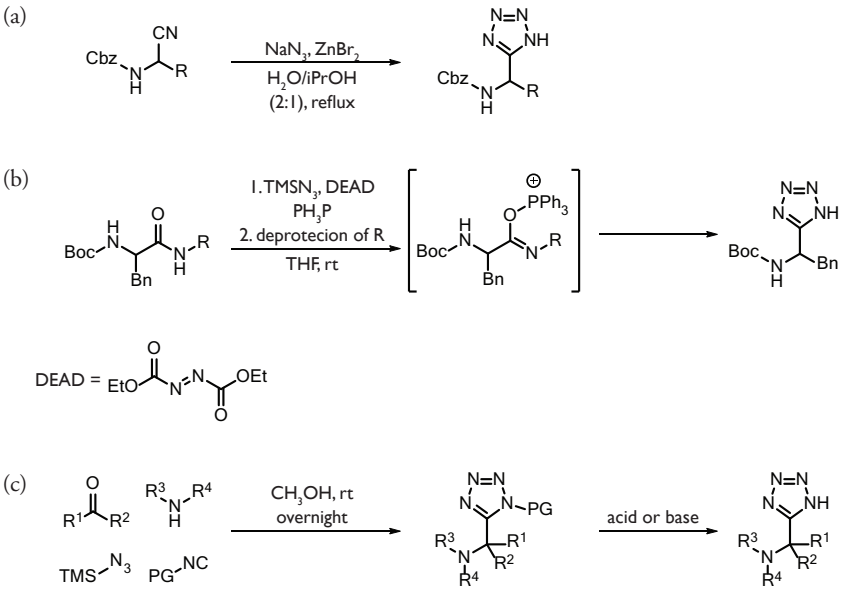

Scheme 2. Different routes to 5-substituted 1*H*-tetrazoles though (a) azide addition to a nitrile (b) azide addition to an imidoyl derivative or (c) Ugi reaction with a cleavable isocyanide.

others (Figure 1).[15–28]

Convertible isocyanides are highly useful in that they can be transformed into other functional groups during a multistep synthesis of complex molecules, e.g., natural products.[29] However, the majority of work performed concerns the transformation of the secondary amide formed during the Ugi and Passerini reactions into esters, thioesters, ketones, carboxylic acids, and other groups. For other isocyanide-based multicomponent reactions (IMCRs) not all the above quoted cleavable isocyanides may be used.

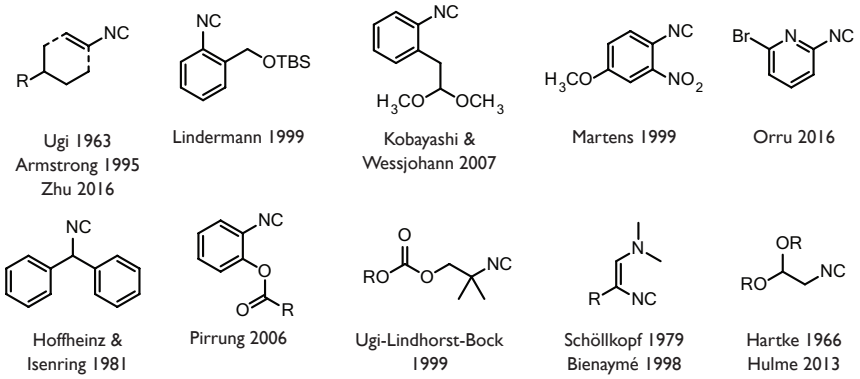

Figure 1. Previously described convertible isocyanides.

3.2.1 Cleavable isocyanides in the Ugi tetrazole synthesis

Previous acidic cleavage of isocyanides leading to tetrazoles include *tert*-butyl isocyanide (**1**),[30] benzotriazol-1-yl-methyl isocyanide (BetMIC, **2**),[31] and *tert*-octyl isocyanide (Walborsky's reagent, **3**),[31] but we were interested in the development of a cleavable isocyanide deprotected under mild conditions due to our recent focus on the Ugi tetrazole reactions (Figure 2).[32–34] The amino acid derived isocyanides **3** and **4** are cleaved under basic conditions,[35] but these cleavable isocyanides display some drawbacks. First, the deprotection takes a considerable time (overnight) with the possibility of unwanted side reactions and, second, especially the amino acid derived isocyanides require a multistep synthesis from benzaldehyde or aspartic acid (for isocyanides **3** and **4**, respectively).

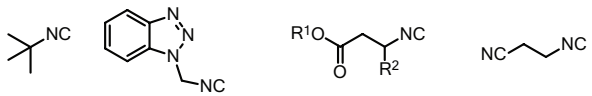

Figure 2. Cleavable isocyanides used in the synthesis of 1*H*-tetrazoles.

To overcome these issues we wanted to introduce the β-cyanoethyl protecting group which is a common phosphotriester protecting group in solid-phase oligonucleotide synthesis and cleaved under mild basic conditions (Scheme 3).[36] The β-cyanoethyl protection was previously employed in the synthesis of 5-substituted-1*H*-tetrazoles, however, it was never introduced as isocyanide component.[35] Moreover, the β-cyanoethyl isocyanide **5** (Figure 2) was described before,[37] nevertheless, it was never employed in isocyanide based multicomponent reactions. Herein an improved synthesis of β-cyanoethyl isocyanide is described as well as its use as cleavable isocyanide in the synthesis of 5-subsituted-1*H*-tetrazoles.

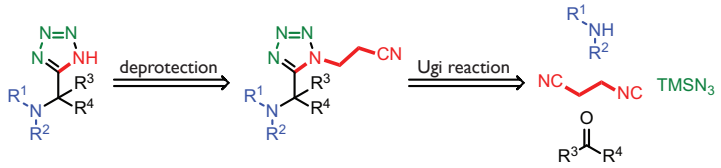

Scheme 3. Retrosynthethic pathway for our approach.

3.3 Synthesis of β-cyanoethyl isocyanide

The first step in the synthesis of β-cyanoethyl isocyanide was the formylation of commercial available 3-aminopropionitrile (**6**) with ethyl formate to obtain *N*-(cyanoethyl)formamide (**7**) in excellent yield (98%). Subsequent dehydration of the formamide was performed using standard conditions ($POCl_3/Et_3N$) to yield the isocyanide **5** in 69% yield (Scheme 4).[38] This compared well to the poor yield (16%) obtained with the Appel-type conditions used in the original procedure.[37,39] Our high purity β-cyanoethyl isocyanide, solidified at room temperature, therefore, making it practical in use and, noteworthy, lacking the appalling smell of volatile isocyanides.[40] Furthermore, the isocyanide was prepared on a large scale by this method and can be stored in the refrigerator for months.

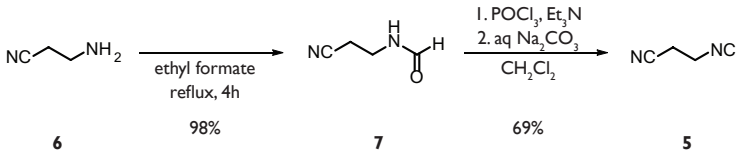

Scheme 4. Synthesis of isocyanide **5**.

3.4 Synthesis of 5-substituted-1*H*-tetrazoles

The reactivity of β-cyanoethyl isocyanide (**5**) was tested for the first time in the Ugi tetrazole reaction where it reacted smoothly with cyclohexanone (**8**), aniline (**9**) and TMS-N_3 (**10**) in methanol to obtain the Ugi product **11** in good yield (64%, Scheme 5). The overall structure of **11** was confirmed by X-ray crystallography (Figure 3).

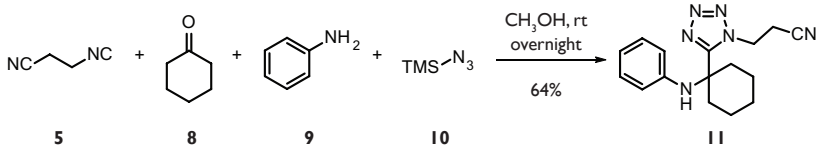

Scheme 5. First Ugi reaction with β-cyanoethyl isocyanide.

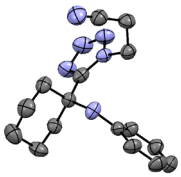

Figure 3. Single crystal X-ray strucutre of **11**.

After this initial promising result the scope of the reaction was investigated by reacting a diverse set of carbonyl components and amines to isolate the 1,5-disubstituted tetrazoles **12**–**21** in moderate to good yield (24–68%, Table 1). Aliphatic, alicyclic, and (hetero)aromatic aldehydes are accepted as carbonyl compounds and generally gave good yields; however, the Ugi products **16** and **20** containing 1-naphthaldehyde or benzo[*b*]thiophene-2-carboxaldehyde, respectively, gave a fair yield. Additionally, ketones such as cyclohexanone (**8**, Scheme 5) and acetone performed well and the Ugi products **11** and **19**, with a quaternary carbon center, were obtained in good yield. Primary aliphatic and (hetero)aromatic amines as well as secondary amines are suitable amine components, but sterically hindered 2,4,6-trimethylaniline resulted in a slightly lower yield for the Ugi product **13** (35%). Overall this shows that this particular reaction has a broad scope and, moreover, exhibits a high tolerance toward functional or protecting groups including the nitrile, Boc, trityl, and alcohol; products **14**, **17**, **18**, and **21**, respectively

Table 1. Scope of the Ugi tetrazole reaction.

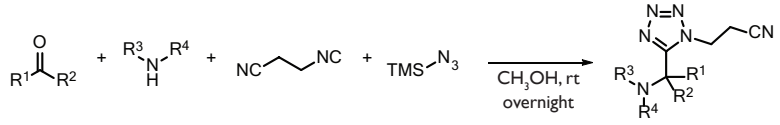

Aldehyde/ketone	amine	Product	Yield[a]
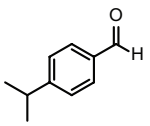	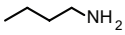	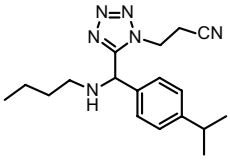 **12**	47%

[a] Isolated yield.

Aldehyde/ketone	amine	Product	Yield[a]
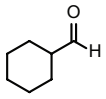	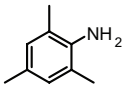	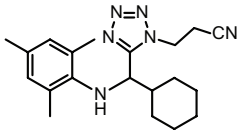 **13**	35%
	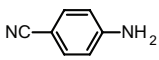	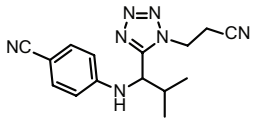 **14**	66%
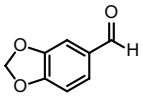		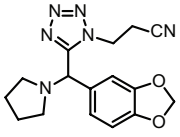 **15**	48%
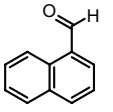		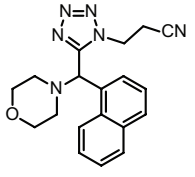 **16**	36%
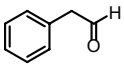	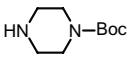	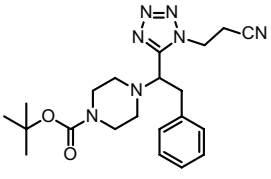 **17**	55%
	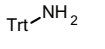	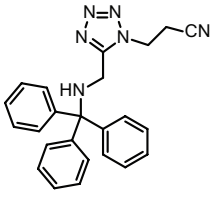 **18**	68%
	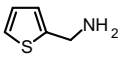	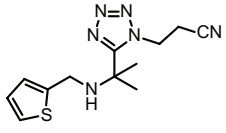 **19**	65%

[a] Isolated yield.

Aldehyde/ketone	amine	Product	Yield[a]
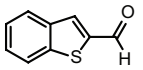		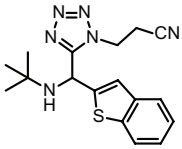 **20**	24%
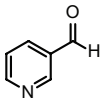	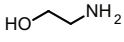	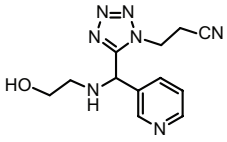 **21**	53%

[a] Isolated yield.

3.4.1 Deprotection of β-cyanoethyl isocyanide.

Attempts to cleave the Ugi products under similar conditions that are typical for β-cyanoethyl deprotection, such as DBU (1,8-Diazabicyclo[5.4.0]undec-7-ene), failed and no reaction occurred.[41] However, we were pleased to find that deprotection with lithium hydroxide gave a clean reaction and full conversion was obtained at room temperature within thirty minutes. After acidification (pH 4–5 to pH-paper), the 1*H*-tetrazole was obtained as a solid, which allowed for the convenient isolation of the products in good to excellent yield (59–93%, Table 2). Compounds that possess more bulky substituents tend to give excellent yields [**24** (91%), **28** (93%), and **29** (87%)]. Moreover, this method did not hamper the isolation of 1*H*-tetrazoles that contain highly water-soluble groups such as morpholine (**27**, 77%) and ethanolamine (**32**, 81%,).

Table 2. Deprotection of N_1-protected tetrazoles.

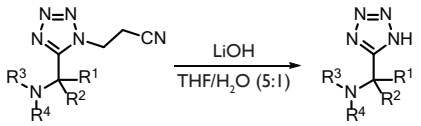

Ugi product	1*H*-tetrazole	Yield[a]
11	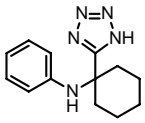 **22**	73%

[a] Isolated yield.

Ugi product	1*H*-tetrazole	Yield[a]
12	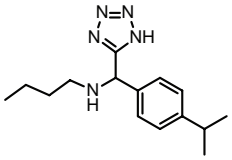 **23**	84
13	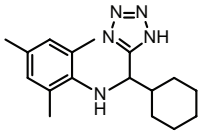 **24**	91
14	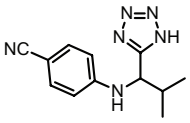 **25**	76
15	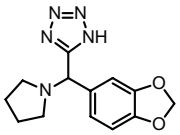 **26**	69
16	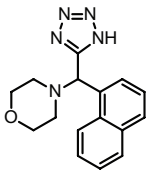 **27**	77
17	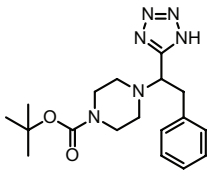 **28**	93

[a] Isolated yield.

Ugi product	1*H*-tetrazole	Yield[a]
18	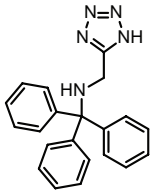 **29**	87
19	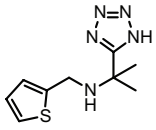 **30**	83
20	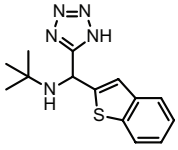 **31**	59
21	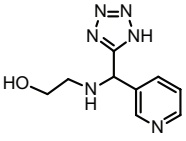 **32**	81

[a] Isolated yield.

3.4.2 Deprotection of orthogonal protecting groups

Finally, deprotection of the orthogonal acid-labile protecting groups from 1*H*-tetrazoles **17** (Boc) and **18** (trityl) was achieved under normal conditions (Scheme 6). Cleavage of the Boc group led to compound **33** that contained a highly water-soluble piperazine and, potentially, allowed for further reactions on the secondary amine. After deprotection of the trityl group from **18**, the (1*H*-tetrazol-5-yl)methanamine hydrochloride (**34**) was obtained, which is the α-amino tetrazole analogue of glycine.[42]

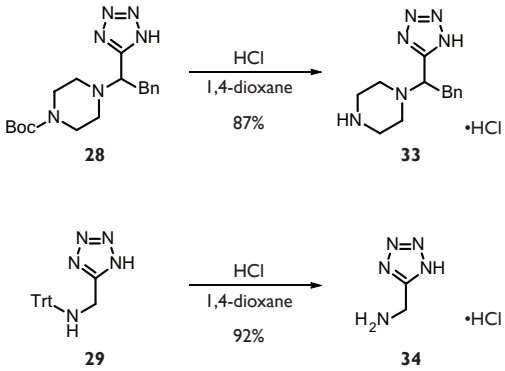

Scheme 6. Deprotection of orthogonal protecting groups.

3.5 Application of β-cyanoethyl isocyanide in the Ugi reaction

After the successful application of β-cyanoethyl isocyanide in the Ugi tetrazole reaction we wanted to extend this isocyanide to other IMCR. Reacting isobutyraldehyde (**35**), benzylamine (**36**), benzoic acid (**37**), and β-cyanoethyl isocyanide (**5**) in methanol gave the Ugi product **38** in satisfactory yield (Scheme 7).

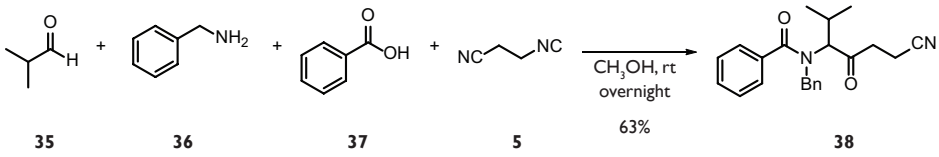

Scheme 7. Synthesis of Ugi product **38**.

Then the Ugi product was subjected to the deprotection conditions used for the Ugi tetrazole products, however, no reaction took place and starting material was recovered. Moreover, attempted deprotection with DBU resulted in the same result, starting material (Scheme 8).

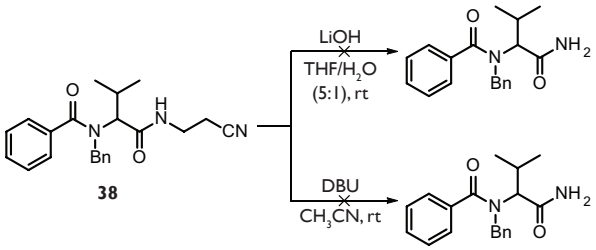

Scheme 8. Attempted deprotection of β-cyanoethyl from **38**.

The rationale behind this observation most likely lies in the intermediate that is formed during the deprotection. In the case of a β-cyanoethyl protected tetrazole **39** the intermediate's negative charge is delocalized over the aromatic ring **40** and protonation leads to the 1*H*-tetrazole 41 (Scheme 9).

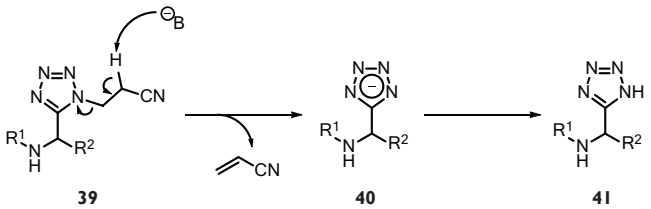

Scheme 9. Mechanism for β-cyanoethyl deprotection.

In the case of an Ugi product **42**, the primary amide anion **43a** or its resonance structure **43b**, obtained after deprotonation of the β-cyanoethyl side chain is much less stabilized than tetrazolate **40** and, thus, not forming the primary amide **44** (Scheme 10). Application of stronger bases like LiHMDS, would give a higher chance on the formation of the amidate of **42**, again not resulting in the product **44**.

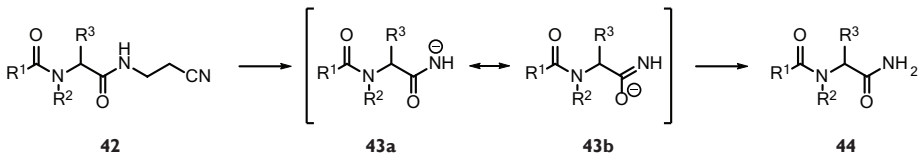

Scheme 10. Illustrative pathway of β-cyanoetyhl deprotection from Ugi product **42**.

3.6 Conclusions and outlook

The β-cyanoethyl group is widely used during the solid-phase synthesis of polynucleotides, but rarely used otherwise, despite its mild and efficient cleavage conditions. Hence, here we reported the use of the protecting group for the tetrazole moiety and its introduction in one step using β-cyanoethyl isocyanide. The herein described β-cyanoethyl isocyanide was readily synthesized from commercially available 3-aminopropionitrile in two steps and obtained as an easy to handle solid isocyanide that reacts together with a broad range of diverse ketones, aldehydes, primary or secondary amines, and TMS-azide to yield 1,5-disubstitued tetrazoles.

The 5-substituted 1*H*-tetrazoles were obtained after mild basic deprotection of the β-cyanoethyl group with short reaction times reducing unwanted side reactions and in high yields outperforming and being a vital addition to other cleavable isocyanides that are described for the Ugi tetrazole reaction.

Unfortunately, at the moment this isocyanide could not be used in other MCRs; β-cyanoethyl isocyanide could not be deprotected from an Ugi reaction product. Nevertheless, the isocyanide presented here may be valuable in the synthesis of biologically active compounds containing the 1*H*-tetrazole moiety.

3.7 Experimental section

For general remarks, see Chapter 2, Section 2.5.

_N_-(2-Cyanoethyl)formamide (7)

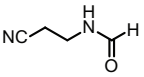

A solution of 3-aminopropionitrile (203 mmol, 15 mL) in ethyl formate (200 mL) was refluxed for five hours and subsequently stirred at room temperature overnight. The reaction was concentrated *in vacuo* and further dried under high vacuum. The product was obtained as a light yellow oil (199 mmol, 19.5 g, 98%). ^{1}H NMR (500 MHz, $CDCl_3$) δ 8.21 (s, 1H), 7.35 (br, 1H), (q, J = 12.7, 6.3, 2H), 2.66 (t, J = 6.4, 2H); ^{13}C NMR (126 MHz, $CDCl_3$) δ 165.00, 162.25, 118.29, 117.67, 37.80, 34.13, 20.36, 18.23 (a mixture of amide rotamers is observed).

3-Isocyanopropanenitrile (5)

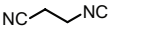

To a solution of *N*-(2-cyanoethyl)formamide (199 mmol, 19.5 g) in CH_2Cl_2 (400 mL) was added Et_3N (1.0 mol, 139 mL, 5.0 equiv.). The mixture was cooled to -5 °C at which $POCl_3$ (209 mmol, 19.5 mL, 1.05 equiv.) was added dropwise over 60 minutes maintaining the temperature below 0 °C. After the addition the reaction was stirred at 0°C for an additional hour. An aqueous solution of Na_2CO_3 (0.6 M, 100 mL) was added carefully while the temperature increased to 20°C. Additional water was added until all salts were dissolved (~300 mL). The mixture was transferred to a separatory funnel and the organic layer was separated. The water layer was extracted with CH_2Cl_2 (200 mL). The combined organic layers were washed with brine (100 mL), dried over $MgSO_4$, and concentrated *in vacuo*. The crude product was purified by filtration over silica (100% CH_2Cl_2) and after evaporation of the solvent obtained as a pale yellow oil (11 g, 138 mmol, 69 %) which solidified upon standing. A pure sample (white solid) was obtained by trituration of a concentrated CH_2Cl_2 solution with petroleum ether at 0 °C. Melting point: 32 °C (lit.[37] 32 °C); IR (neat, υ, cm^{-1}): 2256 (w), 2151(s), 1453 (m), 1425 (m), 1358 (m), 1335 (w), 1259 (w), 1219 (w), 1015 (m), 978 (m), 926 (w), 818 (m, br), 586 (m); ^{1}H NMR (500 MHz, $CDCl_3$) δ 3.72 (t, J = 6.6, 2H), 2.81 (t, J = 6.5, 2H); ^{13}C NMR (126 MHz, $CDCl_3$) δ 160.01, 115.92, 37.68, 18.85.

General procedure for the Ugi tetrazole reaction

A solution of aldehyde or ketone (1.05 mmol) and amine (1.0 mmol) in methanol (1 mL, 1.0 M) was stirred at room temperature for 15 minutes. Subsequently, isocyanide (1.0 mmol, 80 mg) and TMS azide (1.0 mmol, 133 μL) were added and the reaction

was stirred at room temperature overnight. The reaction was concentrated *in vacuo* and purified by column chromatography.

3-(5-(1-(Phenylamino)cyclohexyl)-1*H*-tetrazol-1-yl)propanenitrile (11)

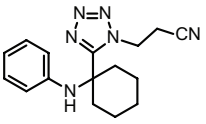

Obtained from cyclohexanone (109 µL) and aniline (91 µL) as a white solid (189 mg, 0.64 mmol, 64%). R_f = 0.50 (60% EtOAc/petroleum ether); ^{1}H NMR (500 MHz, $CDCl_3$) δ 7.09 (t, *J* = 7.5, 2H), 6.79 (t, *J* = 7.4, 1H), 6.25 (d, *J* = 7.7, 2H), 4.86 (t, *J* = 7.4, 2H), 4.18 (s, 1H), 2.81 (t, *J* = 7.4, 2H), 2.29 (d, *J* = 13.6, 2H), 2.24 – 2.10 (m, 2H), 1.78 – 1.71 (m, 3H), 1.64 – 1.49 (m, 2H), 1.49 – 1.37 (m, 1H);^{13}C NMR (126 MHz, $CDCl_3$) δ 159.61, 143.56, 129.74, 119.99, 115.95, 115.08, 99.98, 54.26, 43.90, 34.31, 24.74, 20.96, 18.11; MS (ESI): *m/z* (%): 242.03 (100)[M^+-$(CH_2)_2CN$].The overall structure was determined by single crystal X-ray crystallography. The supplementary crystallographic data can be obtained, free of charge, from the Cambridge Crystallographic Data Centre (CCDC 1479665).

3-(5-((Butylamino)(4-isopropylphenyl)methyl)-1*H*-tetrazol-1-yl) propanenitrile (12)

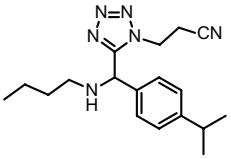

Obtained from n-butylamine (99 µL) and 4-isopropylbenzaldehyde (159 µL) as a pale yellow oil (154 mg, 0.47 mmol, 47%). R_f = 0.33 (40% EtOAc/petroleum ether); ^{1}H NMR (500 MHz, $CDCl_3$) δ 7.29 (d, *J* = 7.9, 2H), 7.25 (d, *J* = 8.3, 2H), 5.39 (s, 1H), 4.74 – 4.57 (m, 2H), 2.91 (quint, *J* = 7.0 , 1H), 2.85 – 2.60 (m, 4H), 2.52 (dt, *J* = 11.4, *J* = 7.2, 1H), 1.95 (br, 1H), 1.61 – 1.44 (m, 2H), 1.44 – 1.28 (m, 2H), 1.23 (d, *J* = 7.0, 6H), 0.89 (t, *J* = 7.4, 3H); ^{13}C NMR (126 MHz, $CDCl_3$) δ 156.14, 149.69, 134.63, 127.41, 126.91, 116.04, 57.46, 47.83, 43.03, 33.79, 32.01, 23.90, 20.37, 17.92, 13.96; MS (ESI): *m/z* (%): 327.28 (100)[M^++H].

3-(5-(Cyclohexyl(mesitylamino)methyl)-1*H*-tetrazol-1-yl)propanenitrile (13)

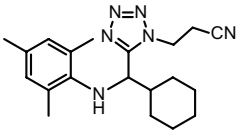

Obtained from cyclohexylcarboxaldehyde (127 µL) and 2,4,6-trimethylaniline (140 µL) as a white solid (122 mg, 0.35 mmol, 35%). R_f = 0.37 (25% EtOAc/petroleum ether); ^{1}H NMR (500 MHz, $CDCl_3$) δ 6.77 (s, 2H), 4.04 – 3.85 (m, 2H), 3.70 (ddd, *J* = 13.7, *J* = 8.9, *J* = 4.5, 1H), 3.27 (d, *J* = 12.3, 1H), 2.76 – 2.57 (m, 2H), 2.44 – 2.29 (m, 1H), 2.20 (s, 3H), 2.01 (s, 6H), 1.94 – 1.81 (m, 2H), 1.80 – 1.67 (m, 2H), 1.52 – 1.13 (m, 5H), 1.10 – 0.90 (m, 1H); ^{13}C NMR (126 MHz, $CDCl_3$) δ 157.43, 140.35, 133.54, 130.82, 130.29, 115.64, 56.86, 42.10, 42.02, 30.59, 30.41, 26.56, 26.19, 26.08, 20.68, 18.19, 18.07; MS (ESI): *m/z* (%):

375.33 (100)[M^++Na].

4-((1-(1-(2-Cyanoethyl)-1*H*-tetrazol-5-yl)-2-methylpropyl)amino)benzonitrile (14)

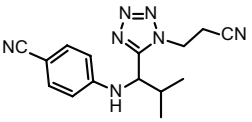

Obtained from 4-aminobenzonitrile (118 mg) and isobutyraldehyde (96 µL) as a white gummy solid (179 mg, 0.66 mmol, 66%). R_f = 0.26 (50% EtOAc/petroleum ether); ^{1}H NMR (500 MHz, $CDCl_3$) δ 7.39 (d, *J* = 8.6, 1H), 6.73 (d, *J* = 8.7, 1H), 5.70 (d, *J* = 7.3, 1H), 4.86 – 4.70 (m, 2H), 3.06 (qt, *J* = 17.1, *J* = 6.8, 1H), 2.54–2.34 (m, 1H), 1.16 (d, *J* = 6.6, 3H), 0.96 (d, *J* = 6.7, 3H); ^{13}C NMR (126 MHz, $CDCl_3$) δ 155.53, 150.04, 134.01, 120.15, 116.38, 112.89, 100.00, 54.55, 43.37, 32.56, 19.34, 19.16, 18.34; MS (ESI): *m/z* (%): 241.06 (100) [M^--$(CH_2)_2CN$].

3-(5-(Benzo[*d*][1,3]dioxol-5-yl(pyrrolidin-1-yl)methyl)-1*H*-tetrazol-1-yl) propanenitrile (15)

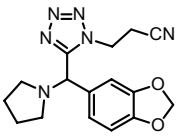

Obtained from piperonal (158 mg) and pyrrolidine (84 µL) as a white solid (156 mg, 0.48 mmol, 48%). R_f = 0.26 (50% EtOAc/petroleum ether); ^{1}H NMR (500 MHz, $CDCl_3$) δ 7.00 – 6.88 (m, 2H), 6.82 – 6.78 (m, 1H), 5.97 (s, 2H), 4.99 (s, 1H), 4.85 – 4.66 (m, 1H), 3.05 – 2.86 (m, 1H), 2.84 – 2.72 (m, 2H), 2.72–2.57 (m, 2H), 2.49 – 2.33 (m, 2H), 1.93 – 1.76 (m, 4H); ^{13}C NMR (126 MHz, $CDCl_3$) δ 155.75, 148.61, 148.10, 130.12, 121.44, 115.94, 108.77, 108.31, 101.71, 64.33, 53.10, 43.18, 23.65, 18.01; MS (ESI): *m/z* (%): 327.33 (100)[M^++H], 349.24 (55) [M^++Na].

3-(5-(Morpholino(naphthalen-1-yl)methyl)-1*H*-tetrazol-1-yl)propanenitrile (16)

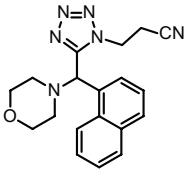

Obtained from 1-naphthaldehyde (143 µL) and morpholine (87 µL) as a pale yellow oil (125 mg, 0.36 mmol, 36%). R_f = 0.26 (50% EtOAc/petroleum ether); ^{1}H NMR (500 MHz, $CDCl_3$) δ 8.43 (d, *J* = 8.5, 1H), 7.87 (dd, *J* = 8.1, *J* = 4.2, 2H), 7.68 (d, *J* = 7.2, 1H), 7.57 (t, *J* = 7.7, 1H), 7.52 (t, *J* = 7.6, 2H), 5.87 (s, 1H), 4.51 (ddq, *J* = 21.0, *J* = 14.0, *J* = 7.1, 2H), 3.82 – 3.71 (m, 4H), 2.91 – 2.76 (m, 2H), 2.69 (dt, *J* = 16.9, *J* = 7.0, 1H), 2.53 (dt, *J* = 16.9, *J* = 7.1, 1H), 2.49 – 2.38 (m, 2H); ^{13}C NMR (126 MHz, $CDCl_3$) δ 154.03, 134.36, 131.35, 130.22, 129.79, 129.19, 127.46, 126.68, 126.04, 125.08, 123.34, 115.87, 67.01, 61.79, 52.12, 43.25, 17.85; MS (ESI): *m/z* (%): 371.25 (100)[M^++Na].

***tert*-Butyl 4-(1-(1-(2-cyanoethyl)-1*H*-tetrazol-5-yl)-2-phenylethyl)piperazine-1-carboxylate (17)**

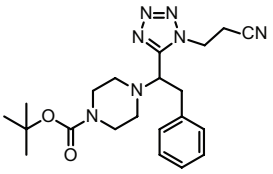

Obtained from phenylacetaldehyde (123 μL) and 1-Boc-piperazine (186 mg) as an off-white solid (125 mg, 0.30 mmol, 30%). R_f = 0.27 (50% EtOAc/petroleum ether); ^{1}H NMR (500 MHz, $CDCl_3$) δ 7.32–7.16 (m, 3H), 7.13 (d, *J* = 6.9, 2H), 4.51 – 4.24 (m, 2H), 4.15 (dd, *J* = 10.2, *J* = 3.8, 1H), 3.55 – 3.36 (m, 5H), 3.30 (dd, *J* = 13.2, 3.7, 1H), 2.96 – 2.79 (m, 1H), 2.70 (br, 2H), 2.65 – 2.50 (m, 3H), 1.45 (s, 9H); ^{13}C NMR (126 MHz, $CDCl_3$) δ 154.70, 154.15, 137.51, 129.54, 129.06, 127.23, 115.80, 80.27, 62.24, 49.23, 42.63, 33.86, 28.58, 18.24; MS (ESI): *m/z* (%): 334.26 (100) [(*M*-Boc)$^+$+Na], 434.33 (75) [*M*$^+$+Na].

3-(5-((Tritylamino)methyl)-1*H*-tetrazol-1-yl)propanenitrile (18.

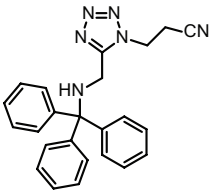

Obtained from paraformaldehyde (32 mg) and tritylamine (259 mg) as a white solid (269 mg, 0.68 mmol, 68%). R_f = 0.24 (40% EtOAc/petroleum ether); ^{1}H NMR (500 MHz, $CDCl_3$) δ 7.45 (d, *J* = 7.8, 6H), 7.33 (t, *J* = 7.6, 6H), 7.29 – 7.17 (m, 3H), 4.44 (t, *J* = 6.9, 2H), 3.85 (d, *J* = 7.6, 2H), 2.94 (t, *J* = 6.9, 2H); ^{13}C NMR (126 MHz, CDCl3) δ 154.11, 144.24, 128.55, 128.32, 127.14, 115.58, 71.33, 42.61, 36.87, 18.62; MS (ESI): *m/z* (%): 340.33 (100)[*M*$^+$-$(CH_2)_2$CN].

3-(5-(2-((Thiophen-2-ylmethyl)amino)propan-2-yl)-1*H*-tetrazol-1-yl) propanenitrile (19.

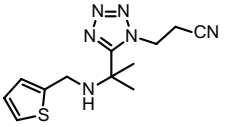

Obtained from acetone (88 μL) and 2-thiophenemethylamine (103 μL) as a pale yellow solid (180 mg, 0.65 mmol, 65%). R_f = 0.25 (40% EtOAc/petroleum ether); ^{1}H NMR (500 MHz, $CDCl_3$) δ 7.23 (dd, *J* = 5.1, *J* = 1.1, 1H), 6.94 (dd, *J* = 5.1, 3.5, 1H), 6.86 (dd, *J* = 3.3, *J* = 0.8, 1H), 5.11 (t, *J* = 7.3, 2H), 3.80 (d, *J* = 5.8, 2H), 3.12 (t, *J* = 7.3, 2H), 1.75 (s, 6H); ^{13}C NMR (126 MHz, $CDCl_3$) δ 158.64, 142.53, 127.00, 124.92, 124.73, 116.02, 53.74, 44.08, 42.71, 27.66, 18.39; MS (ESI): *m/z* (%): 299.22 (100)[*M*$^+$+Na].

3-(5-(Benzo[*b*]thiophen-2-yl(*tert*-butylamino)methyl)-1*H*-tetrazol-1-yl) propanenitrile (20.

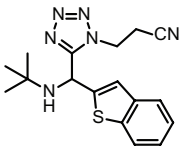

Obtained from 2-benzothiophene (170 mg) and *tert*-butylamine (105 μL) as a white solid (82 mg, 0.24 mmol, 24%). R_f = 0.25 (25% EtOAc/petroleum ether); ^{1}H NMR (500 MHz, $CDCl_3$) δ 7.86 – 7.75 (m, 1H), 7.75 – 7.63 (m, 1H), 7.44 – 7.30 (m, 1H), 7.01 (s, 1H), 6.06 (s, 1H), 5.01 – 4.77 (m, 2H), 3.08 (ddd, *J* = 16.8, *J* = 8.0, *J* = 6.8, 1H), 2.97 (ddd, *J* = 16.8, *J* = 8.0, *J* = 6.5, 1H), 1.87 (s, 1H), 1.14 (s, 9H); ^{13}C NMR (126 MHz, $CDCl_3$) δ 156.79, 143.38, 139.28, 139.22, 125.46, 125.30, 124.17, 122.64, 122.24, 116.06, 52.88, 49.63, 43.89, 29.45, 18.09; MS (ESI): *m/z* (%): 363.24 (100)[M^++Na].

3-(5-(((2-Hydroxyethyl)amino)(pyridin-3-yl)methyl)-1*H*-tetrazol-1-yl) propanenitrile (21)

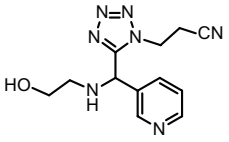

Obtained from ethanolamine (60 μL) and 3-pyridinecarboxaldehyde (122 μL) as a pale yellow oil (144 mg, 0.53 mmol, 53%). R_f = 0.35 (15% CH_3OH/CH_2Cl_2); ^{1}H NMR (500 MHz, $CDCl_3$) δ 8.66 (d, *J* = 1.8, 1H), 8.53 (d, *J* = 4.7, 1H), 7.84 (d, *J* = 8.0, 1H), 7.35 (dd, *J* = 7.9, *J* = 4.8, 1H), 5.49 (s, 1H), 4.97 – 4.66 (m, 2H), 3.81 – 3.50 (m, 2H), 3.21 – 2.98 (m, 2H), 2.84 – 2.54 (m, 2H); ^{13}C NMR (126 MHz, $CDCl_3$) δ 155.56, 149.50, 148.76, 135.40, 133.08, 123.82, 116.54, 60.85, 54.56, 48.96, 43.03, 18.06; MS (ESI): *m/z* (%): 296.22 (100)[M^++Na], 274.24 (40)[M^++H].

General procedure for β-cyanoethyl deprotection

To a solution of protected tetrazole (50 mg) in THF/H_2O (5:1, 1mL) was added LiOH (2.0 equiv.). The resulting suspension was stirred at room temperature for 30 min. The reaction was concentrated to dryness and water (500 μL) was added. The solution was cooled to 0 °C and acidified to pH 4–5 with HCl (0.1 M). The precipitate was collected by filtration, washed with cold water and dried under high vacuum.

***N*-(1-(1*H*-Tetrazol-5-yl)cyclohexyl)aniline (22)**

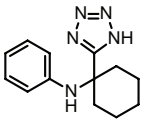

Obtained from protected tetrazole **11** as an off-white solid (30 mg, 0.12 mmol, 73%). ^{1}H NMR (500 MHz, $CDCl_3$) δ 7.04 (t, *J* = 7.9, 2H), 6.72 (t, *J* = 7.4, 1H), 6.25 (d, *J* = 8.0, 2H), 2.21 (d, *J* = 13.4, 2H), 2.14 – 2.02 (m, 2H), 1.73 – 1.60 (m, 3H), 1.60 – 1.46 (m, 2H), 1.46 – 1.32 (m, 1H); ^{13}C NMR (126 MHz, $CDCl_3$) δ 163.17, 143.75, 129.49,

119.56, 115.93, 54.07, 34.84, 25.05, 21.19; MS (ESI): *m/z* (%): 242.13 (100)[*M*$^+$-H].

_N_-((4-Isopropylphenyl)(1_H_-tetrazol-5-yl)methyl)butan-1-amine (23)

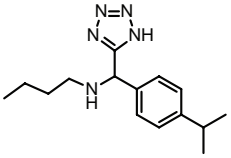

Obtained from protected tetrazole **12** as a white solid (35 mg, 0.13 mmol, 84%). ^{1}H NMR (500 MHz, $CDCl_3$) δ 7.41 (d, *J* = 8.3, 2H), 7.11 (d, *J* = 8.2, 2H), 5.91 (s, 1H), 3.09 – 2.91 (m, 1H), 2.83 (ddd, *J* = 14.0, *J* = 9.6, *J* = 6.3, 4H), 1.72 – 1.57 (m, 1H), 1.57 – 1.47 (m, 1H), 1.23 – 1.17 (m, 2H), 1.16 (d, *J* = 6.9, 7H), 0.74 (t, *J* = 7.4, 3H); ^{13}C NMR (126 MHz, $CDCl_3$) δ 158.00, 150.41, 131.49, 128.33, 127.31, 58.34, 46.72, 33.93, 28.01, 23.91, 23.85, 19.98, 13.55; MS (ESI): *m/z* (%): 272.25 (100)[*M*$^+$-H].

_N_-(Cyclohexyl(1_H_-tetrazol-5-yl)methyl)-2,4,6-trimethylaniline (24)

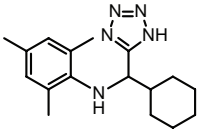

Obtained from protected tetrazole **13** as a white solid (39 mg, 0.13 mmol, 91%). ^{1}H NMR (500 MHz, $CDCl_3$) δ 6.74 (s, 2H), 4.40 (dd, *J* = 9.3, 6.1, 1H), 2.18 (s, 3H), 2.16 – 2.03 (m, 8H), 1.85 – 1.76 (m, 1H), 1.70 (t, *J* = 14.8, 2H), 1.61 (d, *J* = 11.7, 1H), 1.39 – 1.21 (m, 3H), 1.20 – 1.07 (s, 1H), 1.07 – 0.94 (m, 1H); ^{13}C NMR (126 MHz, $CDCl_3$) δ 159.04, 141.40, 132.07, 130.21, 129.14, 58.39, 43.01, 29.73, 29.28, 26.42, 26.29, 26.24, 20.68, 18.85; MS (ESI): *m/z* (%): 298.20 (100)[*M*$^+$-H].

4-((2-Methyl-1-(1_H_-tetrazol-5-yl)propyl)amino)benzonitrile (25)

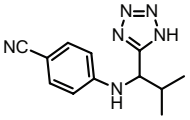

Obtained from protected tetrazole **14** as an off-white solid (31 mg, 0.13 mmol, 76 %). ^{1}H NMR (500 MHz, $CDCl_3$) δ 7.24 (d, *J* = 8.8, 2H), 6.50 (d, *J* = 8.8, 2H), 5.35 (d, *J* = 7.2, 1H), 4.86 (t, *J* = 6.4, 1H), 2.36 (dq, *J* = 13.4, *J* = 6.7, 1H), 1.11 (d, *J* = 6.8, 3H), 0.96 (d, *J* = 6.8, 3H); ^{13}C NMR (126 MHz, $CDCl_3$) δ 158.82, 150.01, 133.95, 120.16, 113.05, 99.85, 54.74, 33.41, 19.06, 18.91. MS (ESI): m/z (%): 241. 17 (100)[*M*$^+$-H].

5-(Benzo[*d*][1,3]dioxol-5-yl(pyrrolidin-1-yl)methyl)-1_H_-tetrazole (26)

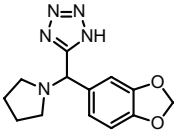

Obtained from protected tetrazole **15** as a white solid (29 mg, 0.11 mmol, 69%). ^{1}H NMR (500 MHz, CD_3OD) δ 7.18 (s, 1H), 7.13 (d, *J* = 8.0, 1H), 6.87 (d, *J* = 8.0, 1H), 5.99 (d, *J* = 6.7, 2H), 5.68 (s, 1H), 3.35 (s, 2H), 3.26 – 3.09 (m, 2H), 2.13 – 1.97 (m, 4H); ^{13}C NMR (126 MHz, CD_3OD) δ 158.03, 149.29, 148.61, 126.59, 123.56, 108.51, 108.30, 101.88, 64.41, 53.61, 22.81; MS (ESI): *m/z* (%): 272.08

(100)[*M*-H].

4-(Naphthalen-1-yl(1*H*-tetrazol-5-yl)methyl)morpholine (27)

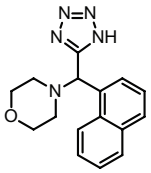

Obtained from protected tetrazole **16** as a white solid (33 mg, 0.11 mmol, 77%). ^{1}H NMR (500 MHz, $CDCl_3$) δ 8.44 (d, *J* = 7.4, 1H), 7.90 – 7.80 (m, 2H), 7.78 (d, *J* = 8.2, 1H), 7.51 – 7.42 (m, 2H), 7.35 (t, *J* = 7.7, 1H), 5.93 (s, 1H), 3.84 – 3.54 (m, 4H), 2.84 – 2.64 (m, 2H), 2.60 – 2.38 (m, 2H); ^{13}C NMR (126 MHz, $CDCl_3$) δ 157.52, 134.25, 131.49, 131.37, 129.89, 129.30, 127.27, 127.19, 126.41, 125.61, 123.22, 66.58, 52.26; MS (ESI): *m/z* (%): 294.12 (100)[*M*-H].

***tert*-Butyl 4-(2-phenyl-1-(1*H*-tetrazol-5-yl)ethyl)piperazine-1-carboxylate (28)**

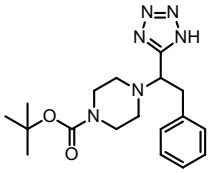

Obtained from protected tetrazole **17** as a white solid (41 mg, 0.11 mmol, 93 %). ^{1}H NMR (500 MHz, $CDCl_3$) δ 7.25–7.00 (m, 5H), 4.45 – 4.23 (m, 1H), 3.48 – 3.17 (m, 6H), 2.51 (dd, *J* = 36.6, *J* = 4.6, 4H), 1.42 (s, 9H); ^{13}C NMR (126 MHz, $CDCl_3$) δ 154.98, 137.47, 129.19, 128.60, 126.80, 80.45, 61.48, 49.33, 36.72, 28.46; MS (ESI): *m/z* (%): 357.18 (100)[*M*-H].

***N*-((1*H*-Tetrazol-5-yl)methyl)-1,1,1-triphenylmethanamine (29)**

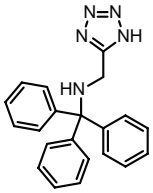

Obtained from protected tetrazole **18** as a white solid (38 mg, 0.11 mmol, 87%). ^{1}H NMR (500 MHz, $CDCl_3$) δ 7.51 (d, *J* = 7.8, 6H), 7.27 (t, *J* = 7.6, 6H), 7.19 (t, *J* = 7.2, 3H), 3.65 (s, 2H); ^{13}C NMR (126 MHz, DMSO) δ 155.82, 145.29, 128.41, 127.88, 126.37, 70.57, 38.04; MS (ESI): *m/z* (%): 340.33 (100)[*M*-H].

2-(1*H*-Tetrazol-5-yl)-*N*-(thiophen-2-ylmethyl)propan-2-amine (30)

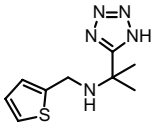

Obtained from protected tetrazole **19** as a white solid (34 mg, 0.15 mmol, 83%). ^{1}H NMR (500 MHz, CD_3OD) δ 7.55 (d, *J* = 5.0, 1H), 7.25 (d, *J* = 3.2, 1H), 7.19 – 7.03 (m, 1H), 4.32 (s, 2H), 1.88 (s, 6H); ^{13}C NMR (126 MHz, CD_3OD) δ 163.42, 134.25, 131.59, 129.32, 128.79, 59.08, 42.07, 25.66; MS (ESI): *m/z* (%): 222.09 (100)[*M*-H].

***N*-(Benzo[*b*]thiophen-2-yl(1*H*-tetrazol-5-yl)methyl)-2-methylpropan-2-amine (31)**

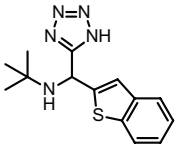

Obtained from protected tetrazole **20** as a white solid (25 mg, 0.09 mmol, 59%). ^{1}H NMR (500 MHz, DMSO) δ 8.03 – 7.86 (m, 1H), 7.80 (dd, *J* = 6.8, *J* = 1.9, 1H), 7.47 (s, 1H), 7.40 – 7.24 (m, 2H), 6.08 (s, 1H), 1.12 (s, 9H); ^{13}C NMR (126 MHz, DMSO)

δ 159.08, 139.55, 138.93, 124.59, 124.46, 123.80, 123.35, 122.45, 49.10, 27.44; MS (ESI): *m/z* (%): 286.09 (100)[*M*-H].

2-((Pyridin-3-yl(1*H*-tetrazol-5-yl)methyl)amino)ethan-1-ol (32)

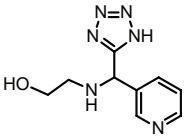

Obtained from protected tetrazole **21** as a white solid (33 mg, 0.15 mmol, 81%). ^{1}H NMR (500 MHz, DMSO) δ 8.76 (s, 1H), 8.56 – 8.54 (m, 1H), 7.98 (d, *J* = 8.0, 1H), 7.43 (dd, *J* = 7.9, *J* = 4.8, 1H), 5.74 (s, 1H), 3.69 – 3.50 (m, 3H), 2.80 (dd, *J* = 9.7, *J* = 5.7, 3H); ^{13}C NMR (126 MHz, DMSO) δ 157.62, 149.97, 149.65, 136.45, 132.46, 123.56, 57.39, 55.39, 48.16; MS (ESI): *m/z* (%): 219.03 (100)[*M*-H].

1-(2-Phenyl-1-(1*H*-tetrazol-5-yl)ethyl)piperazine hydrochloride (33)

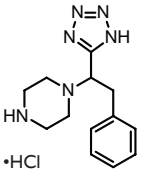

To a suspension of 1*H*-tetrazole **28** (35 mg, 0.1 mmol) in 1,4-dioxane (1 mL) was added 4.0 M HCl in dioxane (125 μL, 0.5 mmol). The reaction became clear and was stirred at room temperature overnight. The reaction was concentrated *in vacuo* and ether (5 mL) was added to the residue. The solid was collected by filtration, washed with ether (2 mL) and dried under vacuum. The product was obtained a white solid (25 mg, 0.085 mmol, 87 %). ^{1}H NMR (500 MHz, D_2O) δ 7.23 (dt, *J* = 8.6, *J* = 6.8, 3H), 7.17 – 7.04 (m, 2H), 4.90 – 4.81 (m, 1H), 3.72 (s, 2H), 3.43 – 3.36 (m, 4H), 3.25 – 3.00 (m, 4H); ^{13}C NMR (126 MHz, D_2O) δ 154.29, 135.35, 129.04, 128.79, 127.27, 66.52, 60.75, 46.11, 42.45, 35.40; MS (ESI): *m/z* (%): 257.21(100) [*M*-H].

(1*H*-Tetrazol-5-yl)methanamine hydrochloride (34)

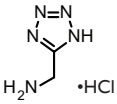

To a suspension of 1*H*-tetrazole **29** (168 mg, 0.49 mmol) in 1,4-dioxane (2.5 mL) was added 4.0 M HCl in dioxane (250 μL, 1 mmol). The reaction was stirred at room temperature for 5 min. The reaction was purified by filtration through silica. The impurities were eluted with EtOAc/petroleum ether (1:1, 30 mL). The product was eluted with CH_3OH/CH_2Cl_2 (3:1, 30 mL), and concentrated *in vacuo*. The product was obtained as a white solid (97 mg, 0.45 mmol, 92%). ^{1}H NMR (500 MHz, D_2O) δ 4.36; ^{13}C NMR (126 MHz, DMSO) δ 34.71; MS (ESI): *m/z* (%): 98.17 (100)[*M*-H].

***N*-Benzyl-*N*-(1-((2-cyanoethyl)amino)-2-methylpropyl)benzamide (38)**

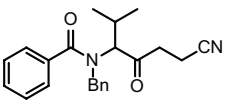

A solution of isobutyraldehyde (91 μL, 1.0 mmol) and benzylamine (109 μL, 1.0 mmol) in methanol (1.0 mL) was stirred at rt for 15 min. Then benzoic acid (122 mg, 1.0

mmol) and β-cyanoethyl isocyanide (80 mg, 1.0 mmol) were added and the reaction mixture stirred overnight at rt. The solvent was evaporated and the residue purified by column chromatography. The product was obtained as a pale yellow oil (219 mg, 0.63 mmol, 63%). R_f = 0.26 (50% EtOAc/petroleum ether); ^{1}H NMR (500 MHz, $CDCl_3$) δ 8.18 (s, 1H), 7.62 – 7.34 (m, 5H),7.22 (t, *J* = 6.0, 3H), 7.05 (d, *J* = 5.7, 2H), 4.57 (dd, *J* = 84.4, 15.6, 2H), 4.04 (d, *J* =10.9, 1H), 3.45 – 3.14 (m, 2H), 2.88 – 2.66 (m, 1H), 2.50 - 2.21 (m, 2H), 1.07 (d, *J* =6.4, 3H), 0.99 (d, *J* = 6.3, 3H); ^{13}C NMR (126 MHz, $CDCl_3$) δ 174.12, 171.01, 136.61, 136.33, 130.07, 128.73, 128.42, 127.75, 127.69, 126.93, 118.21, 68.16, 53.25, 35.40, 26.96, 19.96, 19.42, 17.82; MS (ESI): *m/z* (%): 362.13 (100)[*M*-H].

3.8 References

1 Ugi, I. & Steinbrückner, C. Über ein neues kondensations-prinzip. *Angew. Chem.* **72,** 267–268 (1960).

2 Ugi, I. Neuere methoden der präparativen organischen chemie IV mit sekundär-reaktionen gekoppelte α-additionen von immonium-ionen und anionen an isonitrile. *Angew. Chem.* **74,** 9–22; *Angew. Chem., Int. Ed. Engl.* **1,** 8–21 (1962).

3 Dömling, A. & Ugi, I. Multicomponent reactions with isocyanides. *Angew. Chem., Int. Ed.* **39,** 3168–3210; *Angew. Chem.* **112,** 3300–3344 (2000).

4 Ignacio, J. M., Macho, S., Marcaccini, S., Pepino, R. & Torroba, T. A facile synthesis of 1,3,5-trisubstituted hydantoins via Ugi four-component condensation. *Synlett* **2005,** 3051–3054 (2005).

5 Dömling, A. Recent developments in isocyanide based multicomponent reactions in applied chemistry. *Chem. Rev.* **106,** 17–89 (2006).

6 Dömling, A., Wang, W. & Wang, K. Chemistry and biology of multicomponent reactions. *Chem. Rev.* **112,** 3083–3135 (2012).

7 Khoury, K., Sinha, M. K., Nagashima, T., Herdtweck, E. & Dömling, A. Efficient assembly of iminodicarboxamides by a "truly" four-component reaction. *Angew. Chem., Int. Ed.* **51,** 10280–10283; *Angew. Chem.* **124,** 10426–10429 (2012).

8 Liu, H., William, S., Herdtweck, E., Botros, S. & Dömling, A. MCR synthesis of praziquantel derivatives. *Chem. Biol. Drug Des.* **79,** 470–477 (2012).

9 Zhao, T., Boltjes, A., Herdtweck, E. & Dömling, A. Tritylamine as an ammonia surrogate in the Ugi tetrazole synthesis. *Org. Lett.* **15,** 639–641 (2013).

10 Herr, R. J. 5-Substituted-1*H*-tetrazoles as carboxylic acid isosteres: medicinal chemistry and synthetic methods. *Bioorg. Med. Chem.* **10,** 3379–3393 (2002).

11 Meanwell, N. A. Synopsis of some recent tactical application of bioisosteres in drug design. *J. Med. Chem.* **54,** 2529–2591 (2011).

12 Duncia, J. V., Pierce, M. E. & Santella, J. B. Three synthetic routes to a sterically hindered tetrazole. A new one-step mild conversion of an amide into a tetrazole. *J. Org. Chem.* **56,** 2395–2400 (1991).

13 Demko, Z. P. & Sharpless, K. B. An expedient route to the tetrazole analogues of α-amino acids. *Org. Lett.* **4,** 2525–2527 (2002).

14 Ugi, I. & Rosendahl, F. K. Isonitrile, XV. Δ^1-cyclohexenyl-isocyanid. *Justus Liebigs Ann. Chem.* **666,** 65–67 (1963).

15 Walborsky, H. M. & Niznik, G. E. Synthesis of isonitriles. *J. Org. Chem.* **37,** 187–190 (1972).

16 Schöllkopf, U., Porsch, P.-H. & Lau, H.-H. Synthesen mit α-metallierten isocyaniden, XLIV. Notiz über β-dimethylamino-α-isocyanacrylsäureester und ihre verwendung in der heterocyclenchemie. *Liebigs Ann. Chem.* **1979,** 1444–1446 (1979).

17 Isenring, H. P. & Hofheinz, W. A simple two-step synthesis of diphenylmethyl esters of 2-oxo-1-azetidineacetic acids. *Synthesis* **1981,** 385–387 (1981).

18 Katritzky, A. R., Chen, Y.-X., Yannakopoulou, K. & Lue, P. Benzotriazol-1-ylmethyl isocyanide, a new synthon for CH-N=C transfer. Syntheses of α-hydroxyaldehydes, 4-ethoxy-2-oxazolines and oxazoles. *Tetrahedron Lett.* **30,** 6657–6660 (1989).

19 Keating, T. A. & Armstrong, R. W. Molecular diversity via a convertible isocyanide in the Ugi four-component condensation. *J. Am. Chem. Soc.* **117,** 7842–7843 (1995).

20 Linderman, R. J., Binet, S. & Petrich, S. R. Enhanced diastereoselectivity in the asymmetric Ugi reaction using a new "convertible" isonitrile. *J. Org. Chem.* **64,** 336–337 (1999).

21 Lindhorst, T., Bock, H. & Ugi, I. A new class of convertible isocyanides in the Ugi four-component reaction. *Tetrahedron* **55,** 7411–7420 (1999).

22 Pirrung, M. C. & Ghorai, S. Versatile, fragrant, convertible isonitriles. *J. Am. Chem. Soc.* **128,** 11772–11773 (2006).

23 Isaacson, J., Gilley, C. B. & Kobayashi, Y. Expeditious access to unprotected racemic pyroglutamic acids. *J. Org. Chem.* **72,** 3913–3916 (2007).

24 Hulme, C., Chappeta, S. & Dietrich, J. A simple, cheap alternative to 'designer convertible isonitriles' expedited with microwaves. *Tetrahedron Lett.* **50,** 4054–4057 (2009).

25 Le, H. V., Fan, L. & Ganem, B. A practical and inexpensive 'convertible' isonitrile for use in multicomponent reactions. *Tetrahedron Lett.* **52,** 2209–2211 (2011).

26 Neves Filho, R. A. W., Stark, S., Morejon, M. C., Westermann, B. & Wessjohann, L. A. 4-Isocyanopermethylbutane-1,1,3-triol (IPB): a convertible isonitrile for multicomponent reactions. *Tetrahedron Lett.* **53,** 5360–5363 (2012).

27 Spallarossa, M., Wang, Q., Riva, R. & Zhu, J. Synthesis of vinyl isocyanides and development of a convertible isonitrile. *Org. Lett.* **18,** 1622–1625 (2016).

28 van der Heijden, G., Jong, J. A. W., Ruijter, E. & Orru, R. V. A. 2-Bromo-6-isocyanopyridine as a universal convertible isocyanide for multicomponent chemistry. *Org. Lett.* **18,** 984–987 (2016).

29 Gilley, C. B., Buller, M. J. & Kobayashi, Y. New entry to convertible isocyanides for the Ugi reaction and its application to the stereocontrolled formal total synthesis of the proteasome inhibitor omuralide. *Org. Lett.* **9,** 3631–3634 (2007).

30 Tukulula, M. *et al.* The design, synthesis, in silico ADME profiling, antiplasmodial and antimycobacterial evaluation of new arylamino quinoline derivatives. *Eur. J. Med. Chem.* **57,** 259–267 (2012).

31 Dömling, A., Beck, B. & Magnin-Lachaux, M. 1-Isocyanomethylbenzotriazole and 2,2,4,4-tetramethylbutylisocyanide — cleavable isocyanides useful for the preparation of α-aminomethyl tetrazoles. *Tetrahedron Lett.* **47,** 4289–4291 (2006).

32 Liao, G. P. *et al.* Versatile multicomponent reaction macrocycle synthesis using α-Isocyano-ω-carboxylic acids. *Org. Lett.* **17,** 4980–4983 (2015).

33 Boltjes, A., Shrinidhi, A., van de Kolk, K., Herdtweck, E. & Dömling, A. Gd-TEMDO: design, synthesis, and MRI application. *Chem. – Eur. J.* **22,** 7352–7356 (2016).

34 Patil, P., de Haan, M., Kurpiewska, K., Kalinowska-Tłuścik, J. & Dömling, A. Versatile protecting-group free tetrazolomethane amine synthesis by Ugi reaction. *ACS Comb. Sci.* **18,** 170–175 (2016).

35 Mayer, J. *et al.* New cleavable isocyanides for the combinatorial synthesis of α-amino acid analogue tetrazoles. *Tetrahedron Lett.* **46,** 7393–7396 (2005).

36 Letsinger, R. L. & Ogilvie, K. K. Nucleotide chemistry. XIII. Synthesis of oligothymidylates via phosphotriester intermediates. *J. Am. Chem. Soc.* **91,** 3350–3355 (1969).

37 Schrumpf, G. & Martin, S. Conformational equilibrium and vibrational spectra of 2-isocyano ethylcyanide. *J. Mol. Struct.* **101,** 57–67 (1983).

38 Hoffman, P., Gokel, G., Marquarding, D. & Ugi, I. in *Isonitrile Chemistry* (ed Ugi, I.) 9–17 (Academic Press, 1971).

39 Appel, R. Tertiary phosphane/tetrachloromethane, a versatile reagent for chlorination, dehydration, and P–N linkage. *Angew. Chem., Int. Ed. Engl.* **14,** 801–811; *Angew. Chem.* **87,** 863–874 (1975).

40 "The development of the chemistry of isonitriles has probably suffered only little delay through the characteristic odour of volatile isonitriles, which has been described by Hofmann and Gaultier as highly specific, almost overpowering, horrible, and extremely distressing." from Ugi, I., Fetzer, U., Eholzer, U., Knupfer, H. & Offermann, K. Isonitrile syntheses. *Angew. Chem., Int. Ed. Engl.* **4,** 472–484; *Angew. Chem.* **77,** 492–504 (1965).

41 Tosquellas, G., Bologna, J. C., Morvan, F., Rayner, B. & Imbach, J.-L. First synthesis of alternating SATE-phosphotriester/ phosphodiester prooligonucleotides on solid support. *Bioorg. Med. Chem. Lett.* **8,** 2913–2918 (1998).

42 Zhao, T., Kurpiewska, K., Kalinowska-Tłuścik, J., Herdtweck, E. & Dömling, A. α-Amino acid-isosteric α-amino tetrazoles. *Chem. – Eur. J.* **22,** 3009–3018 (2016).

Chapter 4

4
Be
Beryllium
9.012

Towards a cyclic mixed anhydride in the Castagnoli reaction

In this chapter, we investigate the possibility of extending the Castagnoli reaction towards other cyclic anhydrides. We report a route towards a cyclic mixed anhydride and its attempted application in the Castagnoli reaction.

4.1 The Castagnoli reaction

The Castagnoli (or Castagnoli–Cushman) reaction is the addition of imines to cyclic anhydrides, for the first time described by Neal Castagnoli Jr. He obtained pyrrolidinones **1** from the condensation of benzaldehyde-derived imines **2** with succinic anhydride (**3**, Scheme 1).[1] In a similar fashion piperidinones (six-membered ring) were obtained from the condensation of imines with glutaric anhydride.[2] These chemical structures are prevalent motifs in natural products (*e.g.*, lactacystin **4**) and biologically active compounds like doxapram (**5**) (Figure 1).[3,4]

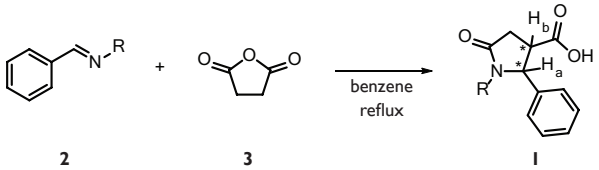

Scheme 1. The first reported Castagnoli reaction.

Theoretically four possible products are possible; two diastereomers (*cis* and *trans*) each consisting of two enantiomers. Although, Castagnoli did not mention diastereomeric ratios, he observed that by preferential crystallization the *trans*-isomer was obtained as major product of the reaction mixture; the *cis*-diastereomer was obtained in small quantities.[1] Nuclear magnetic resonance (NMR) spectroscopy was used as tool to distinguish the diastereomers; based on the estimated dihedral angles and the Karplus relationship the coupling constant between H_a and H_b for the *trans*-isomer is around five hertz (Hz), whereas the *cis*-isomer has a coupling constant around nine Hz.[1,5]

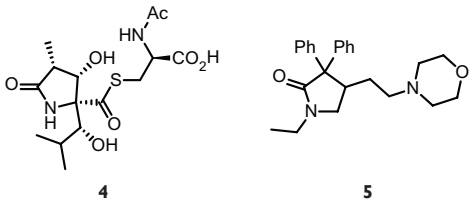

Figure 1. Lactacystin (**4**) and doxapram (**5**).

After the initial disclosure of the Castagnoli reaction, research mainly focused on expanding the cyclic anhydride component of the reaction. It was expanded to homophthalic anhydride (**6**), heterocyclic derivatives of homophthalic anhydride (**7**),

substituted succinc **8** or glutaric anhydride **9** and, more recently, glutaric anhydride derivatives with an additional heteroatom in the ring (e.g. **10**) were introduced (Figure 2).[6,7]

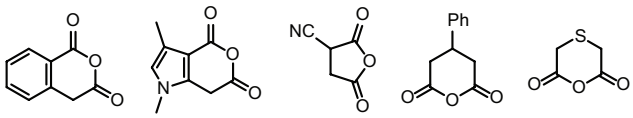

6 **7** **8** **9** **10**

Figure 2. Illustrative examples of cyclic anhydrides.

The imine component, on the other hand, has never been varied since the discovery, it is limited to non-enolizable aliphatic or aromatic imines; enolizable imines tend to be acylated with the cyclic anhydride.[8] In general, non-polar solvents like toluene are used for the Castagnoli reaction; it was observed that the boiling point of the solvent has an influence on the yield of the reaction (after a fixed time); high boiling solvents resulted in high yields and highly diastereoselective formation of the *trans*-isomer.[9] Recently, *N*,*N*-dimethylformamide was used as solvent in the reaction resulting in considerable formation of *cis*-Castagnoli products, moreover, the solvent-free Castagnoli reaction was reported; high temperatures (>150 °C) are still required to obtain satisfactory yields.[10,11] Finally, the Castagnoli is a three-component reaction, thus lending itself greatly for parallel synthesis of lead-oriented libraries.[12]

4.1.1 Reaction mechanism

Since its discovery, three possible reaction pathways were proposed for the Castagnoli reaction including an imino Diels–Alder, Perkin, and iminolysis mechanism (Scheme 2).[13] In the case of succinic or glutaric anhydride, the imino Diels-Alder pathway is not possible, moreover, after performing experiments and examining the substitution effects the Perkin pathway was placed towards the background, supporting the iminolysis pathway.[14] This was later backed-up by molecular orbital (MO) theory and density functional (DFT) calculations, although thought to be more concerted in nature.[13] Recently, the mechanism of the reaction between imines and cyanosuccinic anhydride was examined with DFT calculations, also. There a Mannich-cyclization was proposed, because the zwitterionic intermediates in the iminolysis pathway were calculated to be too high in energy compared to the intermediates in the Mannich-cyclization pathway.[15]

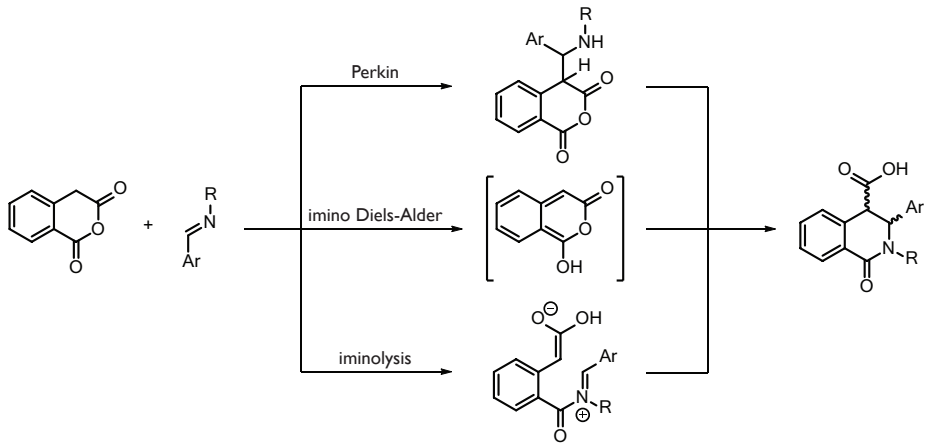

Scheme 2. Three plausible reaction pathways of imine addition to homophthalic anhydride.

The first step in the iminolysis pathway is the formation of the imine **13** through condensation of the aldehyde **11** and amine **12** (Scheme 3). Then the nitrogen lone pair attacks the succinic anhydride (**3**) to form the zwitterionic intermediate **9**, which, after enolization, forms intermediate **15** that cyclizes to the final product **16**.

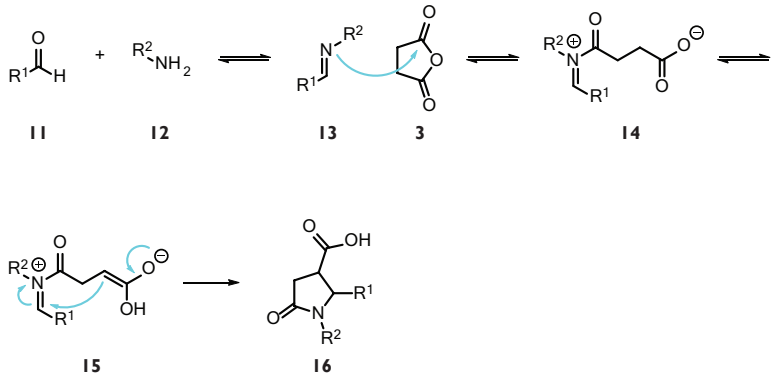

Scheme 3. The iminolysis pathway.

In the Mannich-cyclization pathway, a Mannich reaction occurs between the iminium ion **17** and enolized anhydride **18** to form neutral species **19** (Scheme 4). After intermolecular addition of the amine to the carbonyl of the anhydride followed by anhydride ring opening to the product **16**.

Although, there is evidence supporting both mechanism no consensus has

been reached; less reactive cyclic anhydrides tend to follow the iminolysis pathway, while the intermediates may be high in energy, high temperatures are needed to progress the reaction.[1,13,14,16] The more reactive cyclic anhydrides, with an electron-withdrawing group, are more likely to follow the Mannich-cyclization pathway, these reactions progress well at room temperature.[15,17,18]

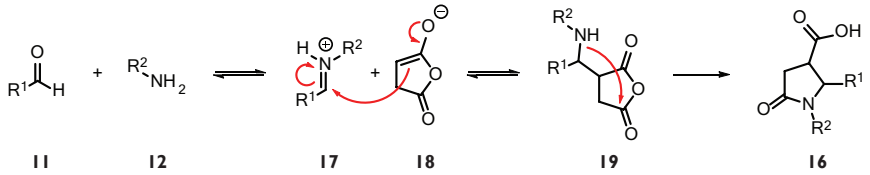

Scheme 4. The Mannich-cyclization pathway.

4.2 Cyclic mixed anhydrides

The majority of the research conducted on the Castagnoli reaction was focused on expanding the scope of the cyclic anhydride component.[6] In all reported cases symmetrical anhydrides were used, nevertheless, several cyclic mixed anhydrides between carboxylic and sulfonic acids are reported that could potentially be applied in the Castagnoli reaction as well. (Figure 3).[19-21]

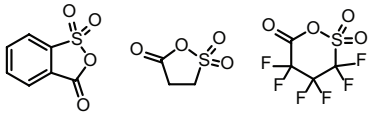

Figure 3. Reported cyclic mixed sulfocarboxylic anhydrides.

These cyclic mixed anhydrides are very moisture-sensitive compounds hydrolyzing back to the di-acid starting material, therefore, *in situ* generation is preferred. The six-membered mixed anhydride **20**, the glutaric anhydride analogue, can be prepared from the corresponding 4-sulfobutanoic acid (**21**) (Scheme 5).

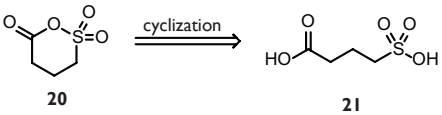

Scheme 5. Retrosynthetic pathway for compound **20**.

4.2.1 Synthesis of 4-sulfobutanoic acid

Synthesis of **21** was attempted by the Strecker sulfite alkylation of 4-bromobutyric acid (**22**) with aqueous sodium sulfite (Scheme 6).[22] However, it proved difficult to obtain the water-soluble acid free from all salts, moreover, column chromatography on silica with methanol as described in literature was not sufficient to even remotely elute the sulfocarboxylic acid.[23]

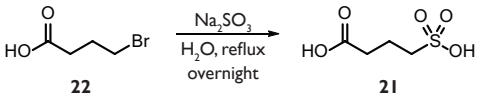

Scheme 6. Attempted synthesis of **21** from 4-bromobutyric acid (**22**).

Fortunately, other strategies to synthesize a precursor for the cyclic mixed anhydride **20** (e.g. sulfonyl chloride) that do not involve large quantities of water are known.[24–26] The sulfonyl chloride **23** can be obtained by oxidation of the corresponding thiol **24** (Scheme 7), while the thiol was commercially available it was relative expensive, however, the corresponding disulfide was reasonably priced and could be converted to the sulfonyl chloride by a similar reaction.

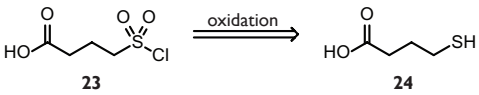

Scheme 7. Retrosynthetic pathway for sulfonyl chloride **23**.

Reduction of the disulfide **25** to the thiol *in situ* and subsequent oxidation to the sulfonyl chloride **23** was achieved in one-pot with *N*-chlorosuccinimide in good yield (67%, Scheme 8).[25]

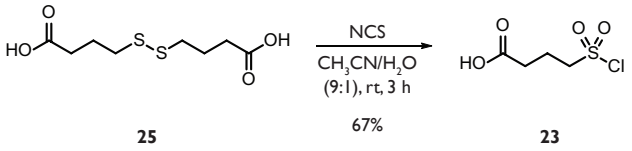

Scheme 8. Synthesis of sulfonyl chloride **21**.

4.3 Castagnoli reaction with a cyclic mixed anhydride

Before attempting the Castagnoli reaction, the cyclization of sulfonyl chloride **23** to the cyclic mixed anhydride **20** was performed with pyridine followed by nucleophilic ring opening.[27] Addition of pyridine to sulfonyl chloride **23** and subsequent addition of two equivalents 4-chlorobenzylamine gave the 4-chlorobenzylammmonium salt of the sulfonic acid **26** in 72% yield (Scheme 9).

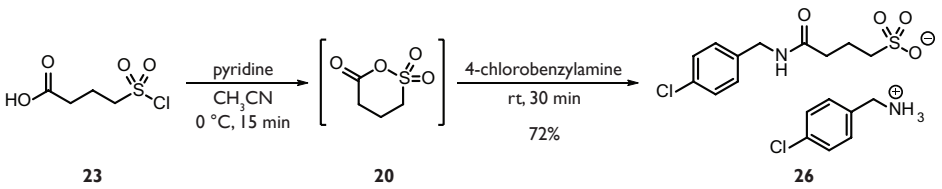

Scheme 9. Confirmation of cyclic mixed anhydride formation.

To investigate the Castagnoli reaction similar conditions were tested as for the formation of **26**, however, in three different dry solvents (THF, CH_3CN, or *p*-xylene) and with pre-formed imine **27** (Scheme 10). After addition of the pyridine, the reaction was stirred for fifteen minutes to facilitate anhydride **20** formation, the imine was added in little solvent and the reaction subsequently heated at 80 °C. In all the cases the reaction did not show any progress towards piperidinone **28** formation, moreover, no useful side product(s) were obtained to investigate what happened during the course of the reaction.

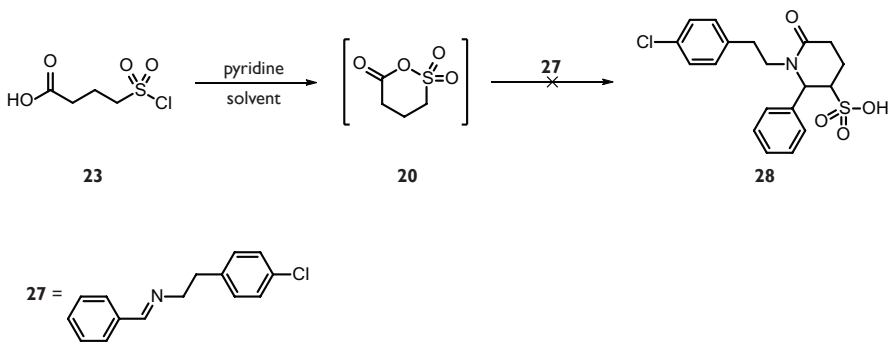

Scheme 10. Attempted Castagnoli reaction with the cyclic mixed anhydride.

Several reasons may have caused a failed reaction: first, if the cyclic mixed anhydride reacted with the carboxylate of unreacted **23**, homocoupling would be the

result. Second, when during the course of the reaction a small amount of imine reversed back to aldehyde and amine, the free amine may have reacted with the anhydride resulting in the formation of sulfonic acid similar to **26**. Third, if the reaction would progress through the iminolysis pathway, at a certain point intermediate **29** would be formed, this type of enol sulfonate is not known (Figure 4). In the other case, when the reaction follows the Mannich-cyclization pathway, intermediate **30** would be formed to get the desired product, which has not been reported before (Figure 4). Finally, formation of aliphatic sulfenes has been described in the literature, thus deprotonation at the α-CH_2 adjacent the sulfonyl chloride would generate sulfene **31**, a highly reactive compound that could react with unreacted sulfonyl chloride (Figure 4).[28–30]

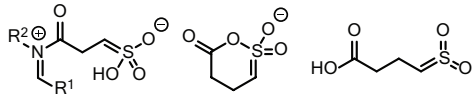

Figure 4. Potential intermediates in the Castagnoli reaction.

4.4 Conclusions and outlook

Unfortunately, obtaining the sulfocarboxylic acid from either γ-butyrolactone or 4-bromobutyric acid was unsuccessful. However, the sulfonyl chloride derivative was obtained by NCS oxidation of the corresponding disulfide in good yield. The formation of the cyclic mixed anhydride appeared to work, the 4-chlorbenzylamide was obtained from the anhydride. Nevertheless, the cyclic anhydride was not successfully applied in the Castagnoli reaction most likely due to the reactivity of the sulfonyl chloride or the cyclic mixed anhydride as well as the potential formation of unlikely intermediates. Nevertheless, the sulfonyl chloride or perhaps a more stable derivative like **32** (Figure 5) could be applied in the synthesis of sulfocarboxylic derivatives by employing different nucleophiles (*e.g.*, alcohols).[27]

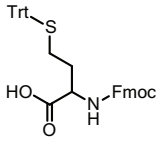

Figure 5. More stable precursor for the cyclic mixed anhydride.

4.5 Experimental section

For general remarks, see Chapter 2, Section 2.5.

4-(Chlorosulfonyl)butanoic acid (23)

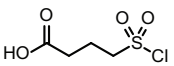

To a 250 mL round bottom flask was added 4,4'-dithiodibutyric acid (2.4 g, 10 mmol) and CH_3CN/H_2O (10:1, 22 mL). The suspension was cooled to 0 °C and NCS (8,0 g, 60 mmol) was added in one portion. The reaction was slowly warmed and at 5 °C a vigorous reaction took place causing the temperature to rise to 35 °C. After stirring the reaction at room temperature for 3 hours the reaction was evaporated to dryness and to the residue was added chloroform. The precipitated succinimide was removed by filtration and the filtrate evaporated to dryness. The residue was purified by column chromatography (SiO_2, EtOAc/petroleum ether) and dried under high vacuum. The title compound was obtained as pale pink solid (2.4 g, 13 mmol, 64%). ^{1}H NMR (500 MHz, DMSO) δ 2.72 – 2.56 (t, *J* = 7.4, 2H), 2.32 (t, *J* = 7.4, 2H), 1.91 – 1.62 (m, 2H); ^{13}C NMR (126 MHz, DMSO) δ 174.29, 50.55, 32.49, 20.46; HRMS (ESI): *m/z*: found: 167.0020, calculated for hydrolysed sulfonyl chloride: 167.0020. Indicating that the sulfonyl chloride is very prone to hydrolysis

(4-Chlorophenyl)methanaminium 4-((4-chlorobenzyl)amino)-4-oxobutane-1-sulfonate (26)

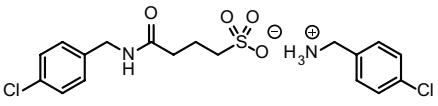

A solution of 4-(chlorosulfonyl)butanoic acid (168 mg, 1.0 mmol) in dry CH_3CN (5 mL) under nitrogen was cooled to 0 °C and pyridine (101 µL, 1.25 mmol, 1.25 equiv.) was added dropwise. After 15 min. at the same temperature, 4-chlorobenzylamine (243 µL, 2.0 mmol, 2.0 equiv.) was added dropwise and the reaction stirred at room temperature for 30 min. The formed precipitate was collected by filtration and recrystallized from ethanol. The title compounds was obtained as white solid (312 mg, 0.72 mmol, 72%). ^{1}H NMR (500 MHz, DMSO) δ 8.35 (s, 1H), 8.17 (s, 1H), 7.52 – 7.47 (m, 2H), 7.36 (d, *J* = 8.3, 1H), 7.25 (d, *J* = 8.3, 1H), 4.23 (d, *J* = 5.9, 1H), 4.04 (s, 1H), 2.42 (t, *J* = 7.6, 1H), 2.22 (t, *J* = 7.5, 1H), 1.86 – 1.77 (m, 1H); ^{13}C NMR (126 MHz, DMSO) δ 172.11, 138.88, 133.23, 132.99, 131.17, 130.88, 128.99, 128.54, 128.19, 50.86, 41.59, 41.31, 34.59, 21.66; HRMS (ESI): *m/z*: calculated sulfonate: 290.02593, found:290.02594.

4.6 References

1 Castagnoli, N., Jr. The condensation of succinic anhydride with benzylidinemethylamine. A stereoselective synthesis of *trans*- and *cis*-1-methyl-4-carbosy-5-phenyl-2-pyrrolidinone. *J. Org. Chem.* **34,** 3187–3189 (1969).

2 Cushman, M. & Castagnoli, N. Novel approach to the synthesis of nitrogen analogs of the tetrahydrocannabinols. *J. Org. Chem.* **38,** 440–448 (1973).

3 O'Hagan, D. Pyrrole, pyrrolidine, pyridine, piperidine and tropane alkaloids. *Nat. Prod. Rep.* **17,** 435–446 (2000).

4 Ng, P. Y., Tang, Y., Knosp, W. M., Stadler, H. S. & Shaw, J. T. Synthesis of diverse lactam carboxamides leading to the discovery of a new transcription-factor inhibitor. *Angew. Chem., Int. Ed.* **46,** 5352–5355; *Angew. Chem.* **119,** 10572–10593 (2007).

5 Karplus, M. Contact electron-spin coupling of nuclear magnetic moments. *J. Chem. Phys.* **30,** 11–15 (1959).

6 González-López, M. & Shaw, J. T. Cyclic anhydrides in formal cycloadditions and multicomponent reactions. *Chem. Rev.* **109,** 164–189 (2009).

7 Krasavin, M. & Dar'in, D. Current diversity of cyclic anhydrides for the Castagnoli–Cushman-type formal cycloaddition reactions: prospects and challenges. *Tetrahedron Lett.* **57,** 1635–1640 (2016).

8 Dar'in, D., Bakulina, O., Chizhova, M. & Krasavin, M. New heterocyclic product space for the Castagnoli–Cushman three-component reaction. *Org. Lett.* **17,** 3930–3933 (2015).

9 Burdzhiev, N. T. & Stanoeva, E. R. Reaction between glutaric anhydride and *N*-benzylidenebenzylamine, and further transformations to new substituted piperidin-2-ones. *Tetrahedron* **62,** 8318–8326 (2006).

10 Lepikhina, A., Bakulina, O., Dar'in, D. & Krasavin, M. The first solvent-free synthesis of privileged γ- and δ-lactams via the Castagnoli-Cushman reaction. *RSC Adv.* **6,** 83808–83813 (2016).

11 Dar'in, D., Bakulina, O., Nikolskaya, S., Gluzdikov, I. & Krasavin, M. The rare *cis*-configured trisubstituted lactam products obtained by the Castagnoli-Cushman reaction in *N,N*-dimethylformamide. *RSC Adv.* **6,** 49411–49415 (2016).

12 Ryabukhin, S. V. *et al.* Toward lead-oriented synthesis: one-pot version of Castagnoli condensation with nonactivated alicyclic anhydrides. *ACS Comb. Sci.* **16,** 146–153 (2014).

13 Kaneti, J., Bakalova, S. M. & Pojarlieff, I. G. Schiff base addition to cyclic dicarboxylic anhydrides: an unusual concerted reaction. An MO and DFT theoretical study. *J. Org. Chem.* **68,** 6824–6827 (2003).

14 Cushman, M. & Madaj, E. J. A study and mechanistic interpretation of the electronic and steric effects that determine the stereochemical outcome of the reaction of Schiff bases with homophthalic anhydride and 3-phenylsuccinic anhydride. *J. Org. Chem.* **52,** 907–915 (1987).

15 Pattawong, O., Tan, D. Q., Fettinger, J. C., Shaw, J. T. & Cheong, P. H.-Y. Stereocontrol in asymmetric γ-lactam syntheses from imines and cyanosuccinic anhydrides. *Org. Lett.* **15,** 5130–5133 (2013).

16 Wei, J. & Shaw, J. T. Diastereoselective synthesis of γ-lactams by a one-pot, four-component reaction. *Org. Lett.* **9,** 4077–4080 (2007).

17 Sorto, N. A. *et al.* Diastereoselective synthesis of γ- and δ-lactams from imines and sulfone-substituted anhydrides. *J. Org. Chem.* **79,** 2601–2610 (2014).

18 Liu, J. *et al. N*-Methylimidazole promotes the reaction of homophthalic anhydride with imines. *J. Org. Chem.* **79,** 7593–7599 (2014).

19 Clarke, H. T. & Dreger, E. E. *o*-Sulfobenzoic anhydride. *Org. Synth.* **9,** 80 (1929).

20 Kharasch, M. S. & Brown, H. C. Chlorinations with sulfuryl chloride. III. (a) The peroxide-catalyzed chlorination of aliphatic acids and acid chlorides. (b) The photochemical sulfonation of aliphatic acids. *J. Am. Chem. Soc.* **62,** 925–929 (1940).

21 Koshar, R. J. Cyclic sulfoperfluoroaliphaticcarboxylic acid anhydrides. US4332954 A (1982).

22 Strecker, A. Ueber eine neue bildungsweise und die constitution der sulfosäuren. *Justus Liebigs Ann. Chem.* **148,** 90–96 (1868).

23 Jariwala, F. B., Wood, R. E., Nishshanka, U. & Attygalle, A. B. Formation of the bisulfite anion (HSO_3^-, *m/z* 81) upon collision-induced dissociation of anions derived from organic sulfonic acids. *J. Mass Spectrom.* **47,** 529–538 (2012).

24 Yang, Z. & Xu, J. Convenient and environment-friendly synthesis of sulfonyl chlorides from *S*-alkylisothiourea salts via *N*-chlorosuccinimide chlorosulfonation. *Synthesis* **45,** 1675–1682 (2013).

25 Kirihara, M. *et al.* Oxidation of disulfides with electrophilic halogenating reagents: concise methods for preparation of thiosulfonates and sulfonyl halides. *Tetrahedron* **70,** 2464–2471 (2014).

26 Qiu, K. & Wang, R. *tert*-Butyl hypochlorite mediated oxidative chlorination of *S*-Alkylisothiourea salts: synthesis of sulfonyl chlorides. *Synthesis* **47,** 3186–3190 (2015).

27 Joyard, Y., Papamicaël, C., Bohn, P. & Bischoff, L. Synthesis of sulfonic acid derivatives by oxidative deprotection of thiols using *tert*-butyl hypochlorite. *Org. Lett.* **15,** 2294–2297 (2013).

28 Opitz, G. Sulfines and sulfenes – the *S*-oxides and *S*,*S*-dioxides of thioaldehydes and thioketones. *Angew. Chem., Int. Ed. Engl.* **6,** 107–123; *Angew. Chem.* **79,** 161–177 (1967).

29 King, J. F. & Lee, T. W. S. Mechanism of formation of sulfenes by dehydrohalogenation of alkanesulfonyl chlorides. *J. Am. Chem. Soc.* **91,** 6524–6525 (1969).

30 King, J. F. Return of sulfenes. *Acc. Chem. Res.* **8,** 10–17 (1975).

Chapter 5

B
Boron
10.811

Domino transformations: additions to C=N bonds and nitriles

In this chapter, we discuss the latest applications of domino transformations in organic synthesis with a special focus on additions to carbon–nitrogen double bonds and nitriles. After a short introduction, different strategies on C=N bonds additions are discussed followed by the last part with an emphasis on the addition to nitriles.

Part of this chapter has been published:

Kroon, E., Zarganes Tzitzikas, T., Neochoritis, C. G. & Dömling, A. in *Science of Synthesis: Applications of Domino Transformations in Organic Synthesis* (ed. Snyder, S. A.) 419–448 (Thieme, 2016).

5.1 Introduction

Domino transformations allow the generation of several new bonds in a single synthetic operation starting from simple substrates, wherein the subsequent reactions result as a consequence of the functionality generated in a previous step. The quality of the domino reaction can be correlated to the number of chemical bonds formed, considering the complexity and diversity that can be achieved in the process, *i.e.*, the bond forming efficiency index defined by Tietze.[1]

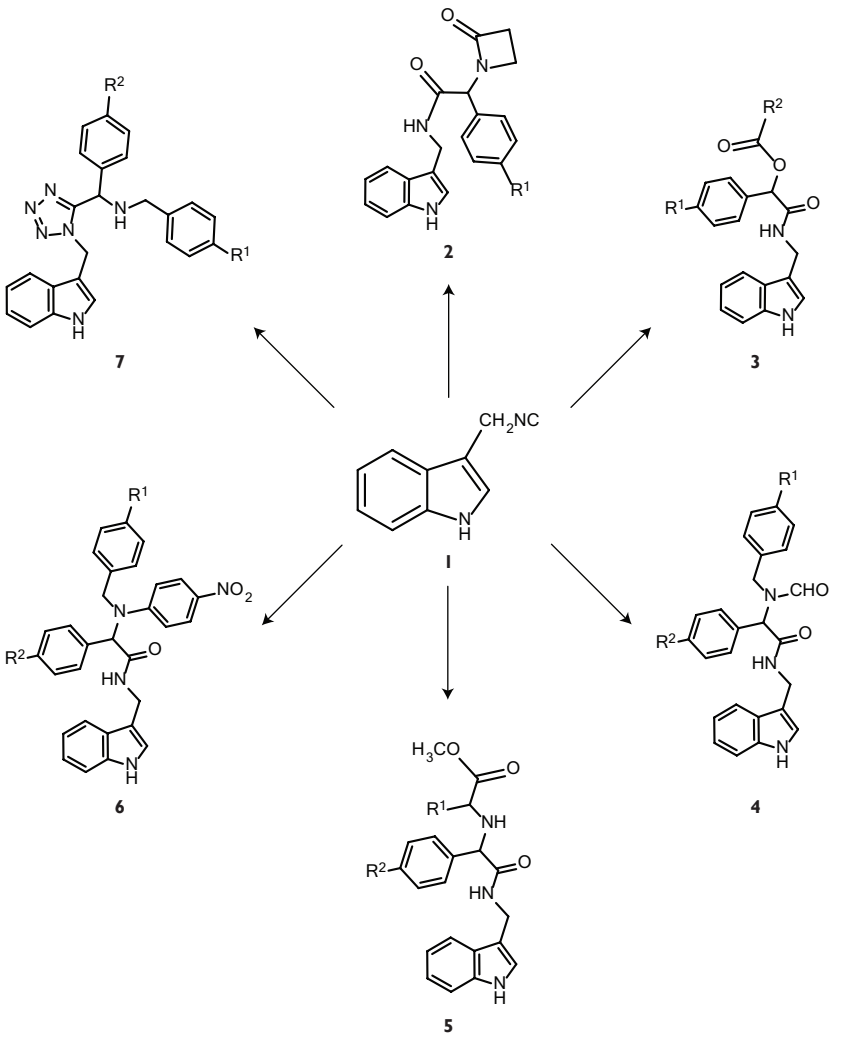

Scheme 1. The power of multicomponent reaction chemistry: one isocyanide, six different scaffolds.

A multicomponent reaction is a process wherein three or more starting materials are combined into one compound in a single chemical operation; thus, it is a domino process. The rapid and facile access to biologically relevant compounds and the scaffold diversity of multicomponent reactions have been recognized by the synthetic community in industry and academia as a preferred method to both design and discover biologically active compounds.[2,3]

Ugi and Ugi-type multicomponent reactions, belonging to the most important transformations in the field, give access to biologically and pharmaceutically relevant compounds, with recent examples including boceprevir, retosiban, and Mandipropamid.[4–6] Classical Ugi four-component,[7,8] Ugi four-component tetrazole,[9] Ugi lactam,[10] Ugi four-component hydantoin,[11] Ugi five-center-four-component,[12] Ugi three-component,[13] and Ugi-Smiles[14] reactions are just a few examples that demonstrate the power of multicomponent reaction chemistry as a key set of domino transformations in organic synthesis. These kinds of reactions start with the formation of the corresponding imine and are followed by addition into the resulting C=N bond by the other reagents (*i.e.*, isocyanide, acid), setting into motion additional events.

Very recently, a facile and convenient synthesis of indole derivatives based on a multicomponent reaction was published (Scheme 1). Employing novel isocyanide **1**, six different scaffolds **2–7** and eighteen new compounds were described. In most of these reactions, the addition to the C=N bond is the initial reaction.[15]

5.2 Addition to C=N and the Pictet–Spengler strategy

Chemical diversity and complexity of scaffolds are the keys for the design and/or screening-based discovery of useful materials. Multicomponent reactions are often highly compatible with a range of unprotected orthogonal functional groups; thus, even more "secondary", scaffolds can be obtained based on bifunctional starting materials or some various subsequent reactions of the initial products. This two-layered strategy has been extremely fruitful in the past, leading to a great array of scaffolds now routinely used in combinatorial and medicinal chemistry for drug-discovery purposes.[3] One characteristic strategy is the combination of the venerable Ugi and Pictet–Spengler reactions, a process which results in polycyclic scaffolds similar to many classes of natural products (Scheme 2).

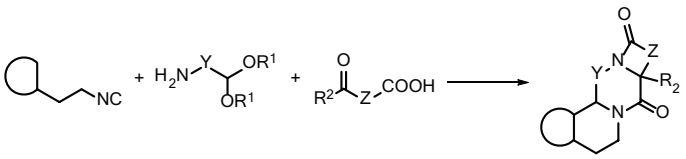

Scheme 2. Ugi and Pictet–Spengler reaction strategy.

In the first reported combination of the Ugi and Pictet–Spengler reactions, electron-rich 2-(1*H*-indol-3-yl)ethan-1-amine-derived isocyanide **8** reacts in the Ugi reaction with a diversity of bifunctional oxocarboxylic acid derivatives **10** and orthogonally protected aminoacetaldehyde **9**, followed by a Pictet–Spengler reaction. This process yields structurally intriguing polycyclic indole type compounds **12** (Table 1). The yields for the Ugi products **11** vary from 50–80% and those for the Pictet–Spengler reactions from 48–90%.[16]

Table 1. Ugi and Pictet–Spengler reaction affording polycyclic indole alkaloid-type compounds.

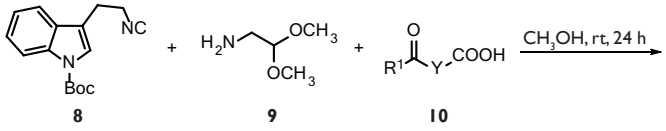

8 **9** **10**

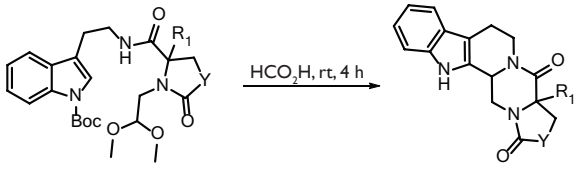

11 **12**

R^1	Y	Yield of 11 (%)	Yield of 12 (%)
CH_3	$(CH_2)_2$	53	48
CH_3	$(CH_2)_3$	80	63
CH_3		60	90
H		60	80

Furthermore, the reaction sequence has been extended to other isocyanides and the synthesis of a small focused library of polycyclic products **16** based on

(2-phenylethyl)amine-derived isocyanides has been described (Table 2). Both syntheses naturally yield different scaffolds with different substitution patterns and likely different biological activities, though these results remain to be reported.

The first step is an Ugi three-component reaction of a (2-phenylethyl) amine-derived isocyanide **13** and aminoacetaldehyde dimethyl acetal (**9**) with a suitable bifunctional oxocarboxylic acid **14**. Both electron-neutral and electron-rich isocyanides can be employed, with the isocyanides being derived from the corresponding amines. The next step involves a Pictet–Spengler reaction of the dimethyl acetal protected Ugi intermediates **15** (Table 2). The conditions for this ring closure require formic acid or methanesulfonic acid and have been chosen according to previous optimizations of this reaction sequence, albeit using different isocyanide inputs. Using formic acid at room temperature for ring closure is good for the more reactive dimethoxyphenyl Ugi products but is ineffective for the less reactive monomethoxyphenyl or phenyl Ugi products; however, in these cases, anhydrous methanesulfonic acid at 70 °C with a longer reaction time is effective. Yields range from moderate to very good, and in some cases high diastereomeric ratios are obtained.[17]

Table 2. Ugi and Pictet–Spengler reactions affording polycyclic products based on (2-phenylethyl) amine-derived isocyanides.

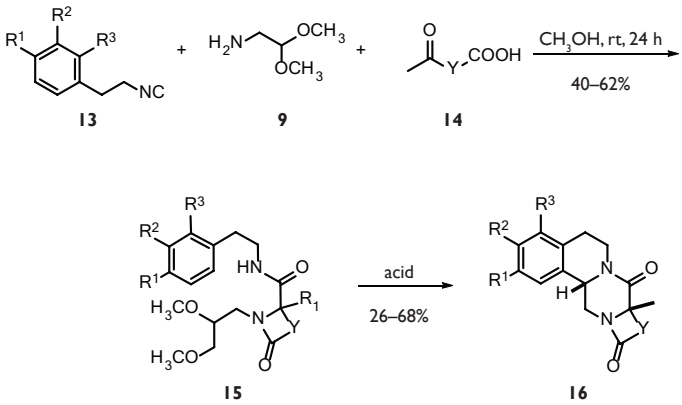

R[1]	R[2]	R[3]	Y	Conditions for cyclization	Yield of 15 (%)	Yield of 16 (%)
H	OCH_3	OCH_3	$(CH_2)_2$	HCO_2H, rt, 4 h	62	62
H	OCH_3	OCH_3	$(CH_2)_3$	HCO_2H, rt, 4 h	40	60
H	OCH_3	OCH_3		HCO_2H, rt, 4 h	55	26
OCH_3	H	H	$(CH_2)_2$	MsOH, 70 °C, 24 h	60	68

An efficient approach to access praziquantel has been described based on an Ugi four-component reaction followed by a Pictet–Spengler reaction.[17] Praziquantel, a tetrahydroisoquinoline derivative, is the only commercially available treatment of schistosomiasis, a high-volume neglected tropical disease affecting more than 200 million people worldwide, and is marketed by Bayer (Biltricide), Merck (Cysticide), and Shin Poong (Distocide), to name a few.

This domino reaction approach comprises an Ugi four-component reaction as the key step, followed by a Pictet–Spengler ring closure. These events were carried out in a sequential one-pot, two-step procedure with an overall yield between 16–58%. Various isocyanides **17**, aldehydes **18**, and acids **19** have been used to define the scope and limitations of the reaction and thirty novel praziquantel derivatives **20** have been successfully synthesized (Table 3).[18] Novel tricyclic indole and isoquinoline derivatives have been synthesized based on a similar approach, thus extending the chemical space accessed even further.

Table 3. Ugi and Pictet–Spengler reaction affording thirty novel praziquantel derivatives.

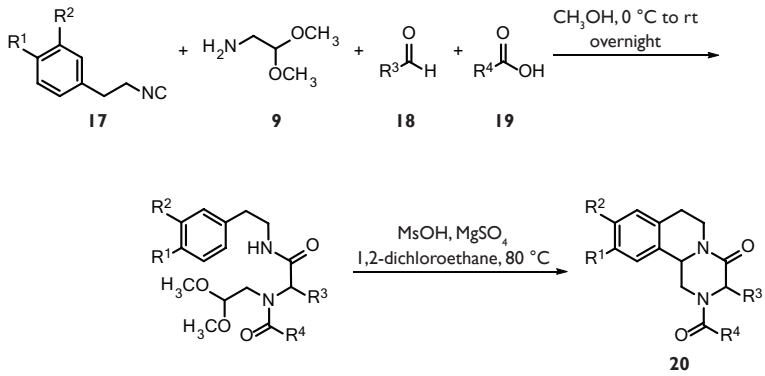

R¹	R²	R³	R⁴	Overall yield of 20 (%)
OCH_3	OCH_3	H	Cy	34
H	H	CH_3	Cy	21
H	H	4-FC_6H_4	Cy	16
H	H	H	cyclopropyl	58
H	H	H	Ph	42

Recently, Khoury and co-workers developed an extension of the Ugi reaction of α-amino acids by introducing primary or secondary amines as additional reactants, thus rendering the Ugi five-center-four-component reaction into a "truly" four-component reaction with four highly variable starting materials (see Section 5.3).[12]

Based on that advance, chiral imino dicarboxamides can be formed by variation of an α-amino acid, an oxo component, an isocyanide, and a primary or secondary amine as previously unprecedented components for this Ugi variation. Critically, the reaction is compatible with many functional groups and different fragments.

A tryptophan amino acid derivative **23**, a ketone **22**, an isocyanide **21**, and aminoacetaldehyde dimethyl acetal (**9**) react in methanol/water (4:1) at room temperature to form the novel Ugi five-center-four-component reaction products **24** (Table 4). Afterwards, by using concentrated formic acid at room temperature, the corresponding Pictet–Spengler cyclization product **25** is formed. The reaction sequence is also conveniently performed in one pot without loss of yield by direct evaporation of the crude Ugi-five-center-four-component reaction mixture followed by addition of formic acid.[19]

Table 4. Ugi and Pictet–Spengler reaction affording novel tricyclic indole and isoquinoline derivatives.

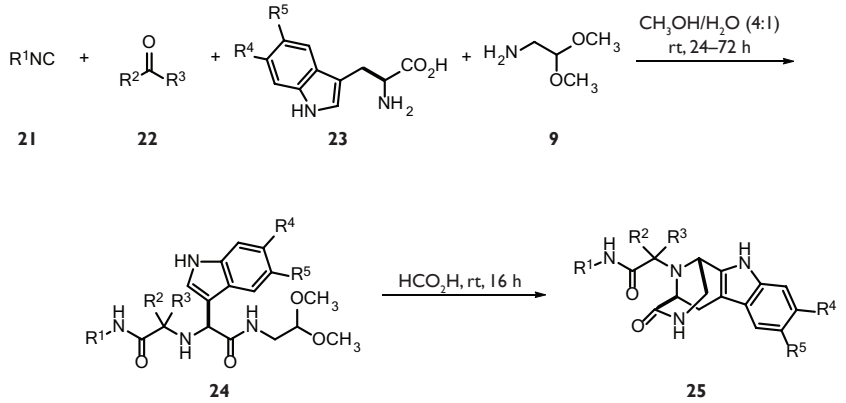

R^1	R^2	R^3	R^4	R^5	Overall yield of 25 (%)
$(CH_2)_2Ph$	$(CH_2)_2NCH_3(CH_2)_2$		H	H	42
$((CH_2)_2Ph$	$(CH_2)_6$		H	H	52
$(CH_2)_2Ph$	$(CH_2)_5$		H	H	48
Bn	$(CH_2)_3$		OH	H	29
Bn	Ph	H	H	H	61
Cy	CH_3	CH_3	OCH_3	OCH_3	52

The advantage of the specific combination of Ugi and Pictet–Spengler reactions is the expedited and convergent access to polycyclic natural product like skeletons. The yields over two steps are acceptable to good. The stereochemistry of the amino

acid is conserved and therefore stereochemically pure (using symmetrical ketones or formaldehyde) or diastereomeric (using aldehydes other than formaldehyde) compounds are obtained. Many variations in the oxo and isocyanide starting materials can lead to synthetic handles to further elaborate the primary structures.[19]

5.3 Ugi five-center-four-component reaction followed by postcondensations

In 1996, Ugi and co-workers described the scope and limitations of a novel variant of the original Ugi reaction.[20] The reaction was termed a five-center-four-component reaction because of the use of bireactive α-amino acids, oxo components, isocyanides, and an alcohol both as solvent and reactant. However, this reaction only comprises a multicomponent reaction where three components show great variability: the α-amino acid, the oxo-component, and the isocyanide. The variability of the alcohol component is rather restricted to low-molecular-weight alcohols such as methanol and ethanol. This restriction is likely a result of the poor solubility of the amino acids in other alcohols as well as the reduced nucleophilicity of the alcohols in general terms. The key reaction intermediate is the six-membered α-adduct **26** of the α-amino acid, the oxo component, and the isocyanide. This α-adduct undergoes nucleophilic attack by the solvent to give the linear product **27** (Scheme 3).

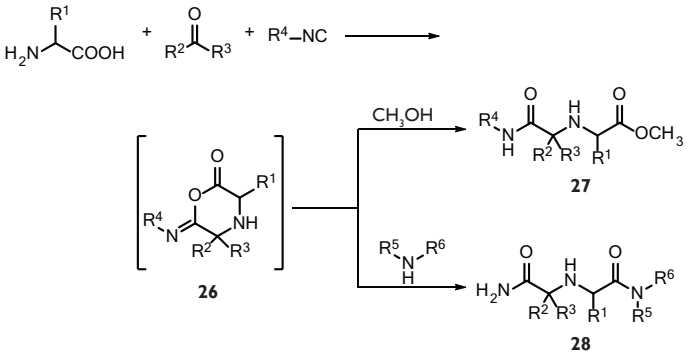

Scheme 3. The Ugi five-center-four-component reaction.

Recently, a novel, stereoselective Ugi-type reaction of four highly variable starting materials has been reported.[12] In this report, the authors envisioned that nitrogen-based nucleophiles, such as primary or secondary amines, could potentially work by successfully competing with the alcohol solvent to attack the six-membered adduct **26**, thus leading to iminodicarboxamide derivatives **28** (Scheme 3).

The optimal solvent for the reaction is a mixture of methanol/water (4:1),

one that allows full solubilization of the starting materials. The reaction is performed at room temperature for 24–72 hours to circumvent the formation of unwanted side products that are formed when the reaction was carried out under microwave conditions instead. The scope of the reaction has been investigated by using representative starting materials of each class (Table 5).

Table 5. A "truly" Ugi five-center-four-component reaction.

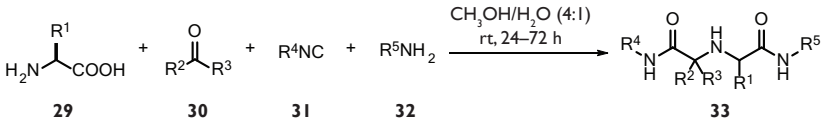

29 **30** **31** **32** **33**

R^1	R^2	R^3	R^4	R^5	Yield (%)
CH_3	$(CH_2)_2O(CH_2)_2$		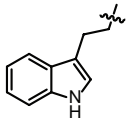	$3,4\text{-}Cl_2C_6H_3CH_2$	54
	$(CH_2)_3$		Bn	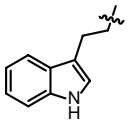	54
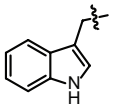	CH_3	CH_3	$CH_2P(O)(OEt)_2$	$3,4\text{-}Cl_2C_6H_3CH_2$	52
iPr	$(CH_2)_5$		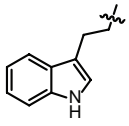	$4\text{-}FC_6H_4CH_2$	54
Bn	$(CH_2)_5$		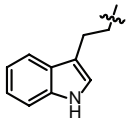	$CH_2CO_2CH_3$	63
$(CH_2)_4NHBoc$	$(CH_2)_5$		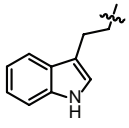	$4\text{-}CH_3OC_6H_4$	62

Not surprisingly, the identity of the starting materials and their specific combinations played a role in the overall yield and selectivity of the reaction.

Virtually all the natural α-amino acids **29** and some non-natural ones can

be used in the reaction; nevertheless, α-amino acids with reactive side chains (e.g. Ser, Glu, Asp, Lys) give lower yields with unprotected side chains and therefore are used in their side-chain-protected form. As oxo-components **30**, symmetrical ketones are used to obtain only one stereoisomer; however, both aldehydes and ketones work equally well in the reaction. Isocyanides **31** that can be used range from (hetero)aromatic, aliphatic, and bulky examples, and mostly primary amines **32** which include functionalized, heterocyclic, and (hetero)aromatic amines (Table 5). All reactions have been performed on a 0.5 mmol scale and the products **33** are separated into their component diastereoisomers by efficient and fast supercritical fluid carbon dioxide (SFC) technology to afford 40–60% yield of the final products. The influence of the amine component was also investigated in relation to the integrity of the stereocenter, and it was found that primary amines lead to retention of stereochemistry, whereas secondary amines lead to partial racemization. The one-pot synthesis towards this scaffold constitutes a major advance and is superior to reported stepwise sequential or multicomponent reaction approaches.[12]

In further elaboration of the Ugi four-component reaction, the synthesis of four heterocyclic scaffolds based on the Ugi four-component reaction of α-amino acids, oxo components, isocyanides, and primary or secondary amines has been described by suitably functionalizing the starting materials of the reaction.[21] Amongst the different strategies for the design of molecular complexity using multicomponent reaction chemistry,[22] post Ugi secondary cyclization has been a very fruitful strategy to accomplish novel scaffolds. Due to the well-known functional group compatibility of the Ugi starting materials, it was envisioned that the construction of heterocyclic scaffolds involving the unique and reactive secondary amine formed during the Ugi reaction variation was feasible. Several intramolecular lactamizations based on different Ugi scaffolds have been reported in the past;[23–26] however, the current synthesis differs from the rest because it yields a unique scaffold under much milder cyclization conditions. When methyl 2-formylbenzoates **37** are used as an oxo-component in the Ugi four-component reaction along with equivalent amounts of amino acid **34**, isocyanide **35**, and a primary or secondary amine **36** with heating (85 °C, 24–72 h), the expected isoindolinone scaffold **38** is formed in moderate yield (Table 6).[21]

Table 6. Cyclization towards isoindolones.

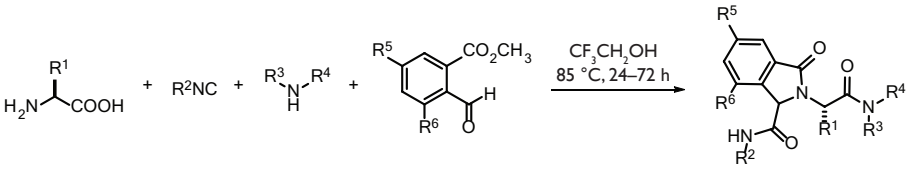

34 **35** **36** **37** **38**

R¹	R²	R³	R⁴	R⁵	R⁶	Yield (%)
iBu	$CHPh_2$	CH_2CHPh	H	H	H	35
Bn	$CHPh_2$	$(CH_2)_3Ph$	H	H	H	50
iBu	Bn	$(CH_2)_2O(CH_2)_2$		OCH_3	OCH_3	40

When a β-oxo ester **42** is employed as a bifunctional orthogonal building block along with an amino acid **39**, an isocyanide **40**, and a primary amine **41** under heating at 85 °C, complete formation of the Ugi product is observed. This material is transformed to the corresponding pyrrolidinedione scaffold **43** upon treatment with three equivalents of cesium carbonate (Table 7).[21] Several analogous reactions yield pyrrolidinediones in satisfactory yields with predominant formation of the *cis*-stereoisomer, as confirmed by X-ray analysis. The discovery of this reaction is remarkable because few other orthogonal methods exist to access a pyrrolidinedione scaffold by isocyanide- based multicomponent reactions.[27]

Table 7. Cyclization towards the pyrrolidinediones.

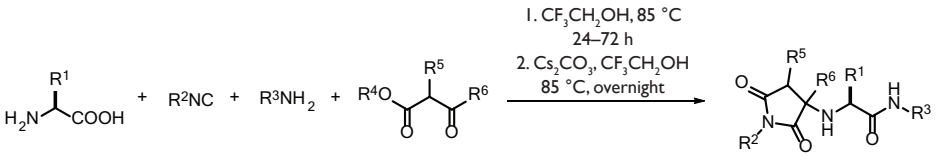

39 **40** **41** **42** **43**

R¹	R²	R³	R⁴	R⁵	R⁶	Yield (%)
H	Bn	Bu	Et	$(CH_2)_4$		40
CH_3	Cy	$(CH_2)_2Ph$	Et	$(CH_2)_4$		49
	$(CH_2)_2Ph$	(CH2)2OEt	Et	$(CH_2)_4$		45
Bn		iPr	Bn	H	CH_3	34

In a final example, the use of electron-rich aromatic α-amino acids, such as phenylalanine **46**, shows applicability in the new Ugi variation to produce compound **47** in good to high yields using aminoacetaldehyde dimethyl acetal (**9**), ketones **44**, and isocyanides **45** (Table 8).[21] In all cases, only the *trans*-diastereomer is observed,

Table 8. Cyclization towards the bicyclic tetrahydroimidazo-[1,2-*a*]pyrazine-2,6(3*H*,5*H*)-diones.

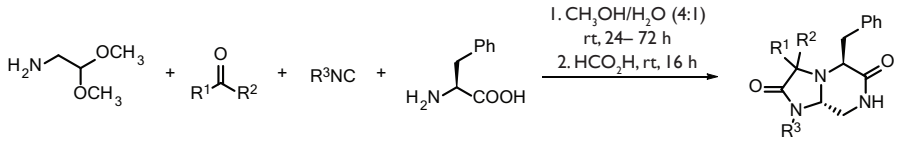

9 **44** **45** **46** **47**

R¹	R²	R³	Yield (%)
CH_3	CH_3	Bn	63
$(CH_2)_5$		Bn	87
$(CH_2)_5$		$(CH_2)_2Ph$	40
$(CH_2)_5$		$(CH_2)_2Ph$	54

as confirmed by X-ray analysis of compound **47**.The Ugi four-component reaction, along with its postcondensation modifications, can also serve as an excellent way to access diverse 1,4-benzodiazepine scaffolds.[28] Such scaffolds are of particular interest in drug design due to a balanced ensemble of beneficial physicochemical properties which includes a semi rigid and compact diazepine ring with spatial placements of several substituents, combined with low number of rotatable bonds, hydrogen bond donors and acceptors, and intermediate lipophilicity. As an alternative to traditional multistep sequential syntheses of these materials, new routes have been designed employing one-pot multicomponent reactions to accelerate access to diverse 1,4-benzodiazepine scaffolds. Novel applications of [(*tert*-butoxycarbonyl)amino]-acetaldehyde in the synthesis of 1,4-benzodiazepines utilizing the Ugi/deprotection/cyclization strategy have been described.[29]

1,4-Benzodiazopine-5-ones **53** can be accessed using methyl 2-aminobenzoate (**49**) as a building block. This compound serves as an amine component for the Ugi four-component reaction together with an isocyanide **48**, [(*tert*-butoxycarbonyl) amino]-acetaldehyde (**50**), and a carboxylic acid **51** to form the Ugi product **52**, which is cyclized to the 1,4-diazepine scaffold (Table 9).[28] The Ugi/deprotection/cyclization strategy allows access to 1,4-benzodiazepine-5-ones **53** with different substitutions derived from the isocyanide and carboxylic acid starting materials.

Table 9. Ugi four-component reaction route to 1,4-Benzodiazepine-5-ones.

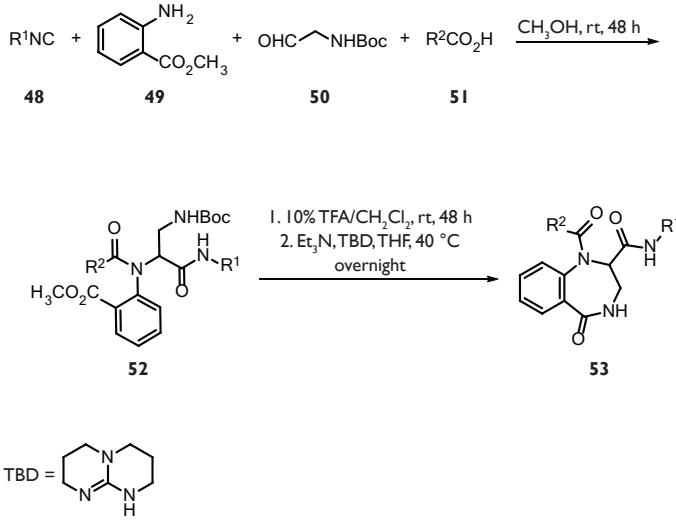

R¹	R²	Overall yield of 53 (%)
t-Bu	CH_3	41
t-Bu	Cy	28
Mes	CH_3	16
t-Bu	Pr	20
t-Bu	Cyclopropyl	38
t-Bu	4-FC_6H_4	22

Because aminophenyl ketones have shown good reactivity in multicomponent reactions as an amine component,[30–32] they are employed in the new Ugi/deprotection/cyclization strategy for the rapid access to as second 1,4-benzodiazepine scaffold **58** (Table 10).[28] Initially, aminophenyl ketones **56** react with an isocyanide **54**, [(*tert*-butoxycarbonyl)amino]-acetaldehyde (**50**), and a carboxylic acid **55** to form the Ugi product **57**. In the second step, the deprotected amino group is immediately cyclized with the ketone functionality to form 1,4-benzodiazepines **58** with four points of diversification.

Table 10. Ugi four-component reaction route to 1,4-Benzodiazepines.

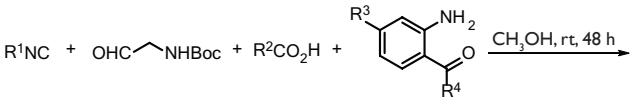

54 **50** **55** **56**

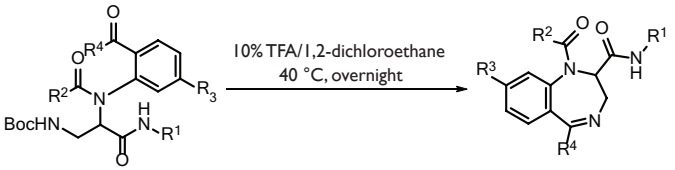

57 **58**

R¹	R²	R³	R⁴	Overall yield of 58 (%)
t-Bu	CH_3	H	Ph	47
Cy	CH_3	H	Ph	36
Cy	CH_3	H	CH_3	43
Bn	CH_3	H	Ph	40
t-Bu	CH_2OH	Cl	Ph	22
t-Bu	Pr	Cl	Ph	24
t-Bu	cyclopropyl	Cl	Ph	25
Bn	CH_3	Cl	2-ClC_6H_4	13

The Ugi/deprotection/cyclization strategy is further applied for the synthesis of a third 1,4-benzodiazepine scaffold **62**. In this case, an aminophenyl ketone **60** reacts with an isocyanide **59**, [(*tert*-butoxycarbonyl)amino]-acetaldehyde (**50**), and azidotrimethylsilane to obtain the Ugi tetrazole product **61**, followed by deprotection/cyclization forming substituted 1,4-benzodiazepines **62** with three points of diversification (Table 11).[28] The scaffolds **58** and **62** are unprecedented in the chemical literature, whereas scaffold **53** is accessed in a new and convenient way.

Table 11. Ugi four-component reaction route to 2-tetrazole-substituted 1,4-benzodiazepines.

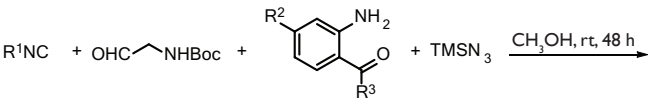

59 **50** **60**

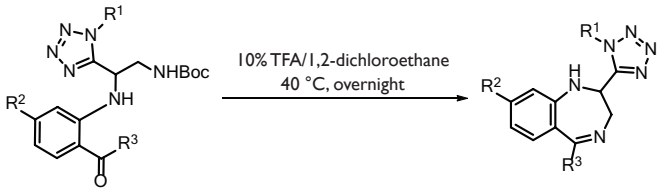

61 **62**

R^1	R^2	R^3	Overall yield of 62 (%)
t-Bu	H	Ph	29
Cy	H	Ph	35
Cy	H	CH_3	49
t-Bu	Cl	Ph	32
Bn	Cl	2-FC_6H_4	12
Bn	H	Ph	26

Further development of an alternative approach towards the 1,4-benzodiazepine scaffold with an additional point of diversification led to the introduction of an "anchor" fragment to the diazepine ring.[28] A technology, referred to as AnchorQuery, performs an exact pharmacophore search of anchor-oriented virtual libraries of explicit conformations. The anchor-oriented libraries are based upon key amino acid residues in, for example, protein–protein interactions where the amino acid residue (e.g. phenylalanine) is used as the anchor.[33] A *N-tert*-butoxycarbonyl-protected amino acid is an ideal building block to introduce anchor fragments, which can then be incorporated into drug-like compounds via multicomponent reactions.[34,35] Hence, the Ugi/deprotection/cyclization strategy is employed to assemble the orthogonal *N-tert*-butoxycarbonyl-protected amino acid building for the synthesis of a 1,4-benzodiazepine scaffold. Aminophenyl ketones **65**, isocyanides **63**, *N*-(*tert*-butoxycarbonyl) glycine (**64**), and aldehydes **66** are employed to give the crude Ugi products **67**, which are not isolated but immediately treated with trifluoroacetic acid in 1,2-dichloroethane to produce 1,4- benzodiazepines **68** in a one-pot procedure (Table 12). These 1,4-benzodiazepines with four points of diversification were isolated in reasonable to good yields.

Table 12. Ugi four-component reaction route to 1,4-Benzodiazepines.

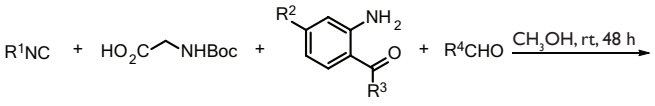

63 **64** **65** **66**

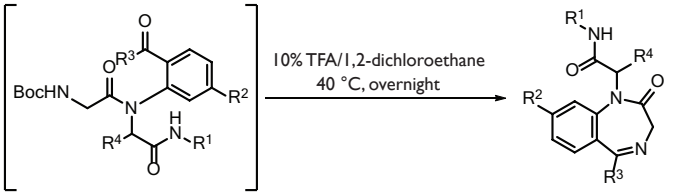

67 **68**

R¹	R²	R³	R⁴	Overall yield of 68 (%)
t-Bu	H	Ph	iPr	38
t-Bu	H	Ph	H	47
t-Bu	H	CH_3	iPr	53
t-Bu	H	CH_3	H	66
Cy	Cl	Ph	H	33
Cy	H	Ph	H	42

As a final example, the synthetic feasibility of "anchor"-biased compound libraries using *N-tert*-butoxycarbonyl-protected amino acid derivatives have also been tested.[28] Phenylalanine, leucine, tryptophan, and tyrosine, amino acids which are abundant in the protein–protein interaction interface, were selected. As shown in Table 13, *N-tert*-butoxycarbonyl-protected amino acid **71** were subjected to the same protocol for the synthesis of 1,4-benzodiazepines **68** with variable aminophenyl ketones **70** and isocyanides **69**. Compounds **72**, with three points of diversification were isolated in 22–69% overall yield. These examples further demonstrate the overall ease of synthesis and increase in molecular complexity during the two-step one-pot procedure, features which are remarkable for the efficient synthesis of 1,4-benzodiazepines containing a variety of "anchor" residues.

Table 13. Synthesis of Anchor-directed 1,4-Benzodiazepines.

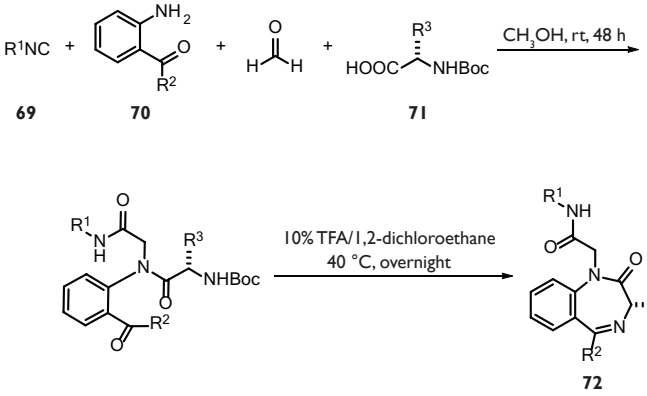

R^1	R^2	R^3	Overall yield of 72 (%)
Cy	Ph	Bn	50
Cy	Ph	iBu	69
t-Bu	CH_3	iBu	46
Cy	Ph	Trp	65
Cy	Ph	4-$HOC_6H_4CH_2$	60

5.4 Addition to nitriles

Cyanoacetic acid derivatives are key starting materials in a plethora of multicomponent reaction yielding carbocycles and their heterocyclic analogous.[36] For instance, in the Gewald multicomponent reaction the α-acidic character of the cyanoacetic acid derivatives **73** is exploited in a Knoevenagel condensation with α-acidic carbonyl compounds **74** (aldehydes, ketones or 1,3-dicarbonyls) to form an acrylonitrile derivative **75**. After sulfanylation with elemental sulfur, the cyano group in **76** is available for intramolecular attack by the sulfur atom, leading to the final Gewald scaffold (e.g. **77**), which possesses an exo-cyclic amine moiety that can be utilized in subsequent chemistry (Scheme 4).[36–38]

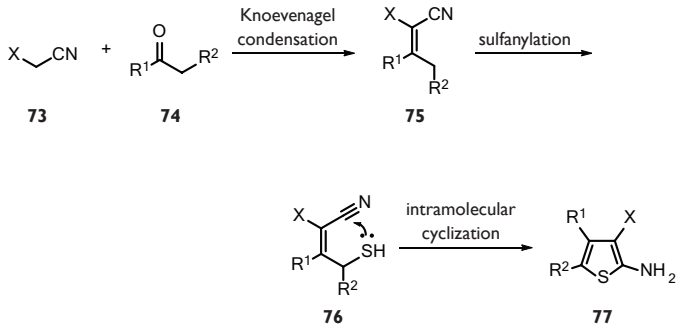

Scheme 4. The Gewald multicomponent reaction.

Unfortunately, only a select few cyanoacetic derivatives, including cyanoacetic acid and esters, malononitrile, and cyanomethyl ketones have been described in such multicomponent reactions, thereby limiting the scope of the reaction to the diversification of the activated carbonyl compounds. Recently, however, an inexpensive, mild, scalable, and simple parallel formation of cyanoacetamides **73** (X = $CONHR_3$) as cyanoacetic acid derivatives in domino multicomponent reactions has been described.[39] With this new access to multigram quantities of a wide range of cyanoacetamides, the application in multicomponent reaction chemistry is described.

The Gewald multicomponent reaction scaffold, 2-aminothiophene, is an important and versatile building block in several drugs (e.g. Olanzapine) and other biologically active compounds. Moreover, the Gewald multicomponent reaction itself constitutes an elegant, convenient, and effective reaction compared to traditional methods for the preparation of such compounds.[40] Wang and co-workers have described the use of their parallel cyanoacetamides methodology in the Gewald multicomponent reaction to broaden its scope. Reacting α-acidic carbonyl

Table 14. Gewald reaction employing cyanoacetamides.

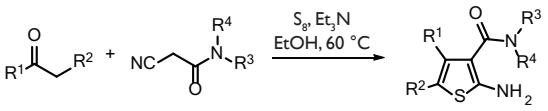

78 **79** **80**

R^1	R^2	R^3	R^4	Yield (%)
H	Ph	H	$CH_2CH{=}CH_2$	82
H	Ph	H	$CH_2C{\equiv}CH$	77
H	Ph	H	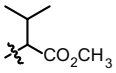	78
H	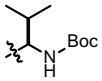		$(CH_2)_2O(CH_2)_2$	75
Ph	H	H	Bu	9
$(CH_2)_4$		H	$(CH_2)_2Ph$	20

compounds **78**, cyanoacetamides **79**, and elemental sulfur in ethanol gives the corresponding 2-aminothiophenes **80** in yields ranging from 9-95% (Table 14).[41]

Acetaldehyde is, due to its low boiling point, not a suitable starting material. However, 1,4-dithiane-2,5-diol **81** [the dimer of 2-mercaptoacetaldehyde (**78**, R^1=H, R^2 = SH) is an effective and commercially available acetaldehyde substitute in the Gewald multicomponent reaction with cyanoacetamides **82**, and no elemental sulfur is required for formation of products **83** (Table 15).[42] Other aldehydes show reasonable Gewald reactivity with a range of cyanoacetamides to give the thiophene products in good yields.

Table 15. Gewald reaction employing cyanoacetamides.

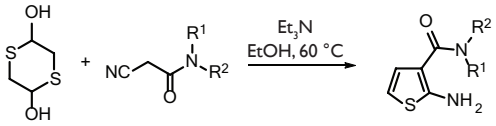

81 **82** **83**

R^1	R^2	Yield (%)
H	cyclopropyl	82
H	Bn	77
H	Bu	78
H	$CH_2CH(OCH_3)_2$	75
$(CH_2)_2NPh(CH_2)_2$		9

tert-Butoxycarbonyl-protected chiral β-amino aldehyde **84** reacts nicely with different cyanoacetamides in good to excellent yields (70–90%). Interestingly, when chiral aldehyde **84** and chiral cyanoacetamide **85** are used, only one diastereomer of 2-aminothiophene **86** is obtained without epimerization in the base-promoted Gewald multicomponent reaction. Nevertheless, when chiral valine methyl ester derived cyanoacetamide **87** reacts with the same aldehyde, the product **88** is generated as two diastereomers in a 2:1 ratio indicating strong epimerization at the valine isopropyl group (Scheme 5). Cyclohexanone and acetophenone give low yields, whereas other ketones do not react at all, presumably due to inferior reactivity compared to the aldehydes. Hence, the use of precondensed acrylonitrile derivatives is described in literature for less reactive aryl alkyl ketones.[43,44]

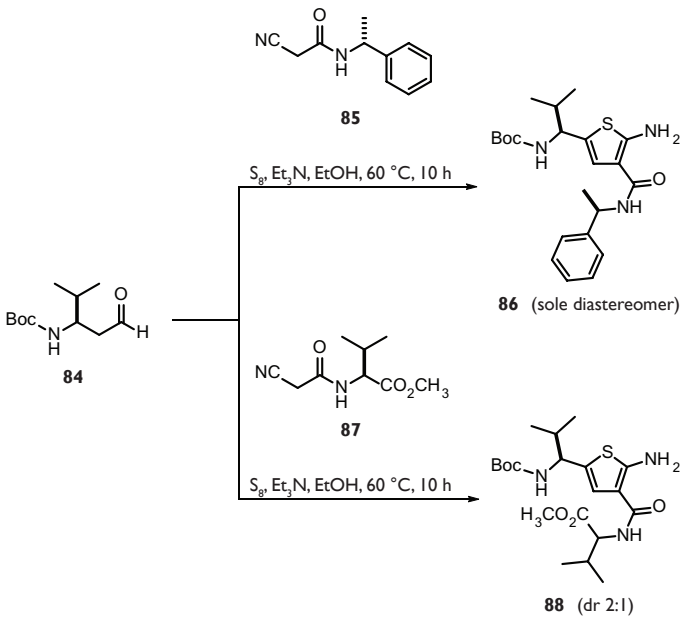

Scheme 5. Stereochemical outcome in the Gewald reaction.

Cyanoacetamides are useful reagents in the formation of 2-aminoindole-3-carboxamides (Table 16).[45] The 2-aminoindole fragment obtained is a key fragment in several biologically active compounds.[46,47] The reaction of 2-halonitrobenzenes or heterocyclic analogues **89** and cyanoacetamide **90** in one-pot produces 2-aminoindole-3-carboxamides **91** in moderate to good yield (42–85%). Various functional groups, including alcohols, alkenes, and alkynes, are introduced into the 2-aminoindole scaffold without any protecting groups allowing for direct follow-up chemistry to reach additional materials. In addition to 2-fluoronitrobenzene

derivatives, some heterocyclic starting materials offer easy access to pyrrolopyridines, a result indicating that this one-pot procedure is quite general.

Table 16. Synthesis of 2-aminoindole-3-carboxamides employing cyanoacetamides.

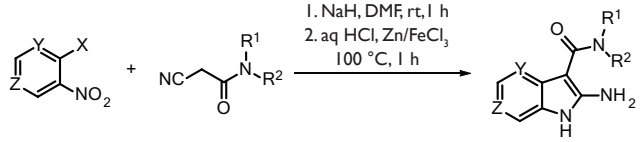

89 **90** **91**

X	Y	Z	R^1	R^2	Yield (%)
F	CH	CH	H	Bu	85
F	CH	CH	H	$CH_2CH{=}CH_2$	77
F	CH	CH	H	$(CH_2)_2OH$	52
F	CH	CCF_3	H	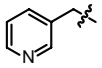	71
F	CH	CCl	$(CH_2)_2O(CH_2)_2$		55
F	N	CH	$(CH_2)_4$		45
Cl	CH	N	H	$CH_2C{\equiv}CH$	42

Classical methods for the synthesis of quinoline derivatives include the Combes, Conrad-Limpach, Doebner-Miller, and Gould–Jacobs syntheses to name a few.[48] The Friedländer reaction is another named reaction for the general preparation of quinolines,[49] and the Friedländer annulation is used in the synthesis of 2-aminoquinoline-3-carboxamides **94** (Table 17).[50]

Table 17. Synthesis of 2-aminoquinoline-3-carboxamides using cyanoacetamides.

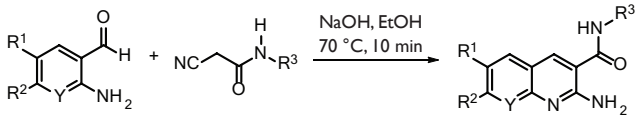

92 **93** **94**

R^1	R^2	Y	R^3	Yield (%)
H	H	CH		67
H	H	CH	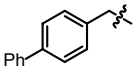	96
Cl	H	CH	$(CH_2)_2OH$	66
Cl	H	CH	$4\text{-}H_2NC_6H_4CH_2$	87
H	Cl	CH	$4\text{-}H_3COC_6H_4(CH_2)_2$	75
H	CF_3	CH	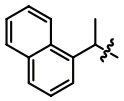	88
OCH_2O		CH	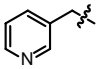	67
OCH_3	OCH_3	CH	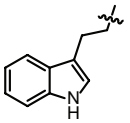	87
H	H	N	cyclopropyl	78

Heating a mixture of a 2-aminobenzaldehyde **92** and a cyanoacetamide **93** with sodium hydroxide in ethanol (70 °C, 10 min) yields the corresponding 2-aminoquinoline-3-carboxamides **94**, following a simple filtration step, in good to excellent yields (60–96%). For more expensive, or commercially limited 2-aminobenzaldehydes, the nitro analogue can be reduced (Fe/HCl) in situ.[51] Remarkably, the reaction of 2-cyano-*N*-(prop-2-ynyl)acetamide (**95**) with 2-amino-5-chlorobenzaldehyde (**98**) shows isomerization of the propargyl amide to the more

thermodynamically stable prop-1-ynyl amide **99** under strong basic conditions. However, with a mild base (such as *N*-methylpiperidine) the corresponding 2-aminoquinoline-3-carboxamides **97** can be obtained in 97% yield from 2-amino-3,6-dibromobenzaldehyde (**96**; Scheme 6).[50]

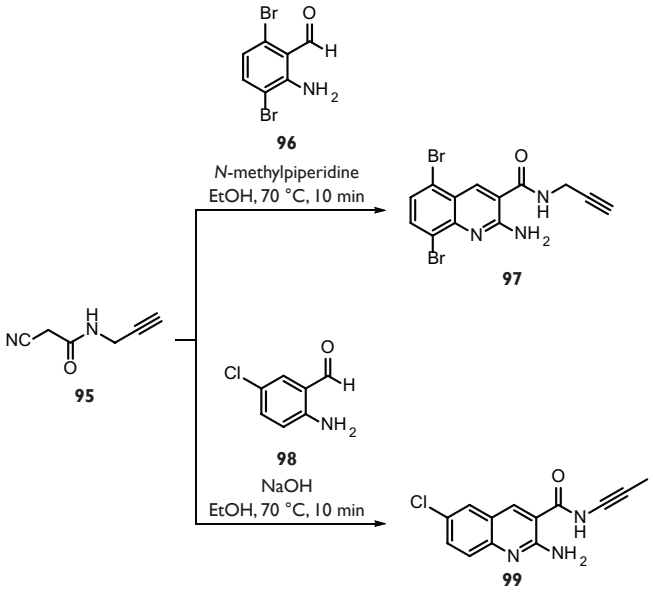

Scheme 6. Isomerization of 2-cyano-*N*-(prop-2-ynyl)acetamide under basic bonditions.

2-Aminoquinoline-3-carboxamides (e.g. **100**) could be further transformed into scaffold **103** by heating the carboxamide neat with 1,1-dimethoxy-*N*,*N*-dimethylmethanamine (**101**, dimethylforamide dimethyl acetal). The products are precipitated upon the addition of EtOH, thus simplifying the workup procedure. With bulky substituents [R^3= Cy or (1-naphthyl)ethyl], the expected product is not obtained; instead, the dimethylamino adduct **102** is isolated (Table 18).[50]

Table 18. Synthesis of pyrimido[4,5-*b*]quinolin-4(3*H*)-ones from 2-aminoquinoline-3-carboxamides.

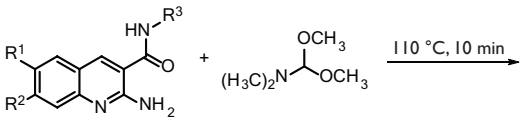

100 101

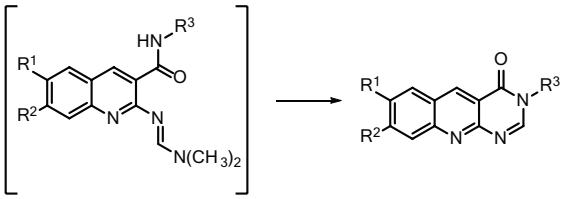

102 103

R^1	R^2	R^3	Yield (%)
H	H	4-$ClC_6H_4(CH_2)_2$	65
Cl	H	piperidino	82
Cl	H	$CH_2CH{=}CH_2$	56
H	Cl	4-$H_3COC_6H_4(CH_2)_2$	78
OCH_2O		$(CH_2)_2Ph$	65

5.5 Conclusions

Additions to C=N bonds and nitriles, specifically in multicomponent reactions, give rise to novel scaffolds that, potentially, can be used in the synthesis of biologically active compounds. Aminoacetaldehyde dimethyl acetal is a convenient aldehyde protected amine that can be applied to the Ugi reaction, setting the stage for a subsequent Pictet-Spengler reaction, hence, the formation of complex polycyclic scaffolds. One of these Ugi/Pictet-Spengler strategies was reported for the synthesis of praziquantel, a drug against schistosomiasis. Furthermore, a 'truly' Ugi-five-center-four-component reaction was described, by appropriately choosing the starting materials a wide array of scaffolds is obtained including several 1,4-benzodiazepines. Finally, easy to perform parallel synthesis of cyanoacetamides has been reported, recently; application in several new reactions give some interesting scaffolds such as: 2-aminothiophene (Gewald reaction), 3-aminoindole, and quinolines.

5.6 References

1 Tietze, L. F. Domino reactions in organic synthesis. *Chem. Rev.* **96,** 115–136 (1996).

2 Dömling, A. Recent developments in isocyanide based multicomponent reactions in applied chemistry. *Chem. Rev.* **106,** 17–89 (2006).

3 Dömling, A., Wang, W. & Wang, K. Chemistry and biology of multicomponent reactions. *Chem. Rev.* **112,** 3083–3135 (2012).

4 Venkatraman, S. *et al.* Discovery of (1*R*,5*S*)-*N*-[3-amino-1-(cyclobutylmethyl)-2,3-dioxopropyl]-3-[2(*S*)-[[[(1,1-dimethylethyl)amino]carbonyl]amino]-3,3-dimethyl-1-oxobutyl]- 6,6-dimethyl-3-azabicyclo[3.1.0]hexan-2(*S*)-carboxamide (SCH 503034), a selective, potent, orally bioavailable hepatitis C virus NS3 protease inhibitor: a potential therapeutic agent for the treatment of hepatitis C infection. *J. Med. Chem.* **49,** 6074–6086 (2006).

5 Liddle, J. *et al.* The discovery of GSK221149A: a potent and selective oxytocin antagonist. *Bioorg. Med. Chem. Lett.* **18,** 90–94 (2008).

6 Lamberth, C. *et al.* Multicomponent reactions in fungicide research: the discovery of mandipropamid. *Bioorg. Med. Chem.* **16,** 1531–1545 (2008).

7 Ugi, I. & Steinbrückner, C. Über ein neues kondensations-prinzip. *Angew. Chem.* **72,** 267–268 (1960).

8 Sheehan, S. M. *et al.* A four component coupling strategy for the synthesis of D-phenylglycinamide-derived non-covalent factor Xa inhibitors. *Bioorg. Med. Chem. Lett.* **13,** 2255–2259 (2003).

9 Nixey, T. & Hulme, C. Rapid generation of *cis*-constrained norstatine analogs using a $TMSN_3$-modified Passerini MCC/*N*-capping strategy. *Tetrahedron Lett.* **43,** 6833–6835 (2002).

10 Ribelin, T. P. *et al.* Concise construction of novel bridged bicyclic lactams by sequenced Ugi/RCM/Heck reactions. *Org. Lett.* **9,** 5119–5122 (2007).

11 Barrow, J. C. *et al.* Discovery and X-ray crystallographic analysis of a spiropiperidine iminohydantoin inhibitor of β-secretase. *J. Med. Chem.* **51,** 6259–6262 (2008).

12 Khoury, K., Sinha, M. K., Nagashima, T., Herdtweck, E. & Dömling, A. Efficient assembly of iminodicarboxamides by a "truly" four-component reaction. *Angew. Chem., Int. Ed.* **51,** 10280–10283; *Angew. Chem.* **124,** 10426–10429 (2012).

13 Pan, S. C. & List, B. Catalytic three-component Ugi reaction. *Angew. Chem., Int. Ed.* **47,** 3622–3625; *Angew. Chem.* **120,** 3678–3681 (2008).

14 El Kaïm, L., Grimaud, L. & Oble, J. Phenol Ugi–Smiles systems: strategies for the multicomponent *N*-arylation of primary amines with isocyanides, aldehydes, and phenols. *Angew. Chem., Int. Ed.* **44,** 7961–7964; *Angew. Chem.* **117,** 8175–8178 (2005).

15 Neochoritis, C. G. & Dömling, A. Towards a facile and convenient synthesis of highly functionalized indole derivatives based on multi-component reactions. *Org. Biomol. Chem.* **12,** 1649–1651 (2014).

16 Wang, W., Herdtweck, E. & Dömling, A. Polycyclic indole alkaloid-type compounds by MCR. *Chem. Commun. (Cambridge, U. K.)* **46,** 770–772 (2010).

17 Wang, W., Ollio, S., Herdtweck, E. & Dömling, A. Polycyclic compounds by Ugi–Pictet–Spengler sequence. *J. Org. Chem.* **76,** 637–644 (2011).

18 Liu, H., William, S., Herdtweck, E., Botros, S. & Dömling, A. MCR synthesis of praziquantel derivatives. *Chem. Biol. Drug Des.* **79,** 470–477 (2012).

19 Sinha, M. K., Khoury, K., Herdtweck, E. & Dömling, A. Tricycles by a new Ugi variation and Pictet–Spengler reaction in one pot. *Chem. – Eur. J.* 1**9,** 8048–8052 (2013).

20 Demharter, A., Hörl, W., Herdtweck, E. & Ugi, I. Synthesis of chiral 1,1'-iminodicarboxylic acid derivatives from α-amino acids, aldehydes, isocyanides, and alcohols by the diastereoselective five-center–four-component reaction. *Angew. Chem.* **108,** 185–187; *Angew. Chem., Int. Ed. Engl.* **35,** 173–175 (1996).

21 Sinha, M. K., Khoury, K., Herdtweck, E. & Dömling, A. Various cyclization scaffolds by a truly Ugi 4-CR. *Org. Biomol. Chem.* **11,** 4792–4796 (2013).

22 Huang, Y. & Dömling, A. in *Isocyanide Chemistry* (ed Nenajdenko, V. G.) 431–449 (Wiley-VCH Verlag GmbH & Co. KGaA, 2012).

23 Zimmer, R. *et al*. Siloxycyclopropanes in Ugi four-component reaction: a new method for the synthesis of highly substituted pyrrolidinone derivatives. *Synthesis* **2001,** 1649–1658 (2001).

24 Marcos, C. F., Marcaccini, S., Menchi, G., Pepino, R. & Torroba, T. Studies on isocyanides: synthesis of tetrazolyl-isoindolinones via tandem Ugi four-component condensation/intramolecular amidation. *Tetrahedron Lett.* **49,** 149–152 (2008).

25 Gunawan, S., Keck, K., Laetsch, A. & Hulme, C. Synthesis of peptidomimetics, δ- and ε-lactam tetrazoles. *Mol. Diversity* **16,** 601–606 (2012).

26 Gunawan, S. *et al.* Synthesis of tetrazolo-fused benzodiazepines and benzodiazepinones by a two-step protocol using an Ugi-azide reaction for initial diversity generation. *Tetrahedron* **68,** 5606–5611 (2012).

27 Bossio, R., Marcos, C. F., Marcaccini, S. & Pepino, R. Studies on isocyanides and related compounds. An unusual synthesis of functionalized succinimides. *Synthesis* **1997,** 1389–1390 (1997).

28 Huang, Y., Khoury, K., Chanas, T. & Dömling, A. Multicomponent synthesis of diverse 1,4-benzodiazepine scaffolds. *Org. Lett*. **14,** 5916–5919 (2012).

29 Keating, T. A. & Armstrong, R. W. Postcondensation modifications of Ugi four-component condensation products: 1-isocyanocyclohexene as a convertible isocyanide. Mechanism of conversion, synthesis of diverse structures, and demonstration of resin capture. *J. Am. Chem. Soc.* **118,** 2574–2583 (1996).

30 Marcaccini, S. *et al.* One-pot synthesis of quinolin-2-(1*H*)-ones via tandem Ugi–Knoevenagel condensations. *Tetrahedron Lett.* **45,** 3999–4001 (2004).

31 Gordon, C. P., Young, K. A., Hizartzidis, L., Deane, F. M. & McCluskey, A. Investigation of the one-pot synthesis of quinolin-2-(1*H*)-ones and the discovery of a variation of the three-component Ugi reaction. *Org. Biomol. Chem.* **9,** 1419–1428 (2011).

32 He, P., Nie, Y.-B., Wu, J. & Ding, M.-W. Unexpected synthesis of indolo[1,2-*c*]quinazolines by a sequential Ugi 4CC-Staudinger-aza-Wittig-nucleophilic addition reaction. *Org. Biomol. Chem.* **9,** 1429–1436 (2011).

33 Koes, D. *et al.* Enabling large-scale design, synthesis and validation of small molecule protein-protein antagonists. *PLoS ONE* **7,** e32839 (2012).

34 Hulme, C. & Cherrier, M. P. Novel applications of ethyl glyoxalate with the Ugi MCR. *Tetrahedron Lett.* 40, 5295–5299 (1999).

35 Lecinska, P. *et al.* Synthesis of pseudopeptidic (*S*)-6-amino-5-oxo-1,4-diazepines and (*S*)-3-benzyl-2-oxo-1,4-benzodiazepines by an Ugi 4CC Staudinger/aza-Wittig sequence. *Tetrahedron* **66,** 6783–6788 (2010).

36 Gewald, K. Heterocyclen aus CH-aciden nitrilen, VII. 2-Amino-thiophene aus α-oxo-mercaptanen und methylenaktiven nitrilen. *Chem. Ber.* **98,** 3571–3577 (1965).

37 Gewald, K., Schinke, E. & Böttcher, H. Heterocyclen aus CH-aciden Nitrilen, VIII. 2-Amino-thiophene aus methylenaktiven nitrilen, carbonylverbindungen und schwefel. *Chem. Ber.* **99,** 94–100 (1966).

38 Shestopalov, A. M., Shestopalov, A. A. & Rodinovskaya, L. A. Multicomponent reactions of carbonyl compounds and derivatives of cyanoacetic acid: synthesis of carbo- and heterocycles. *Synthesis* **2008,** 1–25 (2008).

39 Wang, K., Nguyen, K., Huang, Y. & Dömling, A. Cyanoacetamide multicomponent reaction (I): parallel synthesis of cyanoacetamides. *J. Comb. Chem.* **11,** 920–927 (2009).

40 Huang, Y. & Dömling, A. The Gewald multicomponent reaction. *Mol. Diversity* **15,** 3–33 (2011).

41 Wang, K., Kim, D. & Dömling, A. Cyanoacetamide MCR (III): three-component Gewald reactions revisited. *J. Comb. Chem.* **12,** 111–118 (2010).

42 Puterova, Z., Krutošíková, A. & Végh, A. Gewald reaction: synthesis, properties and applications of substituted 2-aminothiophenes. *ARKIVOC (Gainesville, FL, U. S.)* **Part (i),** 209–246 (2010).

43 Mohareb, R. M., Ho, J. Z. & Alfarouk, F. O. Synthesis of thiophenes, azoles and azines with potential biological activity by employing the versatile heterocyclic precursor *N*-benzoycyanoacetylhydrazine. *J. Chin. Chem. Soc.* **54,** 1053–1066 (2007).

44 Kim, M. H. *et al.* Novel thienopyrimidine derivatives or pharmaceutically acceptable salts thereof, process for the preparation thereof and pharmaceutical composition comprising the same. PCT Int. Appl. WO 2007102679 (2007).

45 Wang, K., Herdtweck, E. & Dömling, A. One-pot synthesis of 2-amino-indole-3-carboxamide and analogous. *ACS Comb. Sci.* **13,** 140–146 (2011).

46 Eggenweiler, H.-M., Baumgarth, M., Schelling, P., Beier, N. & Christadler, M. Preparation of pyrimidines as phosphodiesterase V inhibitors for the treatment of heart circulation disorders. Ger. Offen. DE 1014883 (2003).

47 Enomoto, H. *et al.* Novel indole derivative having inhibitory activity on IkB kinase β. PCT Int. Appl. WO 2008087933 (2008).

48 Wolfe, J. P. *et al.* in *Name Reactions in Heterocyclic Chemistry* (ed Li, J. J.) 375–494 (John Wiley & Sons, Inc., 2005).

49 Cheng, C.-C. & Yan, S.-J. in *Organic Reactions* Vol. 28, 37–207 (John Wiley & Sons, Inc., 2005).

50 Wang, K., Herdtweck, E. & Dömling, A. Cyanoacetamides (IV): versatile one-pot route to 2-quinoline-3-carboxamides. *ACS Comb. Sci.* **14,** 316–322 (2012).

51 Diedrich, C. L., Haase, D. & Christoffers, J. New octahydropyrido[3,4-*b*]acridine scaffolds for combinatorial chemistry. *Synthesis* **2008,** 2199–2210 (2008).

Summary

The nature of the starting materials in multicomponent reactions allow them to be versatile alternatives to classical chemical synthesis in the preparation of complex organic molecules or pharmaceutical products. The reason why multicomponent reactions have required so much attention is the fact that they have some advantages over classical chemical methods. They exhibit a remarkable atom economy, are efficient, are well suited for parallel synthesis allowing for the generation of large libraries, and the number of compounds that can be formed is enormous with the chemical space largely not overlapping the chemical space that is accessible through classical synthesis.

Many aspects of cell life are regulated through protein phosphorylation, a process that is carried out by kinases. Their main function is signal transduction within cells by alteration of substrate activity, protein kinases also govern many other cellular processes. Protein kinases can be classified according to the amino acids they phosphorylate, the two major groups being serine/threonine kinases and tyrosine kinases. The family of AGC kinases plays a significant role in regulating physiological processes relevant to metabolism, growth, proliferation and survival, therefore dysregulation can have great consequences. Two main diseases associated with dysregulation in these physiological processes are cancer and diabetes mellitus type 2, on the other hand, mutations have been shown to cause various inherited syndromes. Within this family 3-phosphoinositide-dependent kinase-1 (PDK1) is an important member as it has a pivotal role as master kinase in the activation of at least twenty-three other AGC kinases.

The research in this thesis is focused on the application of new starting materials in multicomponent reactions and on the development of small molecules that target the kinasePDK1.

In the first part of chapter 1, we introduce multicomponent reactions and their advantages over classical chemistry. An example for the utilization of multicomponent reactions in medicinal chemistry is presented. In the second part, the general aspects of the protein kinase PKD1 are described as well as the allosteric site (PIF pocket) that is present on this protein. Furthermore, the currently known small molecules targeting this allosteric site are discussed.

In chapter 2, we describe how we used the freeware, AnchorQuery, to design scaffolds for the PIF pocket. Several compounds from the Castagnoli reaction turned out to be active and molecules with good affinity for the PIF pocket were synthesized and tested (Figure 1). The pharmacokinetic properties of these compounds have to be further developed, because these compounds do not enter cells, easily. Several recommendations were made to further improve this scaffolds and how to proceed towards the design of new scaffolds.

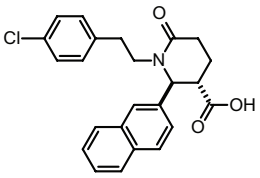

Figure 1. The most active compound towards PDK1 from this research.

In chapter 3, we introduce a new cleavable isocyanide in the Ugi reaction for the potential synthesis of biologically relevant 1*H*-tetrazoles (Scheme 1). In medicinal chemistry these tetrazoles are regarded as bioisosteres of the carboxylic acid moiety, nonetheless, with better pharmacokinetic properties. The β-cyanoethyl isocyanide reacts well with a broad range of starting materials and removal of the isocyanide is fast and proceeds under mild conditions, therefore, providing a valuable alternative to known methods. The application of this isocyanide in other multicomponent reactions is briefly discussed.

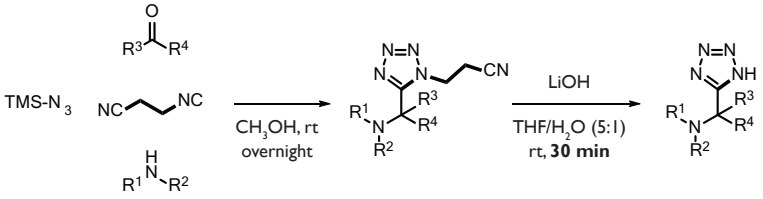

Scheme 1. β-Cyanoethyl isocyanide in the synthesis of 1*H*-tetrazoles.

In chapter 4, we address the introduction of a new type of cyclic anhydride in the Castagnoli reaction to improve the versatility of this reaction. Although, cyclic mixed anhydrides (Figure 2) are known their application in the Castagnoli reaction is not trivial. The synthesis of a cyclic mixed anhydride was achieved and an in-depth discussion is given for the fact that this compound did not perform in the Castagnoli reaction.

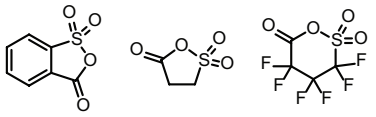

Figure 2. Cyclic mixed sulfocarboxylic anhydrides.

In chapter 5, we give an overview of the latest literature covering the addition to C=N bonds and nitriles, especially focusing on multicomponent reactions. Several useful starting materials are covered that allow for the synthesis of more complex

(biologically active) compounds, based upon known multicomponent reactions. Moreover, the 'truly' Ugi-five-center-four-component reaction is described; by appropriately choosing the starting materials leads this variation of the Ugi reaction to the synthesis of novel compounds.

Samenvatting

De titel van dit proefschrift is *Exploring Multicomponent Reactions: From Chemistry to Drug Design* en gaat over het gebruik van nieuwe startmaterialen in multicomponentreacties en de ontwikkeling van kleine moleculen die een effect hebben op een bepaald lichaamseiwit. Voordat ik uitleg wat er precies in het proefschrift is beschreven geef ik wat achtergrondinformatie om een en ander begrijpelijker te maken.

Moleculen en reacties

Moleculen zijn de kleinste delen van een stof, bijvoorbeeld suiker, die nog de eigenschappen van deze stof hebben. Een molecuul is opgebouwd uit atomen en de belangrijkste voor de organische chemie zijn waterstof (H), koolstof (C), stikstof (N) en zuurstof (O) (Figuur 1). Door chemische reacties uit te voeren met moleculen kunnen we deze aan elkaar vastmaken en zo nieuwe moleculen creëren. In de klassieke chemie gebeurt dit stap voor stap; zie het als een puzzel waarvan je de stukjes één voor één aan elkaar legt. Dit is vaak een lang en relatief ingewikkeld proces. Een andere manier om moleculen te combineren tot een nieuw molecuul is de multicomponentreactie waarbij drie of meer moleculen in één keer worden samengevoegd tot een nieuw molecuul; de puzzelstukjes worden op deze manier in één keer aan elkaar gelegd. Ten opzichte van de klassieke chemie zijn multicomponentreacties: snel, worden ze meestal uitgevoerd bij kamertemperatuur en produceren ze weinig chemisch afval.

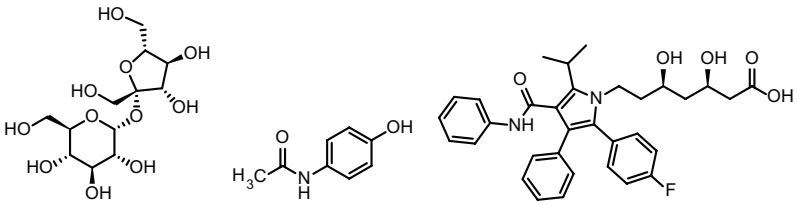

Figuur 1. Moleculen uit het dagelijkse leven, opgebouwd uit atomen.

Een voorbeeld van een multicomponentreactie is de Strecker reactie en sinds de ontdekking halverwege de negentiende eeuw zijn er veel van dit type reacties ontdekt. Een belangrijke groep binnen de multicomponentreacties is de groep reacties waarbij één van de start moleculen een isocyanide is (Figuur 2). Isocyaniden zijn moleculen die een aparte structuur hebben, eerst kunnen ze andere moleculen aanvallen en daarna zelf aangevallen worden. Bovendien hebben ze nog een bijzondere eigenschap, namelijk een vieze penetrante geur. De reactie in Figuur 2 is vernoemd naar de chemicus Ivar Karl Ugi (Ugi reactie) die deze ontdekte in de jaren zestig van

de vorige eeuw.

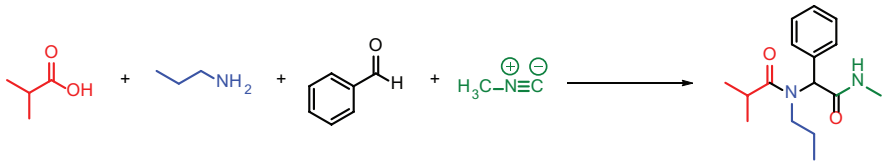

Schema 1. De Ugi vier-componentreactie. Het isocyanide is weergegeven in het groen.

Eiwitten

In ons lichaam hebben we verschillende eiwitten met uiteenlopende functies die ervoor zorgen dat ons lichaam blijft functioneren. Eiwitten zijn ook moleculen, alleen zijn ze heel groot en opgebouwd door het aaneenrijgen van kleine moleculen, de aminozuren. Een goede vergelijking is het rijgen van een snoer met verschillende gekleurde kralen, één voor één worden ze aan een snoer geregen tot er heel veel (soms wel 1000) achter elkaar zitten. Sommige van deze aminozuren hebben bepaalde zijketens die met elkaar een interactie aan kunnen gaan; het snoer van kralen vouwt zich op en een driedimensionale structuur ontstaat (Figuur 3).

Figuur 2. De driedimensionale structuur van een eiwit (PDK1).

Door deze driedimensionale structuur zitten vormt zich een oppervlakte waarin verschillende holtes (*pockets*) zitten. In deze holtes kunnen moleculen binden die nodig zijn voor het eiwit om zijn functie te vervullen of een gedeelte van een andere eiwit waar de functie op uitgevoerd wordt. Het is belangrijk om te beseffen dat deze holtes zeer specifiek zijn en dat alleen moleculen of bepaalde delen van een eiwit kunnen binden, vergelijkbaar met een sleutel en een slot.

Een belangrijk proces in het lichaam is regulatie, ervoor zorgen dat een bepaald proces in het lichaam wordt versneld of vertraagd naar gelang de omstandigheden. Kinasen zijn eiwitten die heel belangrijk zijn bij het reguleren van cellulaire processen;

door een fosfaat groep aan een ander eiwit te bevestigen wordt er een reactie in gang gezet die het betreffende eiwit 'aan' of 'uit' zet (in werkelijkheid is het niet zo 'zwart-wit'). In de driedimensionale structuur heeft een kinase een holte voor het binden van adenosine trifosfaat (ATP, levert de fosfaat groep) en een holte voor het binden van het eiwit dat aan of uit gezet moet worden. Wanneer een van deze twee holtes wordt geblokkeerd door een medicijn kan het eiwit tijdelijk zijn functie niet uitvoeren en wordt een overmatig actief eiwit zo geremd (Figuur 4).

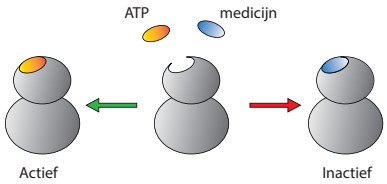

Figuur 3. In het geval een eiwit overmatig actief is kan het geremd worden door een medicijn. Doordat het medicijn bindt kan, in dit geval, geen ATP meer binden en is de kinase inactief.

Omdat kinasen zulke belangrijke eiwitten zijn bij het reguleren van processen in het menselijk lichaam en disregulatie grote gevolgen heeft voor het lichaam is een groot deel van het onderzoek dat wordt uitgevoerd door farmaceutische bedrijven gericht op deze groep eiwitten. Alleen is er een belangrijke horde die het onderzoek bemoeilijkt. Het merendeel van de moleculen die wordt ontworpen voor de kinasen binden aan dezelfde plek, de ATP holte, maar deze holte is voor een groot deel gelijk in alle kinasen (518 stuks). Hierdoor is het moeilijk om een origineel selectief molecuul te maken die een specifieke kinase remt. Gelukkig zijn er andere manieren om dit te bereiken Zogenaamde allosterische holtes zijn holtes die een andere locatie hebben in de driedimensionale structuur, maar wel invloed hebben op de activiteit van het eiwit. Helaas wil dit niet zeggen dat dit de heilige graal is en ook deze methode heeft de nodige uitdaging.

Het proefschrift

In het eerste gedeelte van hoofdstuk 1 worden de multicomponentreacties geïntroduceerd en de voordelen die ze hebben ten opzichte van klassieke chemie genoemd. Een voorbeeld waarbij multicomponentreacties worden gebruikt in de farmacochemie is beschreven. In het tweede gedeelte worden de algemene aspecten van de kinase PDK1 beschreven alsmede de allosterische holte op dit eiwit, de *PIF pocket*. Bovendien wordt er een overzicht gegeven van de kleine moleculen die tot nu toe zijn gemaakt voor deze PIF pocket.

In hoofdstuk 2 beschrijven we hoe de freeware AnchorQuery is gebruikt voor het ontwerpen van scaffolds voor de PIF pocket. Verschillende verbindingen uit de Castagnoli reactie bleken zeer actief en moleculen met een goede affiniteit voor de PIF pocket zijn gesynthetiseerd en getest (Figuur 1). De farmacokinetische eigenschappen zullen verder geoptimaliseerd moeten worden, omdat deze verbindingen nog niet een cel binnen gaan. Enkele aanbevelingen voor vervolg onderzoek aan deze moleculen zijn gegeven en ideeën voor het ontwerpen van nieuwe verbindingen.

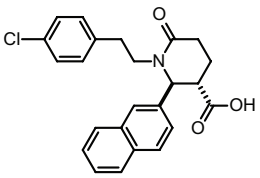

Figuur 4. The most active compound towards PDK1 from this research.

In hoofdstuk 3 introduceren we een nieuw verwijderbaar isocyanide in de Ugi-tetrazoolreactie die zo kan worden toegepast in de synthese van biologisch relevante 1*H*-tetrazolen (Schema 1). In de farmacochemie worden deze tetrazolen namelijk beschouwd als vervanger van een carbonzuur, maar met betere farmacokinetische eigenschappen. Het β-cyanoethyl isocyanide reageert uitstekend met een breed scala aan startmaterialen en het verwijderen van de groep gaat snel en onder milde reactiecondities. Door deze eigenschappen is dit isocyanide een waardevol alternatief voor bestaande methodes. De toepassing van dit isocyanide in andere multicomponentreacties wordt kort beschreven.

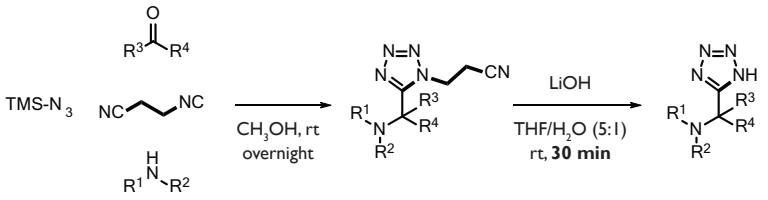

Schema 2. β-Cyanoethyl isocyanide in the synthesis of 1*H*-tetrazoles.

In hoofdstuk 4 proberen we een nieuw type cyclisch anhydride te introduceren in de Castagnoli reactie om zo de bruikbaarheid van deze reactie te vergroten. Hoewel cyclisch gemixte anhydriden (Figuur 2) bekend zijn in de literatuur is hun toepassing in de Castagnoli reactie niet zo eenvoudig. De synthese van een cyclisch gemixt anhydride is bereikt en een uitgebreide discussie waarom deze verbinding mogelijk niet werkt in de Castagnoli reactie is beschreven.

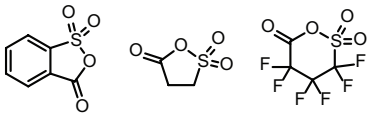

Figuur 5. Cyclic mixed sulfocarboxylic anhydrides.

In hoofdstuk 5 geven we een overzicht van de recente literatuur die zich focust op de additie aan C=N bindingen en aan nitrillen en is hoofdzakelijk gericht op multicomponentreacties. Verschillende bruikbare startmaterialen zijn beschreven die de synthese van meer complexe (biologisch relevante) verbindingen mogelijk maakt. Bovendien komt de Ugi-five-center-four-component reaction aan bod. Door het kiezen van de juiste startmaterialen is deze variatie op de bekende Ugi reactie zeer bruikbaar in de synthese van nieuwe verbindingen.

Acknowledgements

A little over four years my PhD has come to an end, and one of the more difficult things, for me, is to find words to express my gratitude to so many people. I had a wonderful time at the Antonius Deusinglaan; I met a lot of people, made new friends, and witnessed how our research group grew from five to twenty-eight people. Like Ernest Hemingway once said: " It is good to have an end to journey to; but it is the journey that matters, in the end." I think this also applies to a PhD.

First and foremost, Alex. I remember the first time I came to Antonius Deusinglaan to give a presentation about my masters research project. You were sitting in your office, which consisted of a desk laden with papers, a large table also laden with papers, and a comfortable green couch and ditto chair. To be honest, this is exactly how I will remember you: a generous, approachable, funny person that has difficulties to part with paper, sometimes. You give your students plenty of room to develop themselves and your unlimited enthusiasm inspired me to become equally enthusiastic about new experiments or ideas. I admire the way you combine your work with seeing you family only in the weekends, it demands a lot from all of you. I wish you and your family all the best for the future.

I would like to thank the people from the reading committee: Prof. Frank Dekker, Prof. Laurent El Kaïm, and Prof. Anna Hirsch for evaluating my thesis and their useful corrections.

Next, I have to be grateful to my collaborators in Germany and, lately, in Argentina. Ricardo, thank you for introducing met into the wondrous world of the PIF pocket and taking time to learn me all the biochemical aspects that come with it. Thank you, Evelyn and Alejandro, for your efforts to test the different compounds, and to Jörg for performing all the crystallographic work for our project. Finally, thank you Matthias for your ideas regarding the SAR and what to try next.

Dr. Katarzyna Kurpiewska and Dr. Justyna Kalinowska-Tłuścik, thank you for measuring the different single crystal X-ray structures from this thesis.

Behind a good professor is a great secretary and you, Jolanda, are no exception. Thank you for everything you arranged over the years. Especially, the package that had to be send to Argentina was one of the highlights; it never arrived and probably is still gathering dust at the airport of Buenos Aires.

Matthew, although you were not directly involved in my research your advice on other aspects, like measuring solubility, is appreciated. Something else I will remember, is that your were in an euphoric state when Leicester City, out of the blue, had a great season in the Premier League and won the trophy. Go Foxes!

Carlos, you are full of passion for a lot of things (woman), have a great personality and I want to thank you for all the good moments we had.

Then, I would like to be grateful to Kareem. It was great having you here when I just started, you introduced me to the different computer programs we use in our research. I will never forget our Sinterklaas celebration in the first year, and your face when we explained words like negerzoen.

I also supervised students and I would like to thank Fabio and Fanny for the work they did. I hope you learned from the experience, I most certainly did. I wish you all the best in your future careers.

During the four years I have met a lot of people: Ajay, Alaa, Ameena, Atilio, Chary, Eman, Eswar, Fandi, Fernando, Hannah, Jingyao, Kai, Markella, Natalia, Naveen, (Greek) Nick, Niels, Patil, Qian, Robin, Santosh, Sergey, Ting, Vishwanatha, Wenjia, and Yuantze. I am grateful for all the nice memories, for all the gezellige borrels, diners, outings, and for the nice working environment. Moreover, I would like to thank the visiting scientists from all over the world: Arianna, Bupendra, (USA) Nick, Paola, Saad, Samat, Silvia, Shabnam, Soraya, and Shrinidhi. Finally, I would like to thank all the bachelor and master student that visited our lab.

Iris, Marilena, Martijn, Olivia, Thea, thank you for being part of the pub quiz group. I enjoyed all the Wednesdays we visited the Toeter and tried our best...to be somewhere in the middle.

Dinos, I would like to express my gratitude for all the discussion we had over the years, I recall several discussion about the Van Leusen reaction. Moreover, you appeared to have an unlimited knowledge about subjects other than chemistry, very informative. Unfortunately, we never played chess, but perhaps in the future we find the time to play (and I still have time to improve).

André, your work as technician in our group is invaluable and you have my respect for all the things you arrange for the lab. When I started, it was nice to have someone who appreciated de koffietijd as much as I did, it gave us time to discuss other things, besides work. Another recurring theme was troubleshooting and maintenance of the SFC, I believe that after four years we are certified SFC technicians, however, without a certificate. Finally, I want to thank you for being my paranymph during my defence.

Tryfonas, thank you for being my other paranymph. We began our PhD roughly at the same time and when we first met I immediately noticed the kind and generous person you are. Also, for being my partner in crime when travelling to conferences; I am happy that I never had the 'black cat' travelling experience other people seem to have with you. Finally, I would like to thank you and Dinos for arranging the memorable trip to Thessaloniki and Mt. Athos, it was awesome!

I want to express my warmest feelings to Marilena. You became a very good friend with whom I shared so many stories, had numerous good laughs, and dinners in the UMCG. You have a very open, sincere, thoughtful, and generous personality,

and that is what I like about you. I am glad that we have met and hope that we will be friends until we are old and grey. I wish you all the best in pursuing a career at the Greek FDA.

Mijn vrienden Dirk Jan, Gosina, Ilse, Johanna, Jort, Maartje, Nynke en Wytse. Ik wil jullie graag bedanken voor de interesse die jullie altijd hebben gehad in mijn werk. Het is heerlijk om tijdens een weekend weg met elkaar een keer niet te hoeven denken aan experimenten, maar aan gezellig samen zijn.

Renee, Mark, Liona, Trienke, Silke, Jorn, Rixt, Oma, Theo, Henny, Jaring en Tessa, bedankt voor jullie steun en interesse. Ik hoop dat de samenvatting toegankelijk genoeg is, zodat jullie kunnen zien dat ik de laatste jaren toch wat anders heb gedaan dan gif mengen. Ook al wonen we al jaren in Groningen, zal ik dankzij jullie Friesland altijd als thuiskomen zien.

Papa en mama, jullie hebben je vast wel eens afgevraagd of het goed zou komen met mij. Nu ik gepromoveerd ben lijkt me dat wel en ik wil jullie graag bedanken voor de steun die jullie me hebben gegeven in de keuzes die ik maakte; het heeft me gebracht waar ik nu ben. Het is altijd fijn om even thuis zijn bij jullie.

"The meeting of two personalities is like the contact of two chemical substances: if there is any reaction, both are transformed." (C. G. Jung). Lieve Marina, ik denk dat deze quote wel van toepassing is op ons sinds we (lang geleden) samen een profielwerkstuk over esters hebben gemaakt. Je bent slim, zorgzaam en gedreven in de dingen die je doet; eigenschappen die van pas zullen komen als we straks met zijn drieën zijn. Ik hou van je.

Edwin

Groningen, 20 januari 2017